# EFFECT OF SEVERE PLASTIC DEFORMATION AND SUBSEQUENT HEAT TREATMENT ON HARDNESS AND ELECTRICAL CONDUCTIVITY OF OXYGEN-FREE HIGH CONDUCTIVITY (OFHC) COPPER, COMMERCIAL PURE COPPER, AND COPPER CHROMIUM ALLOY

A Thesis

by

YI-TANG KAO

Submitted to the Office of Graduate and Professional Studies of
Texas A&M University
in partial fulfillment of the requirements for the degree of

MASTER OF SCIENCE

| | |
|---|---|
| Chair of Committee, | Karl Ted Hartwig |
| Committee Members, | Ibrahim Karaman |
| | Thomas Lalk |
| Head of Department, | Andreas A. Polycarpou |

December 2014

Major Subject: Mechanical Engineering

# ABSTRACT

Samples of oxygen-free high conductivity (OFHC) copper (C101), commercially pure copper (C110), and copper chromium alloy (C182) were subjected to severe plastic deformation (SPD) using equal-channel angular extrusion (ECAE) to determine the effect of large amounts of plastic strain on the hardness and electrical conductivity for electrical conductor applications. Different levels of plastic strain and strain orientation combinations were applied by ECAE at room temperature. Heat treatments in the range 100°C to 500°C for times from 10 minutes to 4 days were applied to the materials after ECAE. The electrical conductivity and hardness were determined by four-point probe measurement and Vickers microhardness measurement.

The hardness of all test materials increased significantly and the electrical conductivity decreased after ECAE, presumably because of the higher density of dislocations caused by the plastic strain. The properties changed most dramatically after a strain of ~2.3 and reached a near plateau after a strain of ~4. A post-strain heat treatment for temperatures at and above 250°C and for times of at least 1 hr. caused the conductivity and hardness to return to pre-strain levels (near 100 % IACS and VH 50) in C101 and C110, with the change occurring more rapidly for higher temperature annealing. For the case of C182, the post-strain heat treatment induced the highest hardness (VH 162) at 450°C for which the material had a conductivity of 76 %IACS. Copper 101 and 110 showed a plateau in hardness and conductivity after 3 hours heat

treated at 150°C and higher; the hardness and conductivity of C182 did not reach stable values at 350°C and 450°C after 48 hours.

SPD and post SPD heat treatment successfully improved the combination of hardness and electrical conductivity of the three Cu-based alloys studied for room temperature electrical conductor applications. The best combination of hardness and conductivity (99 %IACS and VH 137) occurred in C110 after two passes of ECAE (plastic strain of 2.3) and heat treated at 100 ºC for 1 hour, for which the hardness increased by 58% over the fully annealed condition. The results of this work can be applied to other metals such as aluminum and silver contemplated for electrical conductor applications.

# DEDICATION

To my parents, and all of my family members.

# ACKNOWLEDGEMENTS

I would like to thanks Dr. K. Ted Hartwig for his guidance and support throughout the process of this research. Thanks to my committee members Dr. Thomas Lalk and Dr. Ibrahim Karaman for their enduring patience and helpful suggestions. I would also like to express my gratitude to Mr. Robert Barber for his suggestions and assistance. Thanks to Zach Levin, Shreyas Balachandran, Miao Song, and David Foley for their help in instrument design, execution, and understand.

TABLE OF CONTENTS

Page

LIST OF FIGURES

Page

LIST OF TABLES

Page

# I. INTRODUCTION

## 1.1. Motivations

Over the past few decades, Ultrafine-grained (UFG) and nanocrystalline (NC) materials have gotten wide attention from scientists, because of the potential of improvement of mechanical properties compared to coarse-grained conventional materials. UFG materials are defined as having average grain sizes between 100 nanometer and 1 micrometer. Nanocrystalline materials are defined as having an average grain size below 100 nanometer.

One simple and efficient way to obtain UFG and NC materials is by severe plastic deformation (SPD) such as equal-channel angular extrusion/ pressing (ECAE/ECAP). SPD can impart large imposed strain on the material, and cause grain size refinement in the microstructure. Conventional deformation processes such as drawing, extrusion, and rolling impose strain on the work-piece to refine the grain size as well. However, these conventional process methods carry some disadvantages, such as high fraction of low angle grain boundaries (LAGB), and the samples will go through a significant reduction in initial dimensions. Consequently, strong stress-strain non-uniformity would occur in the materials, and only some limited applications can be produced, such as foil and filament. Moreover, these conventional techniques are not very efficient for grain size refinement, because the amount of imparted strain is limited. By contrast, samples processed by ECAE not only contain ultrafine grain size but also a high fraction of high

angle grain boundaries (HAGB). Compared to other SPD methods, the uniformity of strain and the capability of processing large materials are two advantages of multipass ECAE. Furthermore, ECAE can be conducted at room temperature, which also makes the process attractive.

SPD techniques have always attracted attention from the scientific community. Recently, SPD has been used to obtain UFG and NC materials for electrical conductors. Because poor mechanical properties is the one of the most important issues that needs to be solved for conductor materials, and SPD can be applied to solve this problem. Because of this, some SPD research has focused on aluminum, copper, silver etc., which are the most commonly used materials in conductors. However, the amount of research is limited and showed some inconsistent results. For example, some research has shown that the electrical conductivity decreases while the mechanical properties increase after SPD [1-5]. This property changes are caused by an increased dislocation density and smaller grain size which impede electron flow [5]. On the other hand, some research showed that SPD technique can enhance both mechanical properties and electrical conductivity by proper heat treatment after the process [6], due to the solid solution alloying element precipitated from the matrix [7]. Therefore, these contradictory results and limited reports suggest that there should be more attention on the effect of severe plastic deformation of electrical conductor materials.

In this study, oxygen-free high conductivity (OFHC) copper, commercially pure copper, and chromium copper alloy were subjected to SPD using ECAE. After that, the alloys were heat treated at different temperatures for different times. The microhardness

and conductivity of the materials were investigated to determine if the processed copper alloys might be suitable for future conductor applications.

## 1.2. Objectives

Determine if severe plastic deformation (SPD) resulting from equal-channel angular extrusion (ECAE) and post deformation heat treatment improves the strength and conductivity combination of several copper-based alloys for electrical conductor applications.

In order to achieve the objective, a set of experiments was designed. More specifically, Oxygen-free high conductivity copper (C101), commercially pure copper (C110), and chromium copper alloy (C182) were selected as the test materials. The major experimental tasks are listed below.

- Determine the effect of strain on electrical conductivity and hardness for different numbers of ECAE passes (pass 1, 2, 4, and 8), and the influence of strain path by using different ECAE routes (route A, B, Bc, and E).
- Determine the electrical conductivity and microhardness variation for oxygen-free copper and pure copper caused by different heat treatment temperatures (from 100°C to 400°C) after ECAE. The same for chromium copper alloy, except heat-treated from 350°C to 500°C.
- Determine the time (10 min., 30 min., 60 min., 90 min., 3hr., 12 hr., and 48hr.) effect for different heat treatment temperatures on the materials.

## 1.3. Materials

### 1.3.1. Mechanical and Electrical Properties of Metals

Conduction materials include metals, semiconductors, superconductors, electrolytes, conductive polymers, plasmas and some nonmetallic materials such as graphite. However, metals are the most commonly used material for electrical conductors, due to the high conductivity, high strength, and low cost. Typical mechanical and electrical properties of some common pure metal conductors are shown in Table 1.

Table 1. Mechanical and electrical properties of some pure materials [8-10].

| | Silver | Copper | Gold | Aluminum | Carbon Nanotube |
|---|---|---|---|---|---|
| Tensile Strength (MPa) | 125 | 209 | 103 | 45 | 150000 |
| Electrical Conductivity (%IACS at 20ºC) | 108.4 | 101 | 73.4 | 65-66 | >215 |
| Density ($g/cm^3$ at 20ºC) | 10.49 | 8.93 | 19.3 | 2.70 | 1.60 |

Silver is generally considered the best material for electrical conductors due to its high conductivity and corrosion resistance. However, the high cost, low strength, and the tendency to corrode in an oxygen rich environment limit its application. Nevertheless, there still are some special applications for silver, such as electrical and motor control switches. Gold also has very high electrical conductivity and good corrosion resistance, but the high density and the high cost limit its applications. However, some high-energy applications still use gold as the electrical conductor. Carbon nanotube is an attractive

material, which has extremely high strength and electrical conductivity, but fabrication process is very complicated and expensive. Therefore, this material is still for research use only. Graphene is a great material for electrical conductor applications as well. Its electrical conductivity is around 172 %IACS, and the tensile strength is 130000 MPa. However, the how cost and the complicated manufacturing process are the most important issues that graphene is not commonly used in the industry.

Aluminum and copper are two of the most commonly used materials in electrical conductors. Both of these materials have been used for many years, because of the high conductivity and low cost. A discussion of copper and aluminum is presented in next section.

### 1.3.2. Copper and Aluminum

Which is a better material of conductors between copper and aluminum has been discussed for a long time. Copper has higher conductivity and has a higher strength than Al. However, Aluminum is more available compared to copper. Thus, the price of Al is lower and more stable than that of Cu. Each material has positive and negative features that affect the application for conductors.

Copper has the highest conductivity of all non-precious metals, and possesses good corrosion resistance, excellent workability, good mechanical properties, and good solderability, which explains why copper is preferred for electrical conductors. Pure copper has the highest conductivity compared to other copper alloys, but the strength is

lower. Therefore, adding some alloy element into pure copper is an option to strengthen the material, but it will impair the conductivity.

The main competitor to Cu for commercial electrical conductors is Al. The main advantages for Al are low cost and lightweight. Pure aluminum possesses high conductivity but it is too weak for most applications. Therefore, Al alloy 1350 with 99.5% Al content, and Al alloy 6101 with 98% Al content are the most commonly used materials for conductor applications. Although Al 1350 has 62% the conductivity of Cu, it is poor in mechanical properties. Al alloy 6101 is stronger than Al 1350, but it has lower conductivity as shown in Table 2.

Aluminum alloys always have a lower conductivity than pure Cu. Hence, for the same current-carrying capacity, Al alloys must have a lager cross section. The cost of space increases as well. However, Al alloys possess lower density than Cu. This guides a current-carrying capacity per unit weight for Al that is twice as high as Cu. For some applications where weight is a more important concern, Al would be a better choice. On the other hand, copper has higher tensile strength. For the same current-carrying capacity, although the cross section of aluminum is larger, the tensile strength is still lower than copper. Creep is also an important issue of concern, because creep can cause the mechanical connections to loosen, which can cause the connections to create dangerous arcing or heat. Copper has outstanding creep characteristics compared to aluminum, which can minimize loosening. If the application concerns space and strength more, Cu might be a better option.

Table 2. Mechanical and electrical properties of some Al and Cu alloys [9].

| | Tensile Strength (MPa at 20ºC) | Electrical Conductivity (%IACS at 20ºC) | Density ($g/cm^3$ at 20ºC) |
|---|---|---|---|
| Al 1350-O | 83-195 | 62 | 2.705 |
| Al 6101-T6 | 83-221 | 56 | 2.69 |
| Cu 101 | 221-455 | 101 | 8.94 |
| Cu 110 | 221-455 | 100 | 8.89 |
| Cu 182 | 234-593 | 40 | 8.89 |

(a) rod, 25mm (1 in.) diameter

### 1.3.3. Pure Copper and Copper Alloys

It is known that for electrical conductor applications, the pure coppers, such as oxygen-free high conductivity (OFHC) copper (C101) with 99.99% Cu content, and commercially pure copper (C110) with 99.9% Cu content, possess the highest electrical conductivity compared to other copper alloys. For example, the conductivity of C101 achieves a minimum of 101% IACS. However, the mechanical properties must also be considered. Although the conductivity and strength of annealed pure copper is high, in some applications, the strength is not high enough. In order to solve this problem, one can add some alloying elements into Cu, such as chrome and zirconium. Adding some alloying elements can significantly enhance the strength, but high strength and high conductivity usually cannot exist simultaneously in materials. For instance, chromium copper alloy (C182) is stronger than pure copper, but the conductivity is much lower. The properties of some copper alloys are shown in Table 2.

### 1.3.4. Application of Copper Alloys

The major applications for Cu and Cu alloys are electrical wires, plumbing, and industrial machinery. Moreover, copper has been used for weatherproof architectural materials since ancient times, because of its excellent corrosion resistance. Copper usually is used as a pure metal, but when hardness and strength is a concern, copper alloys are preferred.

OFHC copper (C101) possess high chemical purity and high conductivity, but the recrystallization temperature is below that of commercially pure copper (C110). OFHC copper is widely used for electronic and electrical equipment, which requires high efficiency and a durable material. Especially, C101 is used in application where impurities or oxygen can cause an undesirable chemical reaction with other materials. Such applications include electrical and electronic conductors, solid-state devices, vacuum tube, super conductor matrixes, plasma deposition processes, power substations, and glass-to-metal seals.

Commercially pure copper (C110) has a lower cost compared to C101, but the electrical properties are only slightly different. Thus, C110 is commonly used in various applications, including electrical components, bus bars, cables, power transmission components and high conductivity items for use at higher temperatures. However, C110 has poorer machinability [9], which limited applications where extensive machining is not required.

Chromium copper alloy (C182) is a high copper content alloy, which is usually used where high strength and high conductivity is needed. C182 is an age hardenable material,

which means the properties will change at elevated temperature, due to the precipitation of chromium. The strength of fully aged C182 is nearly twice as high as pure copper where the conductivity is 80% IACS [9]. The corrosion resistance of C182 is also higher than the pure copper since the chromium improves the chemical properties of the oxide film. The features of high strength and high corrosion resistance let C182 has many applications, inc luding cable connectors, seam welding wheels, switchgear, and electrical and thermal conductors that require high strength at elevated temperature.

## 1.4. Severe Plastic Deformation Methods

Several methods exist for severe plastic deformation. Each of them has unique advantages and disadvantages. This section will provide some basic introduction of different SPD methods.

### 1.4.1. High-Pressure Torsion (HPT)

High-pressure torsion (HPT) is illustrated in Fig.1. HPT provides large plastic deformation under high-applied pressure. A disk like sample is held under a high pressure, and then subjected to torsional straining [11]. The friction causes the shear strain in the sample, and the compressive stress prevents the specimen to break under the high strain. One advantage of HPT is that it can produce extremely small grain size, usually in the nanometer range (<100nm). The improved grain size refinement attained by HPT has been confirmed in early research [12]. Furthermore, the capability to process brittle materials is another advantage [11, 13]. However, HPT has some disadvantages as well, such as the

specimen dimensions are limited to 12 mm to 20 mm disk diameter and a thickness between 0.2 mm and 1 mm [14]. This technique needs more investigation for larger samples.

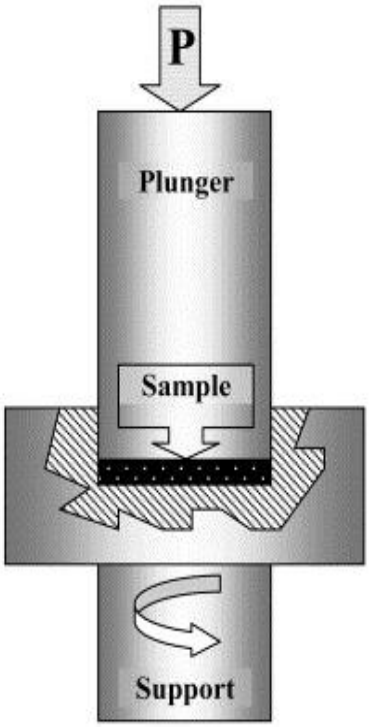


Figure 1. The illustration of high-pressure torsion [15].

### 1.4.2. Repetitive Corrugation and Straightening (RCS)

Repetitive corrugation and straightening (RCS) is illustrated in Fig. 2. In the process, the sample is repetitively bent and straightened with no significant change of the dimensions of sample. During the process, the plastic strain imparted to the sample causes grain size refinement [16]. The advantage of RCS is that it can be easily adapted by current

industrial rolling facilities. Because it is not difficult to substitute corrugated rolls for conventional rolls [17]. However, a disadvantage of RCS is poor homogeneity of microstructure.

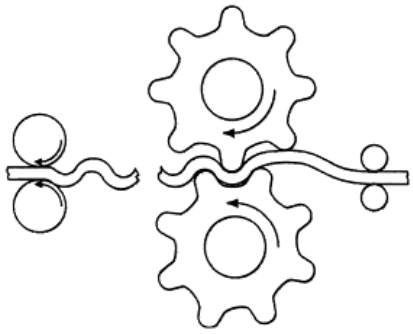

Figure 2. The illustration of repetitive corrugation and straightening (RCS) [16].

### 1.4.3. Accumulative Roll-Bonding (ARB)

The accumulative roll-bonding (ARB) process is shown in Fig.3. ARB can be seen an extension of rolling. A strip is placed on the top of another strip, and in order to have strong bonding between the two strips, the two contact surfaces are degreased and wire-brushed first. Then, these two strips go through the rolling operation and jointed together. After that, the length of the rolled sample is cut into two equal halves, and the same process is repeated [18]. The series of rolling, cutting, degreasing, brushing and stacking are repeated until a large strain occurs in the sample. The key issue to have success with the ARB process is the surface treatment. The surface treatment significantly affects the bond strength between each two strips, and the higher bond strength can cause higher shear

strength on the surface of the sample [19]. Therefore, surface treatment becomes the most important factor to consider during the ARB process. The disadvantage of the ARB method is that the UFG structure of processed material is not three-dimensionally equiaxed. The structure is a pancake like which is elongated in the direction of rolling [17], and thus the material is anisotropic.

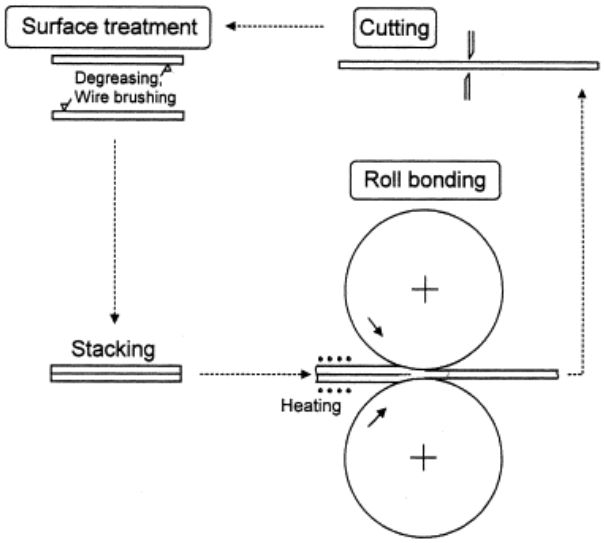


Figure 3. The illustration of accumulative roll-bonding (ARB) [18].

### 1.4.4. Twist Extrusion (TE)

Twist extrusion (TE) is a method that presses a prism shaped sample out through a die as shown in Fig.4. When the specimen is processed, it goes through severe plastic deformation without a dimension change. The method allows the sample to be extruded repetitively for accumulating strain [20]. However, the plastic strain caused by TE is not

uniform across the cross-section of the sample. The strain rises with the distance from the extrusion axis. This means that a more fine grain size is found in the outer regions compared to the core of specimen. It is anticipated that more extrusion passes improve the microstructural homogeneity [17].

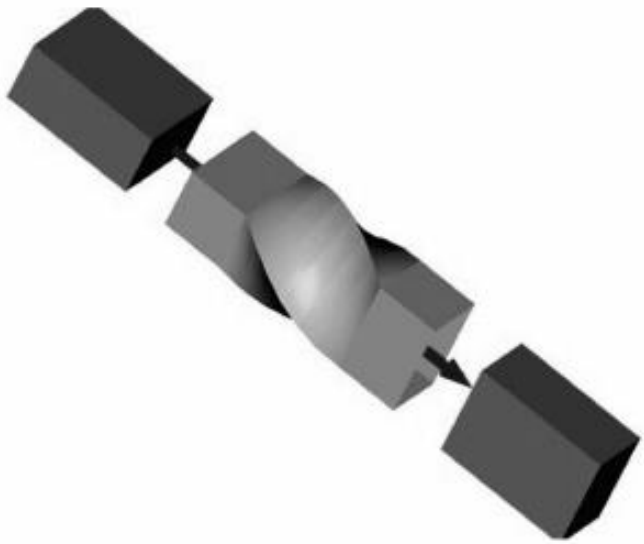

Figure 4. The illustration of twist extrusion [17].

### 1.4.5. Equal Channel Angular Extrusion (ECAE)

Equal-channel angular extrusion (ECAE) is a method of SPD that produces intense plastic strain in materials. ECAE was developed by V.M. Segal and his co-workers in 1972 in Russia [21]. A well-lubricated sample is forced to pass through a die of equal channel sizes, which imparts large plastic strain on the sample through simple shear. After each pass, the shape of the specimen remains approximately the same. The die angle is

one of the most important issues when processing the sample through ECAE, because the die angle determines the shear strain per pass. The variety of the die angle Φ is from 90º to 180º, but the most often used angle is 90º as this provides the highest plastic strain [22]. An illustration of ECAE is shown in Fig.5.

Compared to other conventional metal processes, ECAE presents several significant advantages. First, the billet processed by ECAE keeps a constant shape. Therefore, the method allows for repetitive extrusions until the plastic strain reaches the maximum. On the other hand, there is no geometric restriction for the maximum plastic strain that can be reached [22]. Second, the shear strain caused by ECAE is nearly uniform across the work-piece. Although the strain might show slight differences on work-piece surfaces, it is more uniform than conventional processes [23].

# II. LITERATURE REVIEW

## 2.1. Severe Plastic Deformation Theories

Conventional metal process such as drawing or rolling, are restricted to produce UFG materials. A down side is that the work-piece undergoes a dimension reduction during the process. Hence, the work-piece cannot repeat the process to achieve the maximum strain without a severe dimension change. Second, the strain imposed by conventional metal process can be insufficient [23]. Therefore, over the past decade, attention has been devoted instead to severe plastic deformation (SPD) methods that are not conventional. The formal description of SPD is a metal forming procedure that imposes very high plastic strain to specimens without any significantly shape change in order to produce exceptional grain refinement [23]. The theories of SPD are described below.

The mechanical properties of materials are determined by many different factors, but the average grain size plays a very important role [23]. According to the Hall-Petch relationship, given by Eq. (1):

$$\sigma_y = \sigma_0 + k_y d^{-\frac{1}{2}} \tag{1}$$

where $\sigma_y$ is yield stress, $\sigma_0$ is lattice friction stress required to move a dislocation, $k_y$ is the constant of yield, and d is the grain size [24, 25]. Eq.(1) presents that a grain size reduction will lead to a yield strength increase, and large yield strengths can be obtained from extremely small grain sizes [26].

In order to obtain high mechanical strengths, coarse-grained materials need to be converted to ultrafine-grained (UFG) or nanocrystalline (NC) grained materials. SPD can impose high plastic strain into materials and produce a high density of dislocations. These dislocations can rearrange to form grain boundaries, and refine the grain size [23].

SPD techniques have been found to be suitable for grain size refining. The different methods include equal-channel angular extrusion (ECAE) [2, 5, 7, 27], high-pressure torsion (HPT) [28, 29], twist extrusion [20, 30], repetitive corrugation and straightening (RCS) [16, 31], accumulative roll-bonding (ARB) [18, 19], friction stir processing (FSP) [32, 33], cylinder covered compression (CCC) [34], and reciprocating extrusion [35]. All of these methods are able to introduce large plastic strains and significant grain refinement.

## 2.2. Equal Channel Angular Extrusion

Equal-channel angular extrusion is an especially attractive SPD method for several reasons: First, it has no geometric limitation for the billets so that it can be used in many different applications. Second, ECAE can be applied to different crystal structures and materials. Third, ECAE is relatively easy to perform; it is readily available for most laboratories to use. Fourth, a sufficient and uniform strain can be developed by ECAE. Fifth, the process is repeatable for samples to achieve extend high level of plastic strain [23]. These exceptional features have led to many experimental studies over the last two decades.

2.2.1. Description of Equipment

Different cases of ECAE can induce different strains, which means it will cause different grain sizes in the specimens. Fig.5 shows the two different cases of ECAE. Both of the cases have the same channel angle Φ, and the work-piece cross section. The difference between the two cases is the curvature at the outer point between the two intersecting channels. The curvature angle Ψ for Case A is 0, whereas the curvature angle Ψ of Case B is higher than 0.

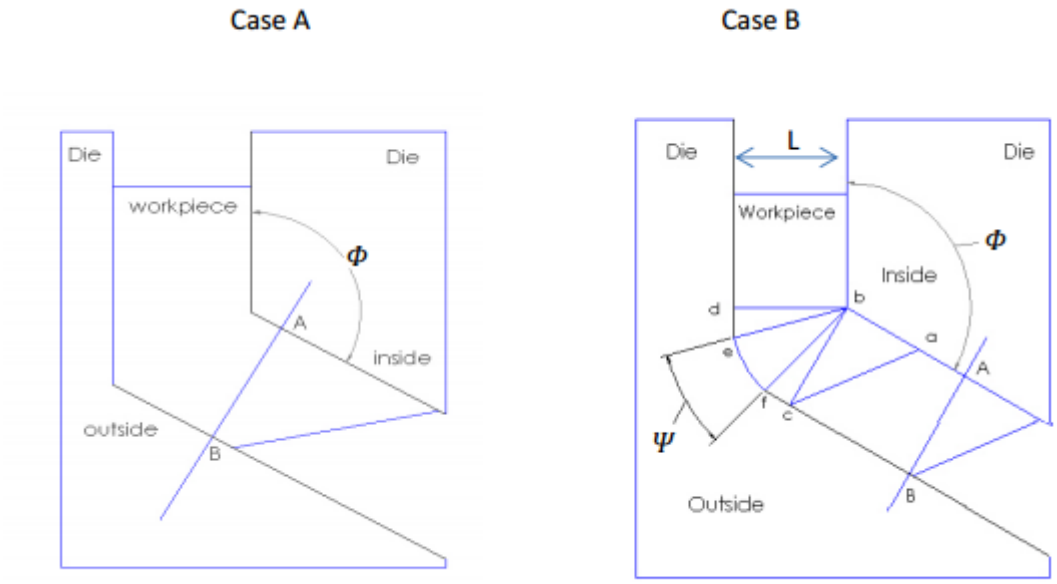


Figure 5. Different ECAE cases, where the curvature angle is: (a) =0 (b) >0.

The relationship derived to distinguish the strain difference caused by the different cases is given by [36]:

$$\epsilon_N = N\left\{\frac{1}{\sqrt{3}}\left[2\cot\left(\frac{\Phi}{2}+\frac{\Psi}{2}\right)+\Psi\csc\left(\frac{\Phi}{2}+\frac{\Psi}{2}\right)\right]\right\} \quad (2)$$

where N is the number of ECAE passes, $\epsilon_N$ the  is strain after N passes, Φ is inner angle and Ψ is outer curvature angle. Eq.(2) shows that the die angle Φ influences the strain more and the strain will decrease when the curvature angle Ψ increases. Because the die channel angle Φ affects the deformation angle of the specimens, lower values of Φ will cause higher strain. However, Nakashima et al. [37] showed that when the channel angle Φ is 90º, the processed samples more quickly achieved a UFG structure with high angle grain boundaries by an intense plastic strain. On the other hand, the higher curvature angle Ψ decreases the strain. Because the higher corner angle will reduce the path length for the bottom part of the specimens. Furthermore, the curvature angle Ψ did not change the deformation angle of specimens, so it has little influence on the strain. Therefore, the strain mostly depends on the channel angle during the ECAE process. The relationship between different angles of ECAE and the equivalent strain are shown in Fig.6. However, a key assumption of Eq.(2) is that the strain during ECAE is homogeneous [36]. Eq. (2) does not describe the non-uniform deformation. Therefore, this solution only can explain the strain occurs at the center part of specimens. Friction, deformation temperature, strain rate, material deformation properties, and other factors can influence the level of non-uniform deformation within the sample [38].

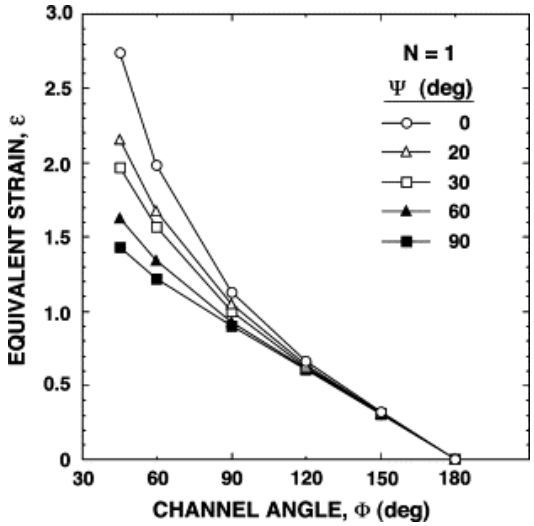


Figure 6. The different angle of the ECAE dies versus different equivalent strain after one pass of ECAE [39].

There has been much more research focus on modeling the actual strain by FEA simulation to explain the non-uniform strain by ECAE [40-42]. The results show that, under the conditions without any friction between the die and specimen. When the curvature angle Ψ is zero, the shear strain on the cross-section of the specimen is uniform with only small non-uniform parts at the top and the bottom. On the other hand, when the curvature angle Ψ increases, the shear strain is uniform at the upper part of the specimen, but non-uniform below [41]. Fig.7 illustrates deformation patterns for different cases of ECAE from the FEA simulation. This figure only shows the steady state condition of the samples; the deformation at the beginning and the end parts of the specimens are not shown [40]. The grid deformation directly shows the strain during ECAE. Furthermore, we also can see the gap between the die and specimen becomes larger when the curvature angle Ψ increases.

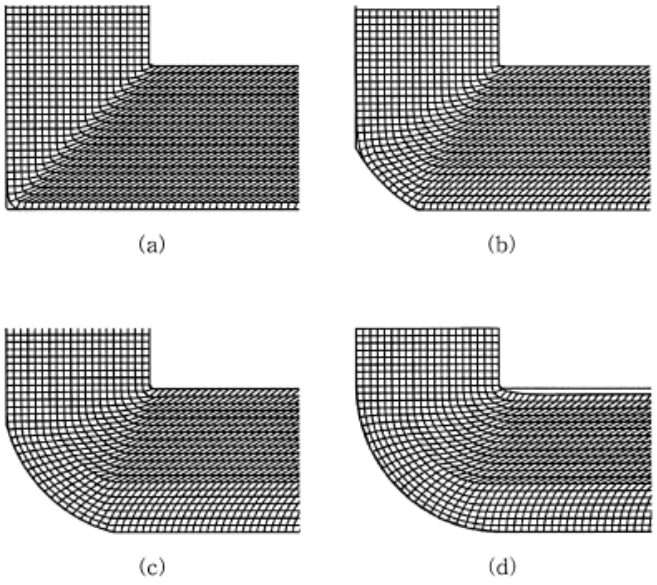


Figure 7. Deformation patterns of samples process by different cases of ECAE. (a) Ψ =0º (b) Ψ =30º (c) Ψ =60º (d) Ψ =90º, when Φ=90 º [40].

### 2.2.2. Factors that Influence ECAE

ECAE usually involves a high-capacity hydraulic press with a high ram speed between 1 to 20 mm $s^{-1}$ [23]. Therefore, the speed variation is also an important factor of concern. Some research has explained different speeds for extrusion [43, 44]. These have shown that process speed has no significant effect on refined grain size. However, microstucture recovery occurs more easily when the pressing speed is slow [43]. Higher speeds can cause temperature increases during the process [44].

Additionally, extrusion temperature is also a significant factor that affects the microstructure of materials during ECAE [45-47]. These results present two significant effects of extrusion temperature. First, the average grain size of specimens increases as the extrusion temperature increases, as shown in Fig.8. Second, the fraction of low angle

grain boundaries formed at higher extruding temperatures [45-47]. The reason for these microstructure changes is that the recovery process become faster as the extrusion temperature increases [46].

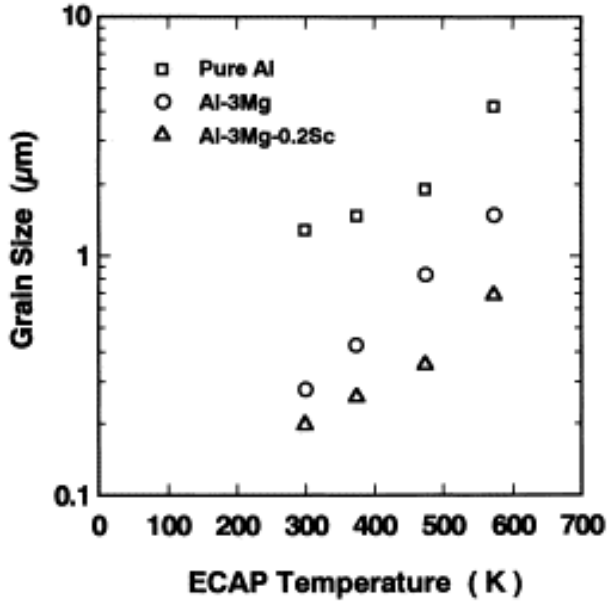


Figure 8. The extrusion temperature versus grain size for some Al and Mg alloys [45].

Back-pressure (BP) is a method that provides an opposite force at the end of sample and which can improve the workability of the specimen during ECAE. An illustration of back-pressure regulation is shown in Fig.9. This topic has been researched for several different experiments already [48-50]. Stolyarov et al. [49] presented that Al-5 wt.% Fe alloy billets failed after a second pass of ECAE, but the alloy keep intact by ECAE with back-pressure after 16 passes. Back-pressure eliminates the gap between the die and the

sample and causes the stress-strain become more uniform in the specimen [50]. Furthermore, back-pressure can also reduce the grain size, but not significantly [23].

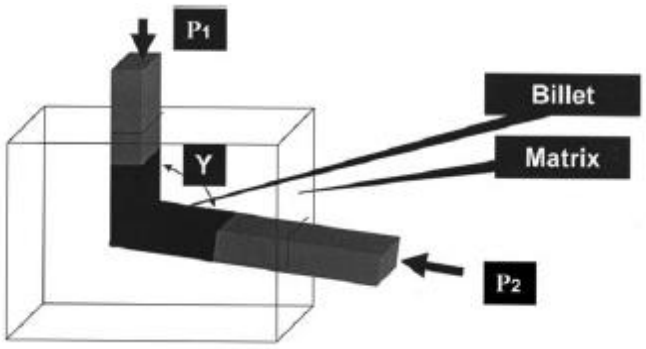


Figure 9. An illustration of an ECAE die with back-pressure. $\boldsymbol{P_1}$ is the force of pressing and $\boldsymbol{P_2}$ is the force of back-pressure [23].

### 2.2.3. Processing Routes

Different strain paths can be produced by changing the rotation pattern of the specimen between each ECAE pass and can lead to significant differences in the microstructure. There are five primary ECAE routes that have been developed; route A, B, Bc, C and E respectively, as summarized in Table 3. Route A is when the billet is extruded without rotation between passes. Route B (also called route $B_A$) is where the billet is rotated through +90° after odd extrusions and rotated -90° after even extrusions. Route $B_C$ (also called route C') is where the billet is rotated through +90° after each pass. Route C is where the billet is rotated through 180° between every pass. Route E is where the billet is rotated through +90° after the first extrusion, then rotated +180° after the second extrusion and repeat this cycle after four-pass sequence.

Table 3.The currently research used routes of ECAE.

| Routes of ECAE | | Route A | Route B | Route $B_C$ | Route C | Route E |
|---|---|---|---|---|---|---|
| Rotation angle | Odd passes | 0° | +90° | +90° | +180° | +180° |
| | Even passes | 0° | -90° | +90° | +180° | +90° |

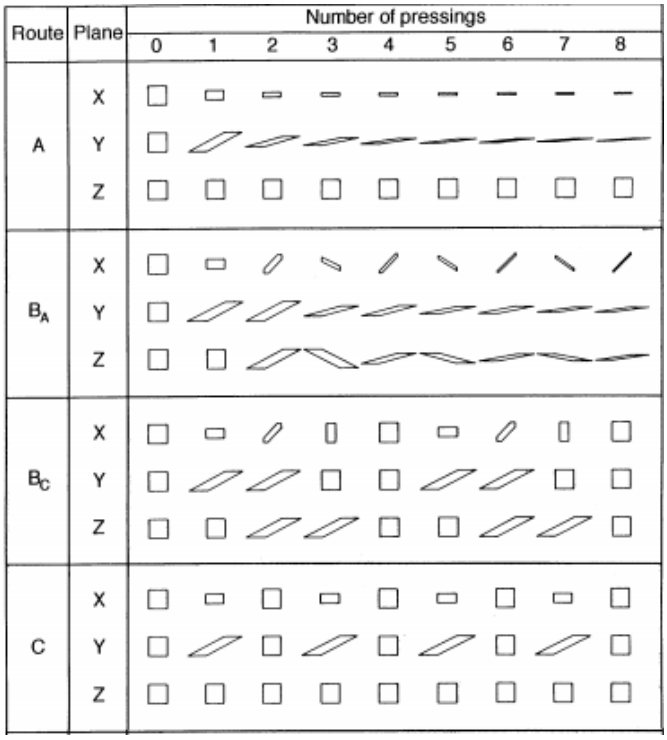


Figure 10. The shear characteristics for different routes of ECAE [51].

The different routes of ECAE have been research in several experiments [51, 52]. The different slip systems are related to different routes of ECAE, and cause different microstructural characteristics in the specimens. The results of shearing characteristics for different routes studied by Furukawa et al. [51] are shown in Fig.10. For the route A, a 3D material element keeps the original shape only in the z plane. For route B, the material

element never keeps the original shape after ECAE. However, for route Bc, the material element returns to the original shape in X, Y, and Z plane after every 4 passes. For route C, the specimen returns to original shape in X, Y, and Z plane after every two passes. Furthermore, the shearing characteristics of route A and route B present similarly, and the shearing characteristics of route Bc and route C present similarly [51].

## 2.3. Previous Work on SPD of Copper and Copper Based Conductor Alloys

Copper and copper alloy processed by SPD can cause grain refinement in the microstructure and lead to increase in strength and hardness [2, 6, 7, 53-56]. However, if the application of the copper is electrical conductor, electrical conductivity or resistivity would be the most important factor. O.F. Higuera-Cobos et al. [57] reported that, for ETP copper (C110) processed by ECAE, conductivity decreases as strain increases, and the reduction of the conductivity is around 2% IACS for the sample through 16 ECAE passes. The reduction of the conductivity can be explained by increases in vacancy and dislocations concentration [57]. The mechanical properties tend to saturate after 2-4 passes. K. Edalati et al. [58] showed results of ECAE processed pure copper: the hardness increased ~270% after ECAE, and the resistivity increased only ~12% [58]. S.A. Hosseini et al. [59] studied commercially pure copper processed by the ARB process. The results show that the mechanical properties significantly increase after ARB process and the conductivity decreases as strain increases. However, the conductivity increases only a small amount after 6 cycles, because the increase of heat caused the recovery. The increase of heat was caused by the previous cold work stored in the sample [59]. These different

researches showed that although the mechanical properties of copper can increase by SPD, SPD negatively affect the conductivity at the same time.

Besides pure copper, different SPD processed copper alloys have been studied. Y.G. Ko et al. [60] studied Cu-3wt%Ag alloy produced by ECAE and ECAE combined with rolling. The mechanical properties of alloy significantly increase, and the conductivity drops in small amount. C.C. Zhu et al. [2] reported the results of the Cu-Mg alloy after ECAE combined rolling and drawing. The microhardness of Cu-Mg alloy significantly increases, but the conductivity decreases. However, the conductivity increases after annealing, but the value is still lower than the as-received material. Moreover, D. V. Shan'gina et al. [61] reported the properties of Cu-Cr alloys after SPD via HPT. Both microhardness and resistivity increase after HPT. However, the heat treatment after HPT can significantly decrease the resistivity and keep the microhardness.

Most previous research shows the similar results: after SPD, the mechanical properties increase, but the conductivity decreases slightly. C.Z. Xu et al. [7] reported that the conductivity of Cu-Cr alloy increases from 25.4%IACS to 78.3%IACS after heat treatment without ECAE. After one pass of ECAE, the conductivity decrease to 77.8%IACS, and the conductivity decreases further with more passes. However, some research successfully found that Cu-Cr alloy with proper heat treatment and ECAE can be enhanced both mechanically and electrically. The result of K.X. Wei et al. [6] showed, the conductivity of Cu-0.5wt.%Cr alloy has no significant change after ECAE combined with cold rolling. However, after heat treatment, the conductivity increases significantly and the microhardness decreases slightly. The best combination of microhardness and

conductivity happened after the heat treatment at 450ºC for 1 hour. Compared to as-received material, the microhardness increased from ~70 Hv to 160 Hv and the conductivity increased from 35 %IACS to 84 %IACS. This result can be explained by the precipitations of Cr. The precipitations of Cr increase the conductivity, and precipitations pinned the dislocations as well [6]. Therefore, high conductivity and high strength can be obtained simultaneously.

These works have attracted attention. For most materials, SPD can significantly enhance the mechanical properties of materials, but decreases the conductivity lightly. The heat treatment after SPD can recover small amounts of conductivity, but decreases the mechanical properties lightly as well. However, some research showed that, the heat treatment after SPD could increase the conductivity and kept the mechanical properties of materials. At the end, both electrical and mechanical properties increase compared to as-received materials.

# III. EXPERIMENTAL MATERIALS AND PROCEDURES

## 3.1. Materials

Three different copper alloys, oxygen-free high conductivity (OFHC) copper (C101), commercially pure copper (C110), and chromium copper alloy (C182), were used in this study. C101 was received from ThyssenKrupp Materials North America. C110 and C182 were received from New Southern Resistance Welding (NSRW). The materials dimensions were: C101 (1 in. × 1 in. × 48 in.), C110 (1 in. × 1 in. × 48 in.), and C182 (1 in. × 1 in. × 72 in.). Their chemical composition is shown in Table 4. C101 has 99.99% Cu content, the alloy with the highest Cu composition. C110 possess 99.9% Cu content (silver counted as copper) and 0.04% O content. C182 contains 99.1% Cu content (Cu+Ag) and 0.6-1.2% Cr content.

Table 4. The chemical composition of C101, C110, and C182.

| Materials | C101 | C110 | C182 |
|---|---|---|---|
| Cu | 99.99 min. | 99.9 min. | 99.1 min.[(a)] |
| O | 0.0005 max. | 0.04 max. | - |
| As | 0.0005 max. | - | - |
| P | 0.0003 max. | - | - |
| Sb | 0.0004 max. | - | - |
| Te | 0.0002 max. | - | - |
| Pb | - | 0.005 max. | 0.05 max. |
| Bi | - | 0.001 min. | - |
| S | - | 0.003 max. | - |
| Cr | - | - | 0.6 to 1.2 |
| Fe | - | - | 0.1 max. |
| Si | - | - | 0.1 max. |

(a) Cu + Ag

3.2. Equal Channel Angular Extrusion Processing

All of the materials were cut by band saw with dimensions of 1 in. × 1 in. × 7 in. for extrusion. The billets of C101, C110 and C182 were pressed through a square channel die at an extrusion speed of 0.1 inch/sec with a channel angle $\Phi=90°$ and a curvature angle $\Psi=0°$ at room temperature. The die of ECAE was designed by Mr. Robert Barber following an original concept by V.M. Segal. Before the extrusion, the billets were painted

with a graphite-based lubricant. The billets were processed via different routes and different passes: 1 pass with route A, 2 passes with route B, 4 passes with route Bc and route E, and 8 passes with route Bc and route E. Route B is where the billet is rotated through ±90° after each extrusion. Route Bc is where the billet is rotated through +90° after each extrusion. Route E is where the billet is rotated through +90° after the first extrusion, and then rotated +180° after the second extrusion, etc. The details of ECAE processing are presented in Chapter 2. After each pass of ECAE, the specimens changed shape slightly. Before the next extrusion started, the specimens were be rolled back to cross section dimesions of ~1.0". The specimens were milled slightly to flatten the surfaces.

After extrusion, the ends of the samples were be cut off by band saw; only the middle parts were kept for the measurements. For the samples that were processed through route B and Bc, two inches were cut off each end and discarded. For the samples that went through routes A and E, one inch were cut off from the ends. After cutting, the samples were milled to make the surfaces flat. Next, cutting was done by a Mitsubishi FX10 wire electrical discharge machine (EDM) for the samples of microhardness and electrical resistivity measurement.

## 3.3. Heat Treatment

### 3.3.1. Heat Treatment Before ECAE

After cutting the specimens to dimensions of 1 in. × 1 in. × 7 in., the samples were initially heat treated before the ECAE process. C101 and C110 were annealed for 2 hours

at 400°C in an air oven, and then cooled down on a metal plate to room temperature. The C182 material was heat treated for 45 minutes at 990°C in an air oven, then quenched into water at room temperature.

### 3.3.2. Heat Treatment After ECAE

After ECAE processes and EDM cutting, the samples were heat treated at different temperatures for different times in a fluidized sand bath, which was designed and built by Mr. Robert Barber. The accuracy of the temperature was around ±3 ºC. After the heat treatment, the samples were placed on a metal plate at room temperature.

The samples of C101 and C110, were heat treated for 1 hour at 100 ºC, 125 ºC, 150 ºC, 175 ºC, 200 ºC, 250 ºC, 300 ºC and 400 ºC, respectively. Moreover, the samples processed by 1 pass route A and 4 passes route Bc were chosen for long-term heat treatments at 100 ºC, 150 ºC and 200 ºC. The samples heat-treated for 1 hour were kept for another heat treatment at the same temperature after measurement. The time of the long-term heat treatments were 1 hr., 3 hr. 12 hr. and 48 hr. The samples were heat-treated, removed from the sand bath for measurement, and then heat-treated at the same temperature until the time for another measurement. This approach was repeated for the long-term heat treatment samples.

The samples of C182 were heat treated at 350 ºC, 400 ºC, 450 ºC, and 500 ºC for 10 min., 30 min., and 90 min. The measurement is the same as for C101 and C110. The same samples were used for heat treatment at the same temperature for different times. The samples processed by 1 pass route A and 4 passes route Bc were chosen to do the long

term heat treatment at 350 ºC and 450 ºC. The time for the long-term heat treatments were 3 hr., 12 hr., and 48 hr.

## 3.4. Microhardness Measurements

### 3.4.1. Samples Preparation

The samples for microhardness measurements were cut by EDM with dimensions of 0.250 ×0.250 ×0.375 inches, and measured on the transverse plane of the samples, are shown in Fig.11. After the EDM cutting and heat treatment, the samples were de-burred by file. Then, the samples of C101 and C110 were mounted in an acrylic mold using epoxy and epoxy hardener. The surface of the samples need to be tested was exposed on one end. After mounting, the samples were cured at room temperature for 24 hour. The samples of C182 were not mounted in epoxy in order to do the next heat treatment. The surface of the samples was polished using an ECOMET 3 variable speed grinder-polisher with 120, 320, 400, 600, 800, 1000, and 1200 grit silicon carbide papers and constant water flow. It was later discovered with the samples of C101 and C110 were to be given a long-term heat treatment. The mounted epoxy samples were broken by hammer in order to take out the samples for next heat treatment.

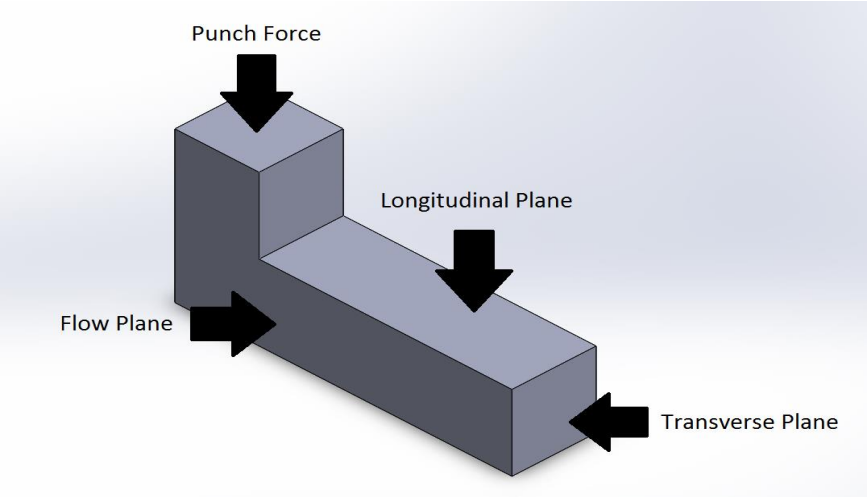


Figure 11. The illustration of the planes on ECAE specimen.

### 3.4.2. Procedure

The Vickers microhardness measurements were performed using a Leco Microhardness Tester LM 300AT. The tester applied a designed single load to a 4-sided pyramidal diamond indenter for a designed period. The angles of the pyramidal diamond indenter were 136º between opposite sides. The indenter gives an angle to the horizontal plane of 22º on each side. In this study, the transverse planes of the samples were imposed with 300g of indenter load and a loading-time of 5s. The Hv numbers are determined by the area of the indentation and the force. This machine calculated the Hv numbers automatically. Therefore, after finishing each indent, and measuring the diagonal length of the diamond indentation on the samples, the Hv numbers were displayed on the screen of the machine. In this study, the average of microhardness for each sample is an average by six measurements.

## 3.5. Resistivity Measurements

### 3.5.1. Sample Preparation

The samples for resistivity measurements were cut by EDM with dimensions of 0.125 × 0.125 × 2.00 inches After the EDM cutting and heat treatment, the samples were de-burred by file to keep the cross section of the samples uniform. Before resistivity testing, the cross-section of the samples was measured by a caliper with 0.001-inch accuracy.

### 3.5.2. Four Point Probe Method

Resistivity was measured by the four-point probe (FPP) method, which is illustrated in Fig.12. The four-point probe was originally proposed by Wenner in 1916 to measure the earth resistivity [62]. In 1954, Valdes adopted the four-point probe for semiconductor resistivity measurement [63]. Today, this technique is widely used in the semiconductor industry for monitoring the production process.

In the method, four probes are forced to the surface of the samples where the current passes through the outer probes (probe 1 and probe 4) and produce the voltage difference in the inner probes (probe 2 and probe 3). A constant direct current (DC) passes between the outer probes. The two inner probes have a constant distance (D2) between each other and used to measure the voltage drop. The resistivity is determined by the following Eq. (3):

$$\rho = \frac{VA}{Il} \tag{3}$$

where $V$ and $l$ stand for the voltage drop and the distance between the two inner probes. $A$ is the cross section of sample, and $I$ is the current that passes through the sample. The equation that converts resistivity to conductivity is shown in Eq.(4):

$$\sigma_{\%IACS} = \frac{172.41}{\rho} \tag{4}$$

where $\sigma_{\%IACS}$ is the electrical conductivity in percent IACS, and $\rho$ is the electrical resistivity in microohm · centimeters [1]. After this chapter, the electrical properties are presented by conductivity.

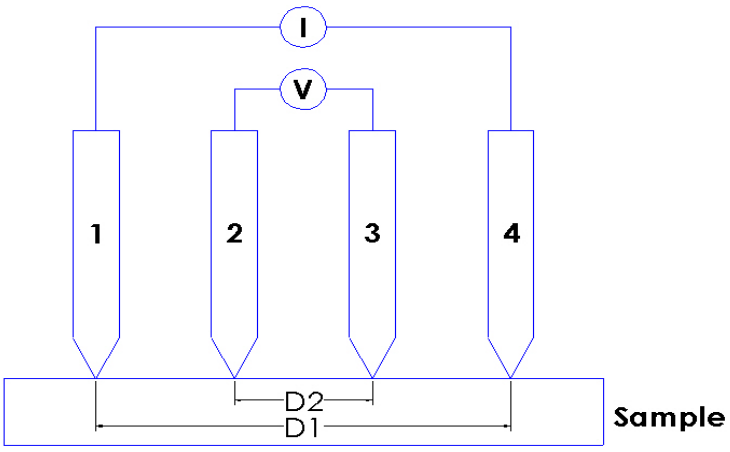


Figure 12. Illustration of the four-point probe resistivity measurement.

### 3.5.3. Procedure

The resistivity measurement in this study was performed by three different machines, power source, ampere meter, and volt meter. A 2600 ± 1 mA constant direct current was supplied by a Hewlett-Packard model 6282A DC power supply with one terminal

connected to probe one. The other terminal was connected to the ampere meter, which was a Keithley Model 199 System DMM Scanner. The other end of the ampere meter was connected to the probe 4. The inner probes were connected to a Keithley Model 181 Nanovoltmeter, which had an accuracy of the voltage of ~nanovolts. The distance between the two inner probes was 1.00 inch. The average voltage drop was measured 30 times for both current directions (reverse and forward). The reasons to reverse the current are: (1) checking the sufficiency of the current input (2) controlling thermal effects. If the voltage drop from the two current directions has a large difference, the current input or the ohmic contact has problem.

# IV. EXPERIMENTAL RESULTS

## 4.1. Microhardness

### 4.1.1. Oxygen-Free High Conductivity (OFHC) Copper (C101)

#### 4.1.1.1. After Equal Channel Angular Extrusion (ECAE)

The microhardness of copper C101 subjected to different passes and routes of ECAE at room temperature is shown in Fig.13. Before ECAE, the annealed material has a much lower microhardness compared to the as-received material because the dislocations in the annealed material are eliminated by annealing. After ECAE, as expected, the microhardness of C101 significantly increased because of strain and the associated increase in dislocation density.

The highest microhardness occurred in route 2B, which increased ~34.7% compared to the as-received material. However, microhardness tends to saturate after two passes of ECAE. In other words, after the second pass of ECAE, more plastic strain does not influence hardness significantly.

Moreover, the samples produced by four passes and eight passes with different routes have a similar hardness. Therefore, the strain path of ECAE has no obvious influence on the hardness of the samples.

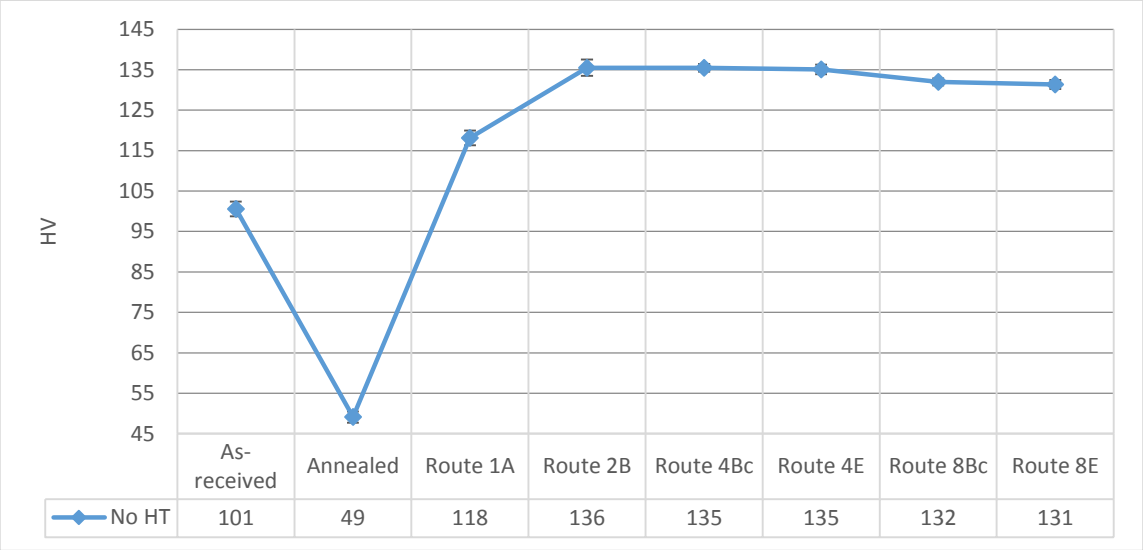


Figure 13. The microhardness of copper C101 after room temperature ECAE without subsequent heat treatment.

#### 4.1.1.2. Different Temperatures of Heat Treatment

The microhardness of copper C101 after a one-hour heat treatment at different temperatures is shown in Fig.14. The hardness of all samples after heat treatment at 100 ºC shows similar results to the samples without heat treatment. This means recrystallization did not occur at 100 ºC. However, the hardness started to decrease when the temperature was above 100 ºC, and a significant drop occurred at 125 ºC and 150 ºC. This can be explained by the recrystallization phenomenon. When the temperature was above 150 ºC, the hardness decreased continuously as the temperatures rose further, but the amount of decrease was miniscule. When the temperature of heat treatment was above 175 ºC, the hardness of the sample processed by more than two passes became lower than

the as-received material. For the sample processed by one pass of ECAE, the hardness became lower than the as-received material when the temperature was above 200 ºC.

The hardness of the sample processed by one pass and route A showed a different tendency compared to other samples. The most significant drop of hardness occurred between 150 ºC to 250 ºC. After a second pass of ECAE, the hardness tends to saturate, so the hardness after different temperatures of heat treatments is similar to each other.

For the samples through the same number of passes but different routes, the results showed no significant difference between them. However, for the samples through route 4Bc and 8Bc, the hardness dropped more significantly between 100 ºC and 125 ºC. On the other hand, for the samples through route 2B, 4E and 8E, the most significant drop occurred at 125 ºC and 150 ºC.

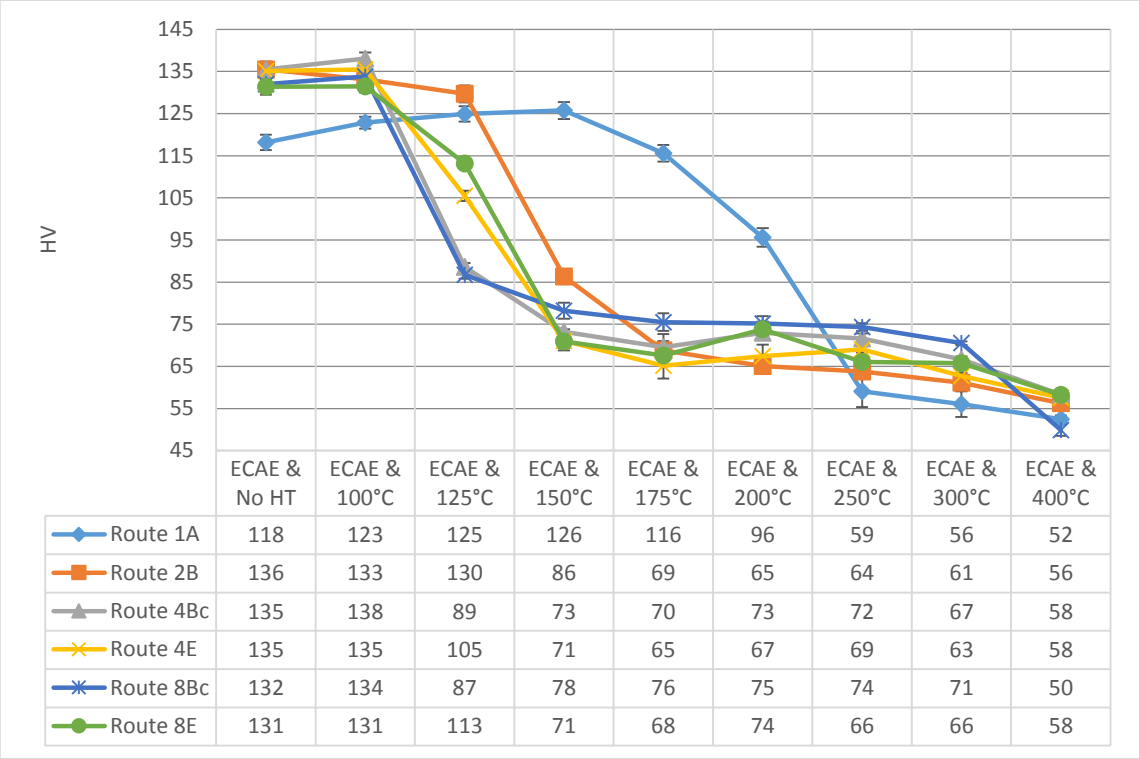


| | ECAE & No HT | ECAE & 100°C | ECAE & 125°C | ECAE & 150°C | ECAE & 175°C | ECAE & 200°C | ECAE & 250°C | ECAE & 300°C | ECAE & 400°C |
|---|---|---|---|---|---|---|---|---|---|
| Route 1A | 118 | 123 | 125 | 126 | 116 | 96 | 59 | 56 | 52 |
| Route 2B | 136 | 133 | 130 | 86 | 69 | 65 | 64 | 61 | 56 |
| Route 4Bc | 135 | 138 | 89 | 73 | 70 | 73 | 72 | 67 | 58 |
| Route 4E | 135 | 135 | 105 | 71 | 65 | 67 | 69 | 63 | 58 |
| Route 8Bc | 132 | 134 | 87 | 78 | 76 | 75 | 74 | 71 | 50 |
| Route 8E | 131 | 131 | 113 | 71 | 68 | 74 | 66 | 66 | 58 |

Figure 14. The hardness of copper C101 after ECAE and one-hour heat treatment at different temperatures.

#### 4.1.1.3. Different Times of Heat Treatment

The samples processed by ECAE routes 1A and 4Bc were selected for the long-term heat treatment. The times of the heat treatment were 1 hr., 3 hr., 12 hr., and 48 hr. The hardness results are shown in Fig.15 and Fig.16, which separately represented the route 1A and route 4Bc samples.

For the samples produced by route 1A, the increasing time decreased the hardness. However, when the temperature of heat treatment was 100 ºC, time had little influence on the hardness. The hardness remained constant with time at 100 ºC. On the other hand, for

the samples heat-treated at 150 ºC and 200 ºC, the hardness kept dropping as time increased; however, the amount of change was relatively small.

On the other hand, for the samples processed by route 4Bc and heat treated at 100 ºC, the hardness significantly decreased after long-term heat treatment. The longer time of heat treatment, the higher degree of decrease for hardness. Moreover, for the samples heat-treated at 150 ºC and 200 ºC, time had no effect on the hardness beyond the first hour. The results show some fluctuation in hardness after different times of heat treatment, but the change of the amount is not obvious.

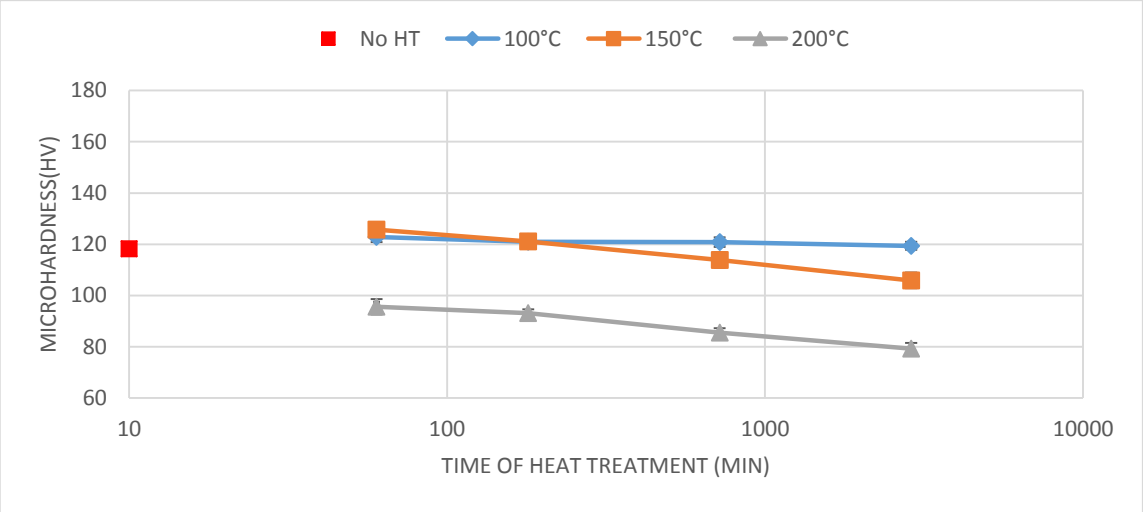


Figure 15. The hardness of copper C101 after route 1A ECAE and long-term heat treatment.

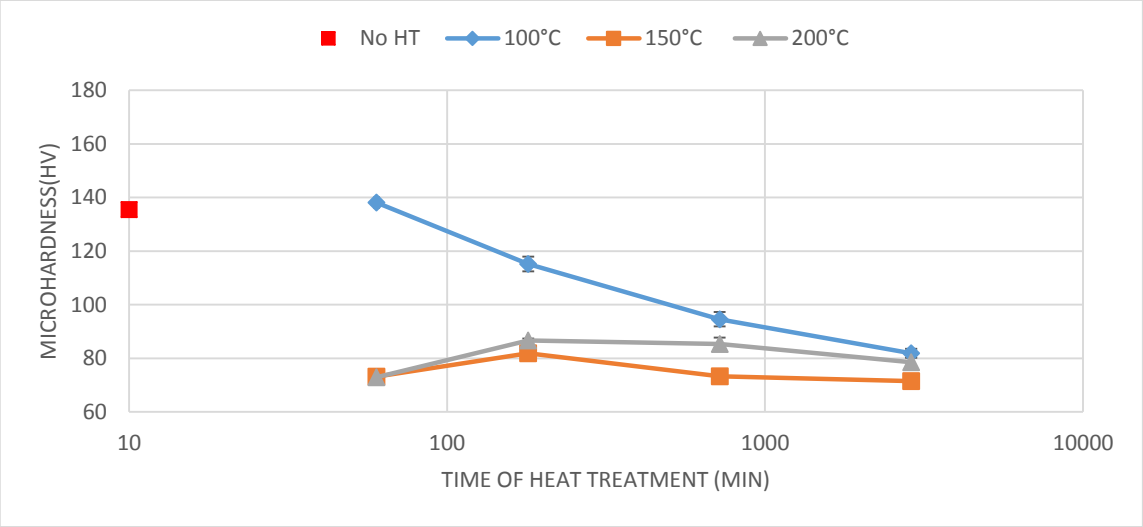

Figure 16. The hardness of copper C101 after route 4Bc ECAE and long term heat treatment.

### 4.1.2. Commercially Pure Copper (C110)

#### 4.1.2.1. After Equal Channel Angular Extrusion (ECAE)

The results of microhardness measurements on copper C110 before and after ECAE without subsequent heat treatment are shown in Fig.17. Before the ECAE process, the hardness decreased after annealing, due to the elimination of dislocations. After ECAE, the hardness increased significantly, because of the increase in dislocation density.

The highest hardness occurred after the second pass of ECAE; it showed ~38% increase compared to the as-received material. After this point, the hardness tends to saturate; the routes and the passes of ECAE show no significant effect beyond two ECAE passes.

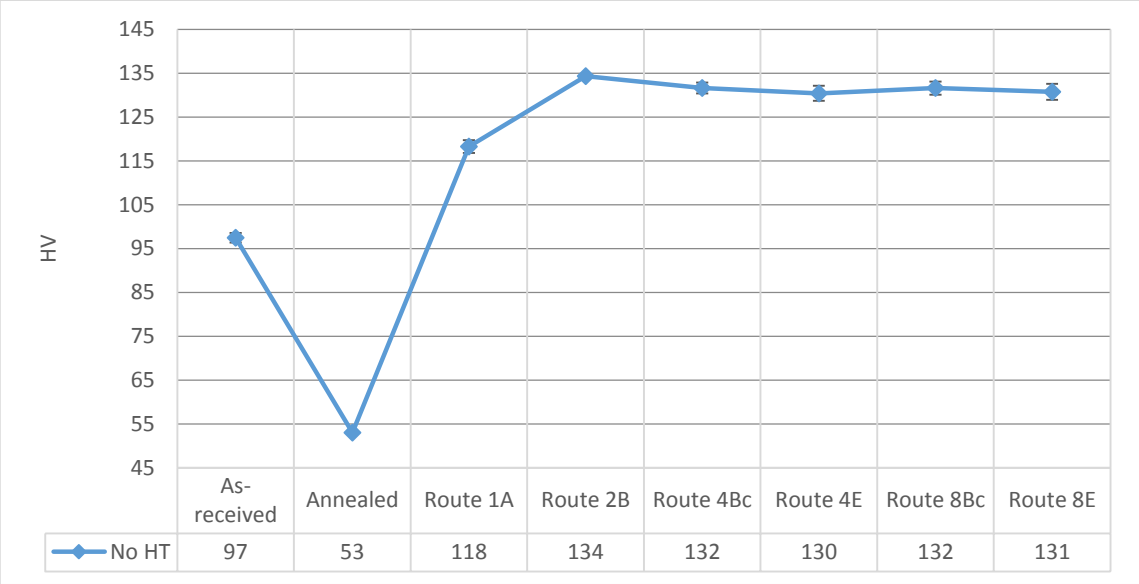


Figure 17. The results of copper C110 before and after ECAE without subsequent heat treatment.

#### 4.1.2.2. Different Temperatures of Heat Treatment

The results of microhardness for copper C110 after ECAE and a one-hour heat treatment at different temperatures are shown in Fig.18. For all of the samples, after the heat treatment at 100 ºC, the hardness is similar to the samples without heat treatment. When the heat-treatment temperature is above 200 ºC, the hardness decreases slightly as temperature increases, and the results were similar for all samples.

However, after the heat treatment at 125 ºC, the hardness of the samples processed by route Bc start to decrease, but the hardness of other samples remains constant. After the heat treatment at 150 ºC, the hardness decreases significantly for all samples except the one processed by one pass of ECAE. This result shows that the samples processed by route Bc start to recrystallize during 100 ºC and 150 ºC. On the other hand, for the samples

processed by route 2B, 4E and 8E, the recrystallization starts at 125 ºC. Moreover, when the temperature of the heat treatment is above 175 ºC, the hardness of all samples becomes similar except the sample processed by route 1A.

For the sample processed by route 1A, when the temperature of heat treatment is 175 ºC, the hardness starts to drop dramatically. For this case, recrystallization occurs in the range 175 ºC and 250 ºC.

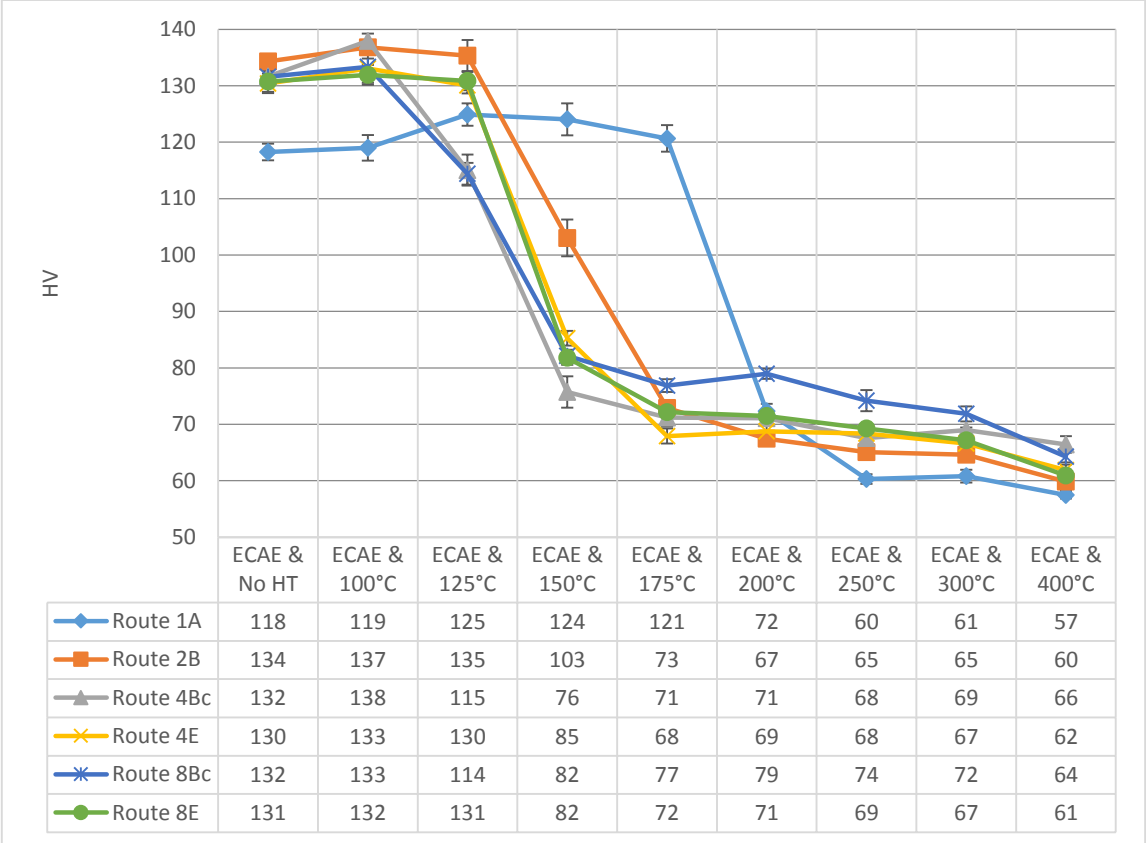


| | ECAE & No HT | ECAE & 100°C | ECAE & 125°C | ECAE & 150°C | ECAE & 175°C | ECAE & 200°C | ECAE & 250°C | ECAE & 300°C | ECAE & 400°C |
|---|---|---|---|---|---|---|---|---|---|
| Route 1A | 118 | 119 | 125 | 124 | 121 | 72 | 60 | 61 | 57 |
| Route 2B | 134 | 137 | 135 | 103 | 73 | 67 | 65 | 65 | 60 |
| Route 4Bc | 132 | 138 | 115 | 76 | 71 | 71 | 68 | 69 | 66 |
| Route 4E | 130 | 133 | 130 | 85 | 68 | 69 | 68 | 67 | 62 |
| Route 8Bc | 132 | 133 | 114 | 82 | 77 | 79 | 74 | 72 | 64 |
| Route 8E | 131 | 132 | 131 | 82 | 72 | 71 | 69 | 67 | 61 |

Figure 18. The microhardness of copper C110 after ECAE and heat treatment at different temperatures for one hour.

#### 4.1.2.3. Different Times of Heat Treatment

The samples processed by route 1A and route 4Bc were selected for the long-term heat treatment to determine the effect of time. The hardness variations are shown in Fig.19 and Fig.20.

For the samples processed by route 1A, time had no effect on the hardness when the temperature of heat treatment is 100 ºC. This result is consistent with the C101. On the other hand, for the sample heat-treated at 150 ºC, the hardness decreased slightly after heat treatment; a longer time decreases the hardness more, but the change is small. For the sample heat treated at 200 ºC, the results are a little unstable, but the variation is small between the different times of heat treatment.

For the samples processed by route 4Bc (see Fig.20), the heat treatment at 100 ºC was able to weaken the hardness, and the hardness decreased as time increased. The hardness did not change after the first one-hour heat treatment, but after 48 hours, the hardness decreased ~29% compared to the sample without heat treatment. This result is similar to that of C101. However, the samples heat-treated at 150 ºC and 200 ºC show a very different tendency. For the samples heat-treated more than one hour, the hardness decreased ~42% (at 150 ºC) and ~46% (at 200 ºC) compared to the sample without heat treatment. However, when the time of heat treatment became longer, the hardness kept constant.

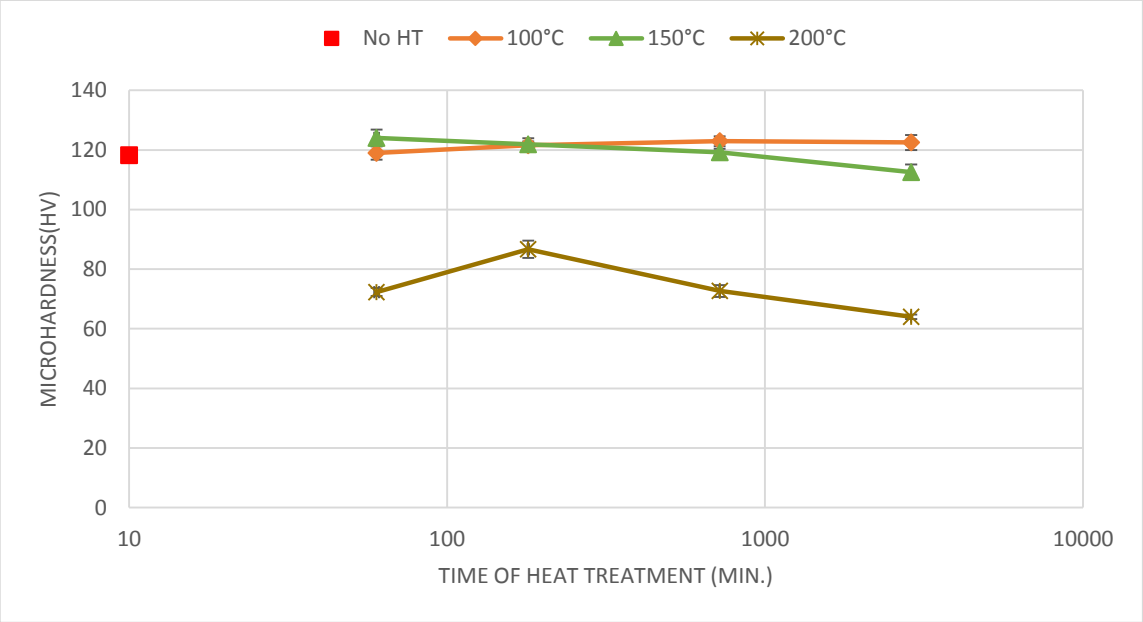


Figure 19. The hardness of copper C110 after long-term heat treatment for 1A ECAE processing.

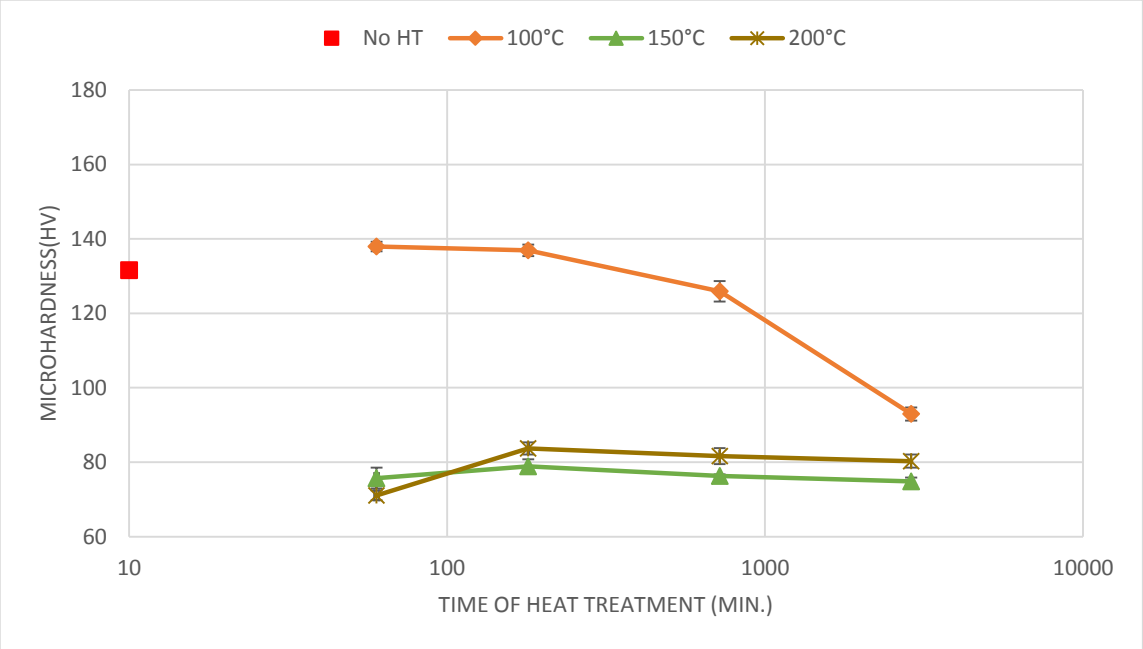


Figure 20. The hardness of copper C110 after long-term heat treatment for 4Bc ECAE processing.

### 4.1.3. Chromium Copper Alloy (C182)

#### 4.1.3.1. After Equal Channel Angular Extrusion (ECAE)

The microhardness measurements of copper C182 before and after ECAE without subsequent heat treatment are shown in Fig.21. The as-received C182 possesses a much higher microhardness than C101 and C110 because the chromium significantly enhances the hardness. However, after solution heat treatment and quenching, the hardness of C182 decreases ~60%, due to dissolved Cr. After ECAE, the hardness increases significantly because of the increase in dislocation density.

After ECAE, the sample processed by route 8Bc shows the highest hardness, but the hardness is still lower than the as-received material. For the samples processed by the same passes but different routes, route Bc produced higher hardness than route E, but the difference is small.

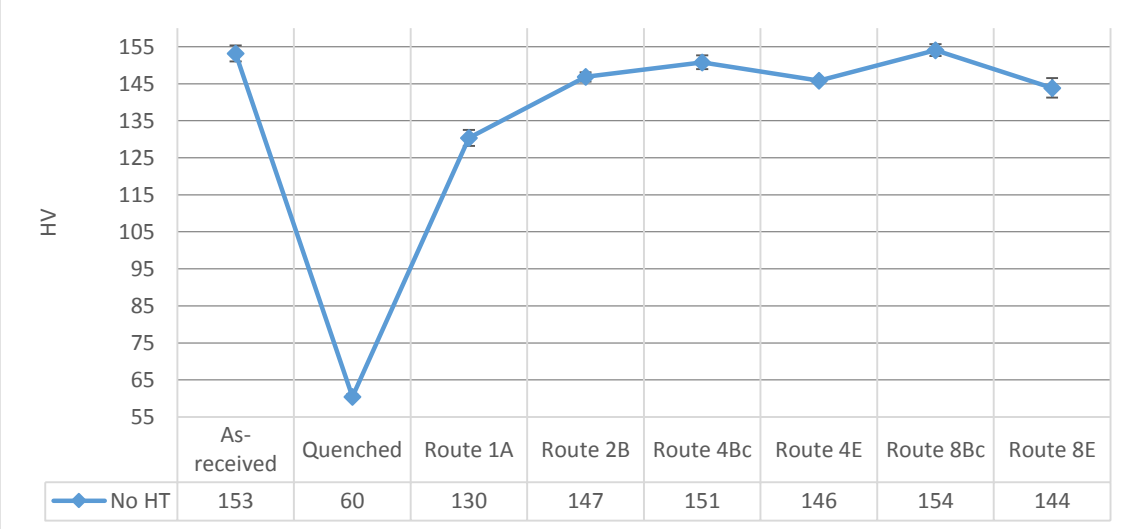


Figure 21. The microhardness of copper C182 before and after ECAE without subsequent heat treatment.

#### 4.1.3.2. Different Temperatures of Heat Treatment

Fig.22, Fig.23, and Fig.24 show the microhardness of copper C182 after ECAE and heat treatment at different temperatures. The times of the heat treatment are 10 min., 10+20 min., and 10+20+60 min., respectively.

For the samples heat-treated at 350 ºC and 400 ºC for 10 min., the hardness decreases slightly after heat treatment. The highest hardness presented when the temperature of heat treatment was 450 ºC for the samples processed by route 1A, 2B, 4E and 8E. This result might indicate effective age hardening occurs at 450 ºC. For the samples produced by route 4Bc and 8Bc, the hardness decreased after heat treatment at any temperature. Moreover, the hardness of the samples heat-treated at 500 ºC were lower than the samples heat-treated at 450 ºC, except the sample processed by route 1A.

For the 10+20 min. heat treatment, the hardness of all samples decreased at 350 ºC, but increased at 400 ºC, which also correlative the highest hardness for the samples processed by route 2B, 4E and 8E. On the other hand, the highest hardness occurred at 450 ºC for the route 1A sample. Differently, the hardness decreased after heat treatment at any temperature for the route 4Bc and route 8Bc samples.

When the time of heat treatment increased to 60 minutes or more, the highest hardness presented when the temperature was 400 ºC. However, for the samples produced by route 4Bc and 8Bc, the hardness decreased after the heat treatment at any temperature.

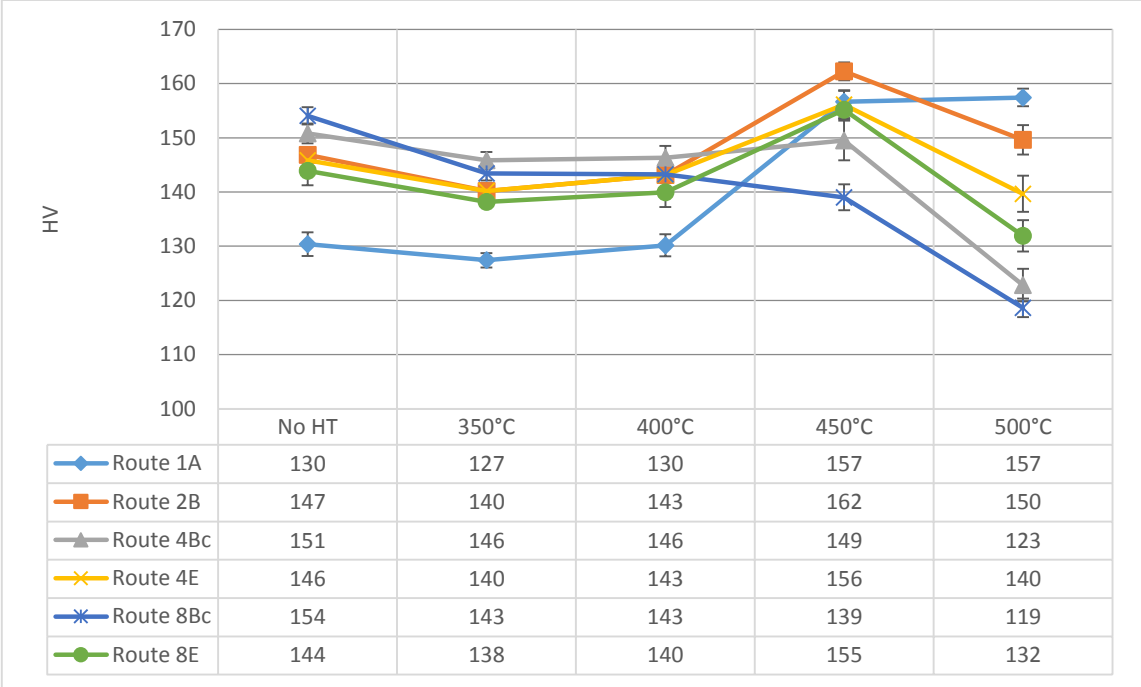


| | No HT | 350°C | 400°C | 450°C | 500°C |
|---|---|---|---|---|---|
| Route 1A | 130 | 127 | 130 | 157 | 157 |
| Route 2B | 147 | 140 | 143 | 162 | 150 |
| Route 4Bc | 151 | 146 | 146 | 149 | 123 |
| Route 4E | 146 | 140 | 143 | 156 | 140 |
| Route 8Bc | 154 | 143 | 143 | 139 | 119 |
| Route 8E | 144 | 138 | 140 | 155 | 132 |

Figure 22. Microhardness of copper C182 after ECAE and a 10-minute heat treatment at different temperatures.

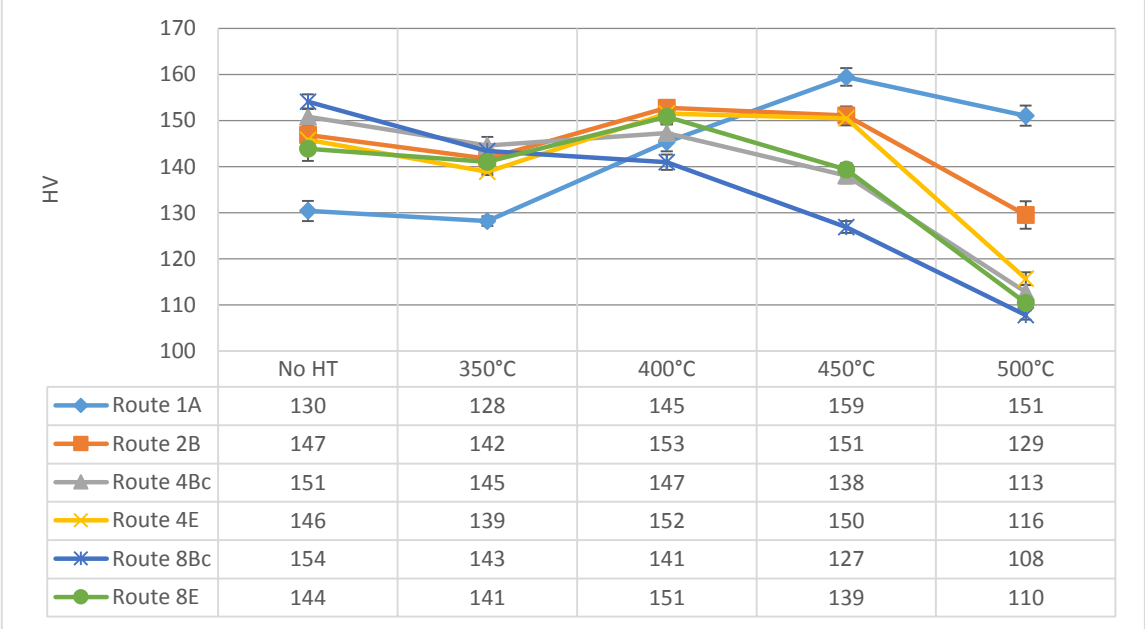


| | No HT | 350°C | 400°C | 450°C | 500°C |
|---|---|---|---|---|---|
| Route 1A | 130 | 128 | 145 | 159 | 151 |
| Route 2B | 147 | 142 | 153 | 151 | 129 |
| Route 4Bc | 151 | 145 | 147 | 138 | 113 |
| Route 4E | 146 | 139 | 152 | 150 | 116 |
| Route 8Bc | 154 | 143 | 141 | 127 | 108 |
| Route 8E | 144 | 141 | 151 | 139 | 110 |

Figure 23. The microhardness of copper C182 after ECAE and heat treated at different temperatures for 10+20 minute.

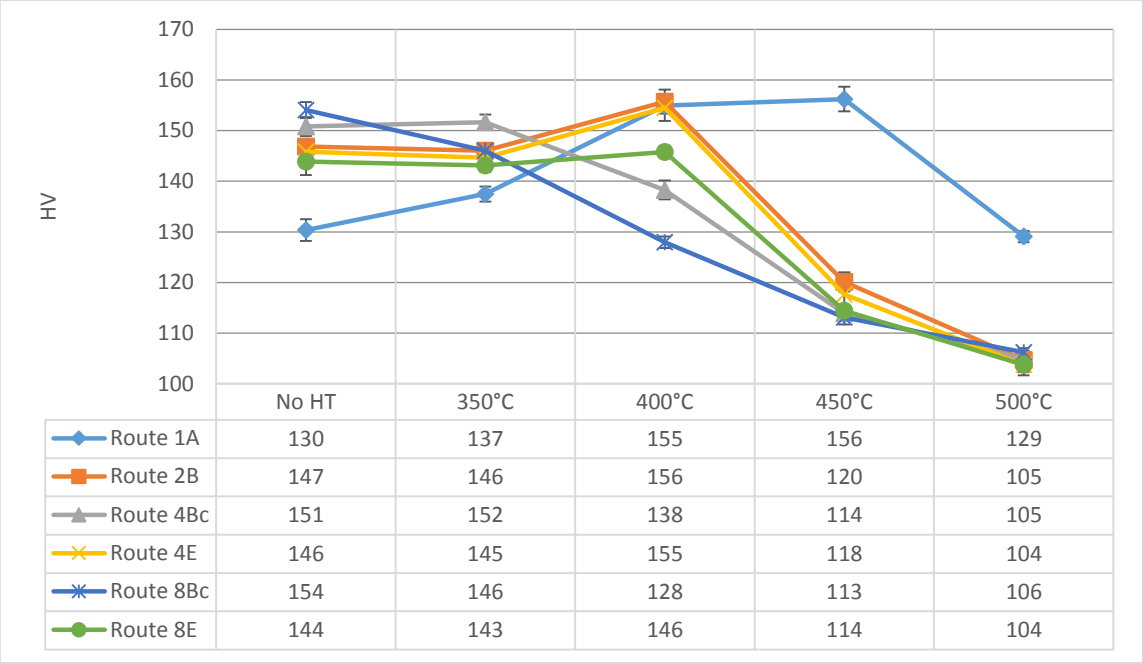


| | No HT | 350°C | 400°C | 450°C | 500°C |
|---|---|---|---|---|---|
| Route 1A | 130 | 137 | 155 | 156 | 129 |
| Route 2B | 147 | 146 | 156 | 120 | 105 |
| Route 4Bc | 151 | 152 | 138 | 114 | 105 |
| Route 4E | 146 | 145 | 155 | 118 | 104 |
| Route 8Bc | 154 | 146 | 128 | 113 | 106 |
| Route 8E | 144 | 143 | 146 | 114 | 104 |

Figure 24. The microhardness of copper C182 after ECAE and heat treated at different temperatures for 10+20+60 minute.

### 4.1.3.3. Different Times of Heat Treatment

The microhardnesses of copper C182 after ECAE and heat treatment at different times are shown in Fig.25, Fig.26, Fig.27, and Fig.28; the temperatures of the heat treatments were 350 ºC, 400 ºC, 450 ºC, and 500 ºC, respectively.

As shown in Fig.4.13, for the samples heat-treated at 350 ºC, the hardness decreased slightly after the first 10 minutes. However, after that, the hardness increased as the time increased. After heat treatment for 90 min., the level of the hardness became similar to the sample without heat treatment. At this temperature, the time tendency shows no difference for all samples processed by different passes and routes.

For the samples heat-treated at 400 ºC, the hardness of all samples decreased after heat treatment for 10 min. However, a longer heat treatment increased the hardness except the samples processed by route Bc. For the samples processed through route 4Bc and 8Bc, the hardness decreased continuously as time increased. Furthermore, for the sample of route 8E, the highest hardness presented after heat treatment for 30 min, but it started to decrease when the time was longer. On the other hand, for the samples processed by routes 1A, 2B and 4E, the hardness increased as the time increased.

The hardness of copper C182 heat-treated at 450 ºC is shown in Fig.4.15. After the heat treatment for 10 min, the samples produced by route 1A, 2B, 4E and 8E possessed a higher hardness than the as-received material. However, when the time of heat treatment started to increase, the hardness dropped significantly except the route 1A sample. The hardness of the route 1A sample remained constant when the time increased. For the samples processed by route 4Bc and 8Bc, the hardness decreased after heat treatment, and it decreased more when the heat treatment was longer.

The hardnesses of the samples heat-treated at 500 ºC after ECAE are shown in Fig.4.16. For the samples processed by more than four passes of ECAE, the hardness decreased after heat treatment as time increased. However, the hardness of the samples processed by route 1A and 2B increased slightly after the 10-minute heat treatment, but the hardness started to decrease after a longer time.

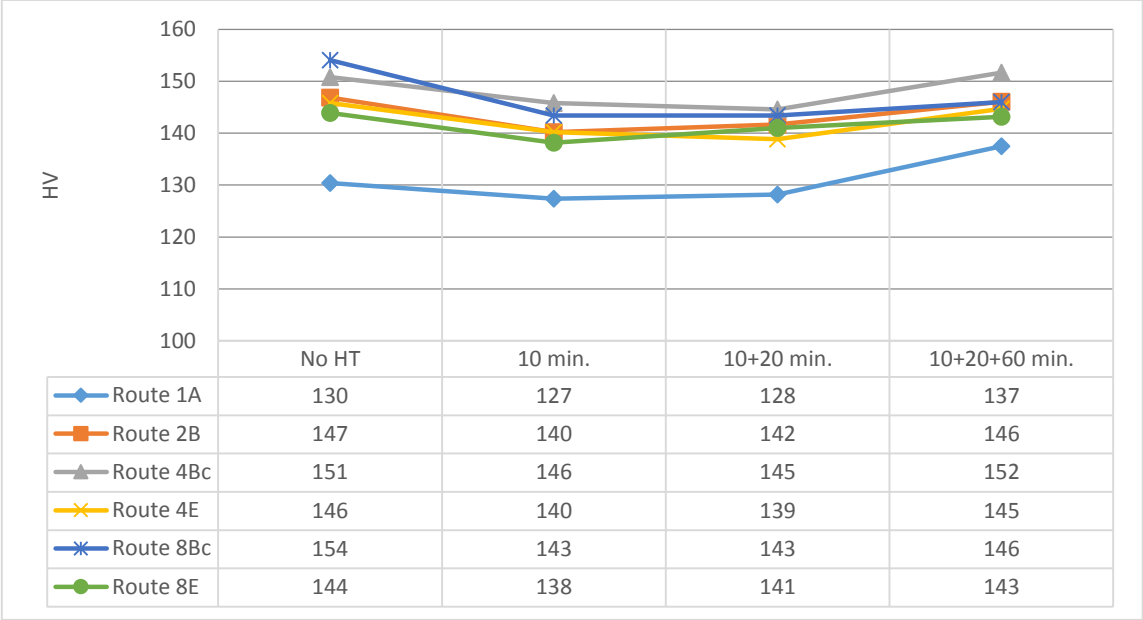


| | No HT | 10 min. | 10+20 min. | 10+20+60 min. |
|---|---|---|---|---|
| Route 1A | 130 | 127 | 128 | 137 |
| Route 2B | 147 | 140 | 142 | 146 |
| Route 4Bc | 151 | 146 | 145 | 152 |
| Route 4E | 146 | 140 | 139 | 145 |
| Route 8Bc | 154 | 143 | 143 | 146 |
| Route 8E | 144 | 138 | 141 | 143 |

Figure 25. The microhardness for copper C182 after heat treatment at 350 ºC for different times.

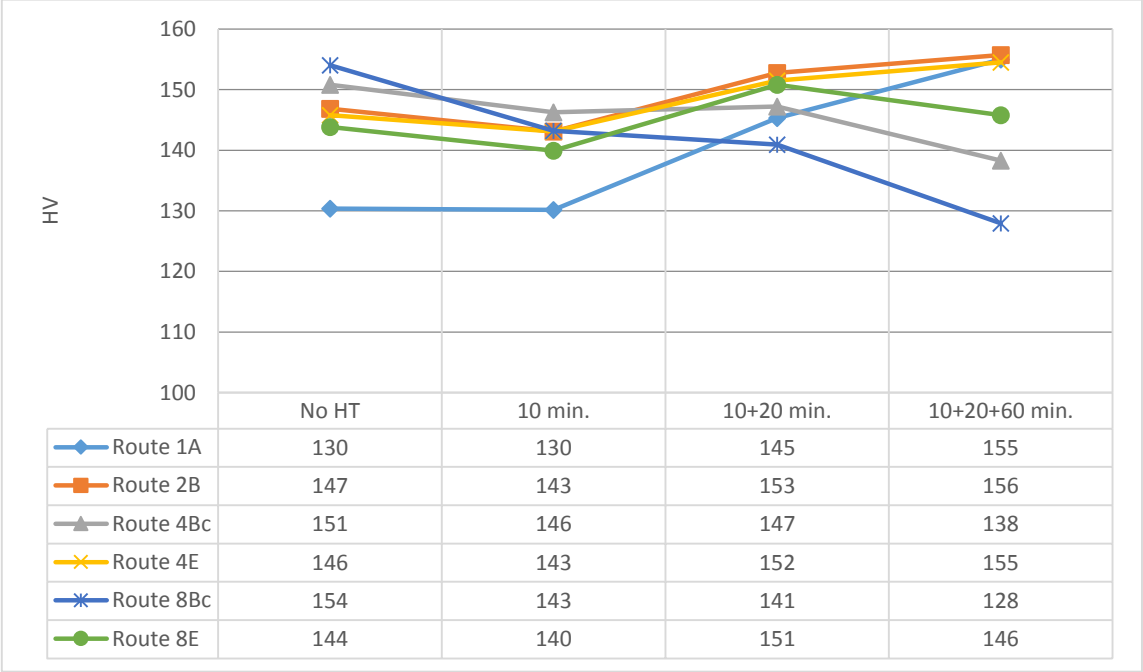


| | No HT | 10 min. | 10+20 min. | 10+20+60 min. |
|---|---|---|---|---|
| Route 1A | 130 | 130 | 145 | 155 |
| Route 2B | 147 | 143 | 153 | 156 |
| Route 4Bc | 151 | 146 | 147 | 138 |
| Route 4E | 146 | 143 | 152 | 155 |
| Route 8Bc | 154 | 143 | 141 | 128 |
| Route 8E | 144 | 140 | 151 | 146 |

Figure 26. The microhardness for copper C182 after heat treatment at 400 ºC for different times.

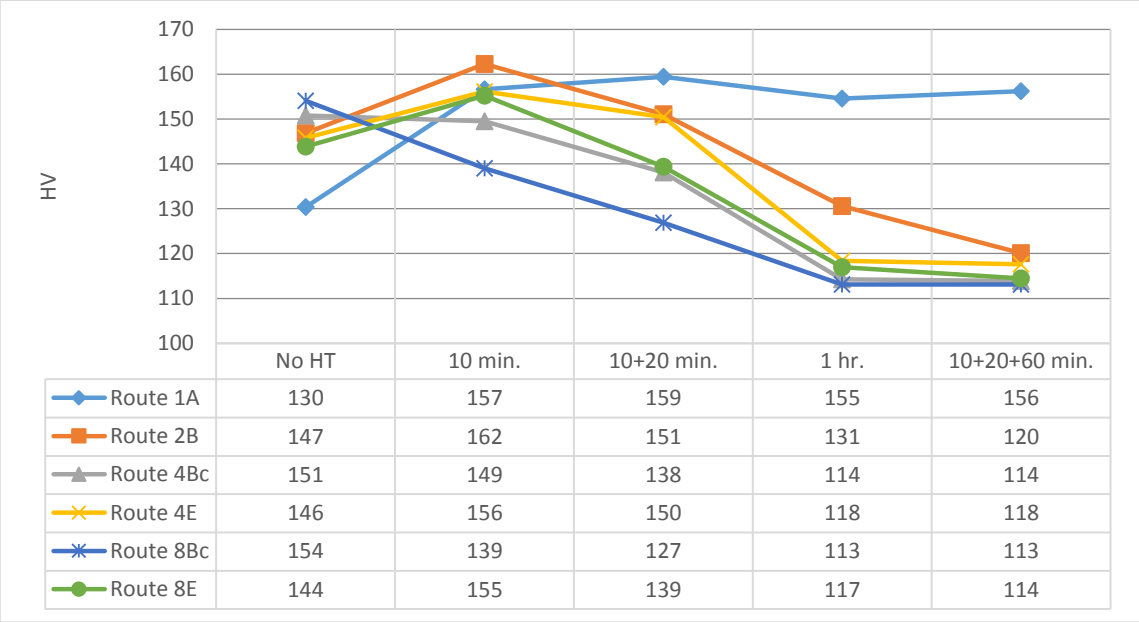


| | No HT | 10 min. | 10+20 min. | 1 hr. | 10+20+60 min. |
|---|---|---|---|---|---|
| Route 1A | 130 | 157 | 159 | 155 | 156 |
| Route 2B | 147 | 162 | 151 | 131 | 120 |
| Route 4Bc | 151 | 149 | 138 | 114 | 114 |
| Route 4E | 146 | 156 | 150 | 118 | 118 |
| Route 8Bc | 154 | 139 | 127 | 113 | 113 |
| Route 8E | 144 | 155 | 139 | 117 | 114 |

Figure 27. The microhardness for copper C182 after heat treatment at 450 ºC for different times.

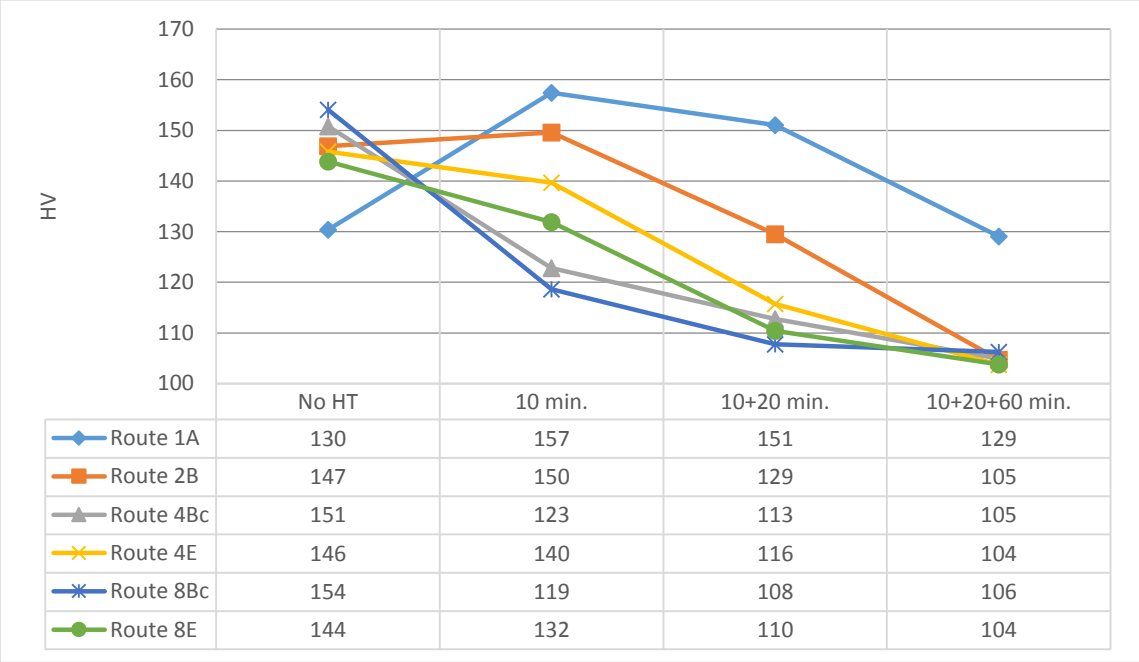


| | No HT | 10 min. | 10+20 min. | 10+20+60 min. |
|---|---|---|---|---|
| Route 1A | 130 | 157 | 151 | 129 |
| Route 2B | 147 | 150 | 129 | 105 |
| Route 4Bc | 151 | 123 | 113 | 105 |
| Route 4E | 146 | 140 | 116 | 104 |
| Route 8Bc | 154 | 119 | 108 | 106 |
| Route 8E | 144 | 132 | 110 | 104 |

Figure 28. The microhardness for copper C182 after heat treatment at 500 ºC for different times.

Furthermore, the samples processed by route 1A and route 4Bc, and heat-treated at 350 ºC and 450 ºC were selected for the long-term heat treatment. The hardness results are shown in Fig.29.

For the samples processed by route 1A, when the temperature of the heat treatment was at 350 ºC, the hardness increased as time increased. However, after the 48-hour heat treatment, the hardness was still lower than the as-received material. This indicates that the quench before ECAE had more influence than the plastic deformation and heat treatment at 350 ºC. On the other hand, the highest hardness was obtained at 450 ºC after 30 minutes' heat treatment. This highest hardness was slightly higher than the as-received material. It might be explained by the precipitation that occurred at this temperature. However, when the time of heat treatment became longer, the hardness decreased as time increased, probably due to over-aging of precipitates.

On the other hand, the hardness of route 4Bc samples showed a different time response. When the heat treatment temperature was 350 ºC, the hardness remained constant until the 3-hour heat treatment. When the time of heat treatment was over three hours, the hardness dropped as time increased, and the lowest hardness presented after the 48-hour heat treatment.

Therefore, long-term heat treatment decreases the hardness of copper C182. However, when the degree of strain is small in the sample and the temperature of the heat treatment is lower than the recrystallization temperature, a longer time could slightly increase the hardness.

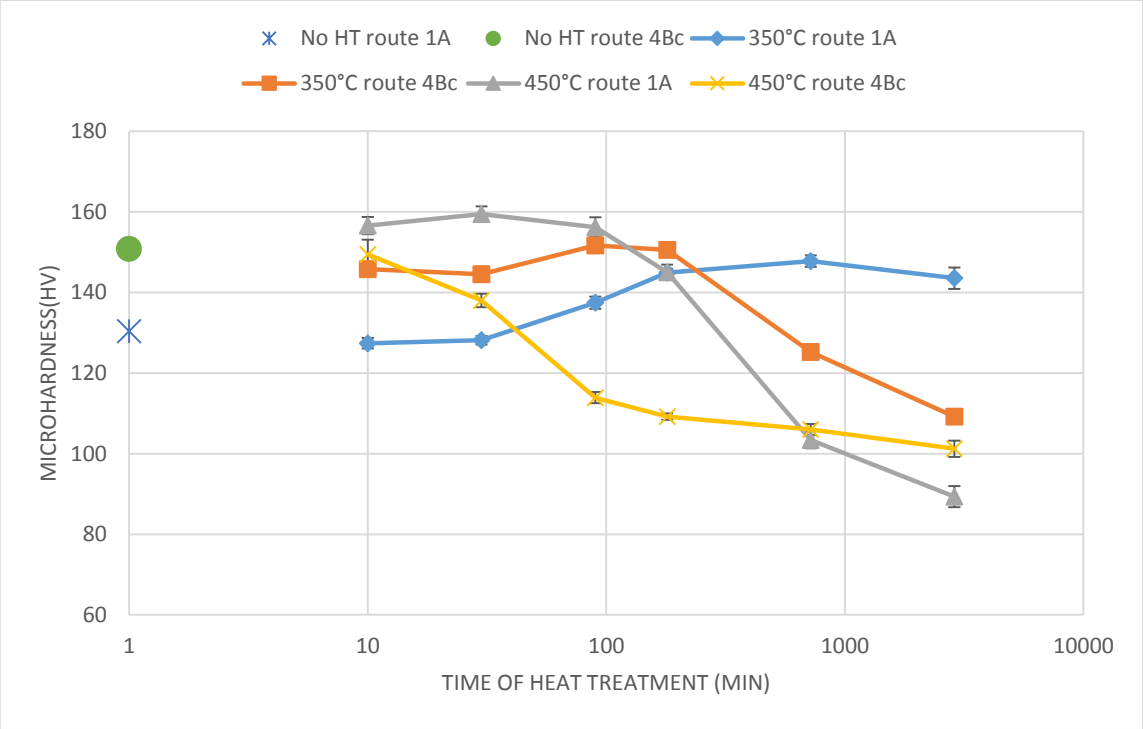


Figure 29. The hardness of copper C182 after ECAE and long-term heat treatment.

## 4.2.Conductivity

### 4.2.1. Oxygen-Free High Conductivity (OFHC) Copper (C101)

#### 4.2.1.1. After Equal Channel Angular Extrusion (ECAE)

The conductivity of copper C101 after ECAE without heat treatment is shown in Fig.30. Before ECAE, the annealed sample had a higher conductivity compared to the as-received material because the dislocation density was lowered by the annealing. After ECAE, a higher density of dislocations formed in the microstructure and caused the conductivity to decrease. Furthermore, the higher degree of plastic strain caused by ECAE, the larger decrease the conductivity. After the fourth pass of ECAE, the conductivity tends

to saturate. However, different strain paths affect the conductivity differently. For the samples processed by route Bc, the material possessed a lower conductivity than the samples processed by route E.

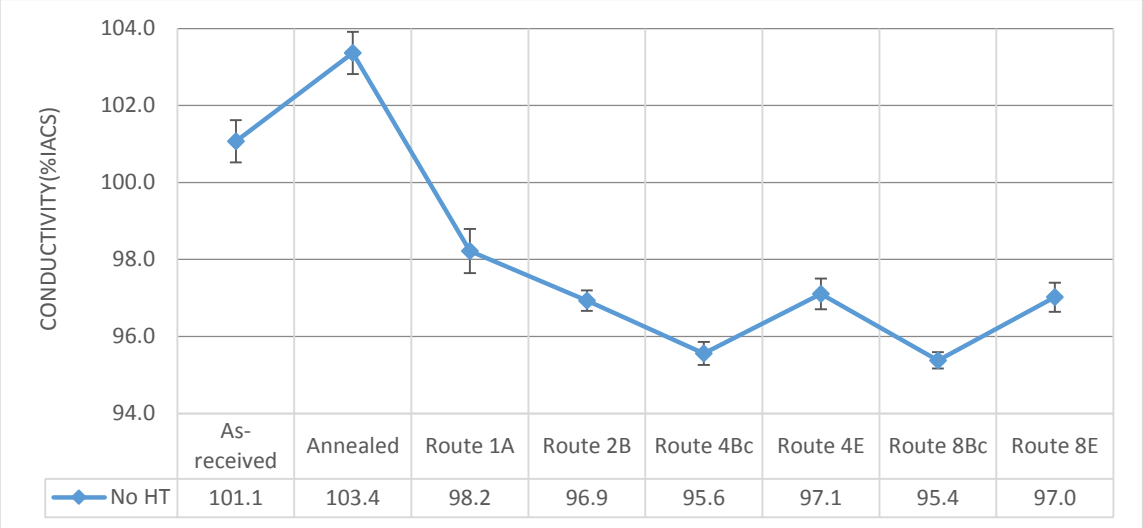


Figure 30. The conductivity of copper C101 before and after ECAE without subsequent heat treatment.

### 4.2.1.2. Different Temperatures of Heat Treatment

The conductivity of copper C101 processed by ECAE and heat-treated at different temperatures is shown in Fig.31. The trends of conductivity for all samples are similar. The conductivity increased as temperature increased. The highest conductivity can be found at 400 ºC.

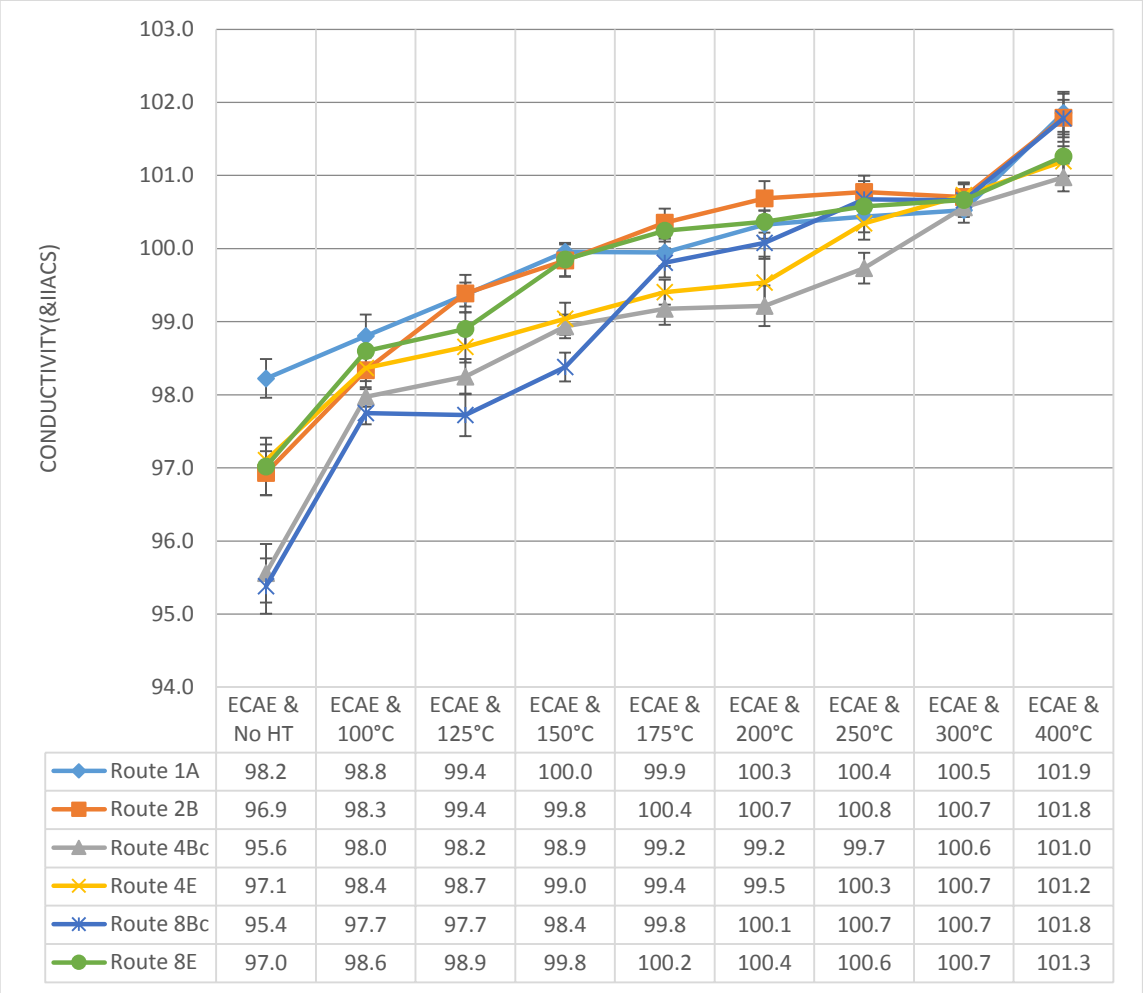


| | ECAE & No HT | ECAE & 100°C | ECAE & 125°C | ECAE & 150°C | ECAE & 175°C | ECAE & 200°C | ECAE & 250°C | ECAE & 300°C | ECAE & 400°C |
|---|---|---|---|---|---|---|---|---|---|
| Route 1A | 98.2 | 98.8 | 99.4 | 100.0 | 99.9 | 100.3 | 100.4 | 100.5 | 101.9 |
| Route 2B | 96.9 | 98.3 | 99.4 | 99.8 | 100.4 | 100.7 | 100.8 | 100.7 | 101.8 |
| Route 4Bc | 95.6 | 98.0 | 98.2 | 98.9 | 99.2 | 99.2 | 99.7 | 100.6 | 101.0 |
| Route 4E | 97.1 | 98.4 | 98.7 | 99.0 | 99.4 | 99.5 | 100.3 | 100.7 | 101.2 |
| Route 8Bc | 95.4 | 97.7 | 97.7 | 98.4 | 99.8 | 100.1 | 100.7 | 100.7 | 101.8 |
| Route 8E | 97.0 | 98.6 | 98.9 | 99.8 | 100.2 | 100.4 | 100.6 | 100.7 | 101.3 |

Figure 31. The conductivity of copper C101 after ECAE and heat treatment for one hour at different temperatures.

The influence of the routes and passes also can be found in the figure, but the differences are small. For the samples processed by route 1A and 2B, they possessed higher conductivity than other samples after the heat treatment at different temperatures. Moreover, when the heat treatment temperature is 300 ºC, all of the samples possessed similar conductivity.

#### 4.2.1.3. Different Times of Heat Treatment

The samples processed by route 1A and 4Bc were selected for the long-term heat treatment at 100 ºC, 150 ºC, and 200 ºC. The conductivity results are shown in Fig.32 and Fig.33.

When the heat-treatment temperature was 100 ºC, the conductivity of route 1A sample increased as time increased, and leveled off after the 12-hour heat treatment. When the temperature was 150 ºC, the conductivity increased slightly as time increased. However, the amount of change was minuscule. On the other hand, the conductivity increased obviously at 200 ºC, but it became constant after the three-hour heat treatment.

For the samples processed by route 4Bc, the conductivity increased as a function of time. When the temperature was higher, the conductivity increased faster. However, after the 48-hour heat treatment, the conductivity of samples heat-treated at different temperatures became similar.

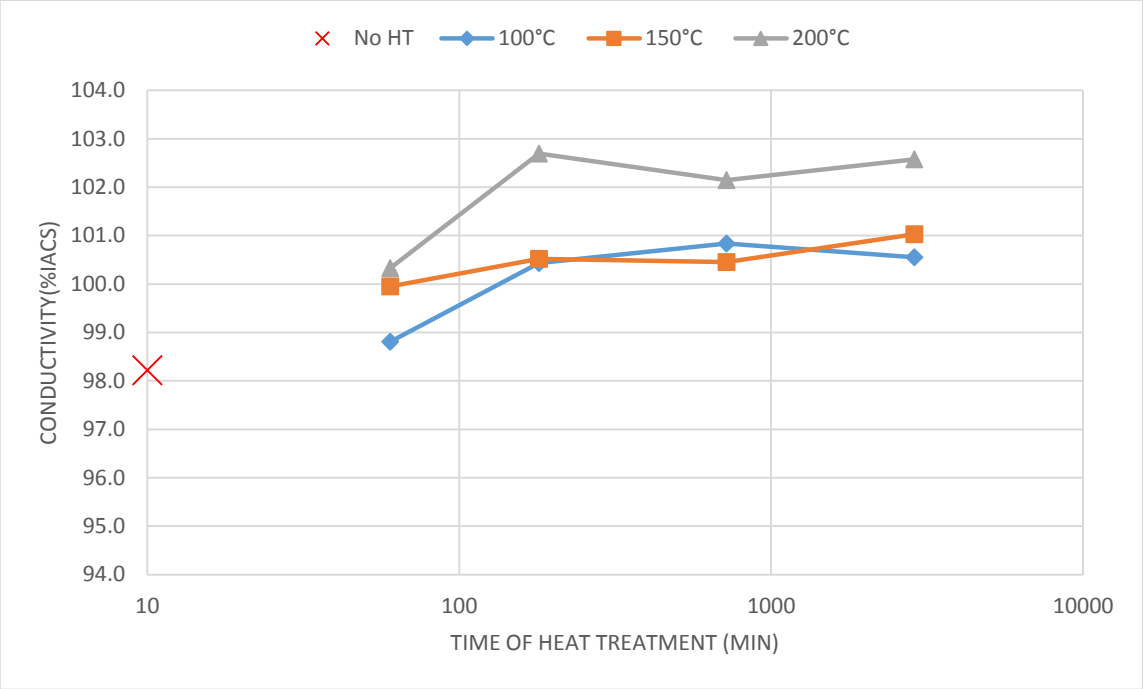


Figure 32. The conductivity of copper C101 after long-term heat treatment (route 1A).

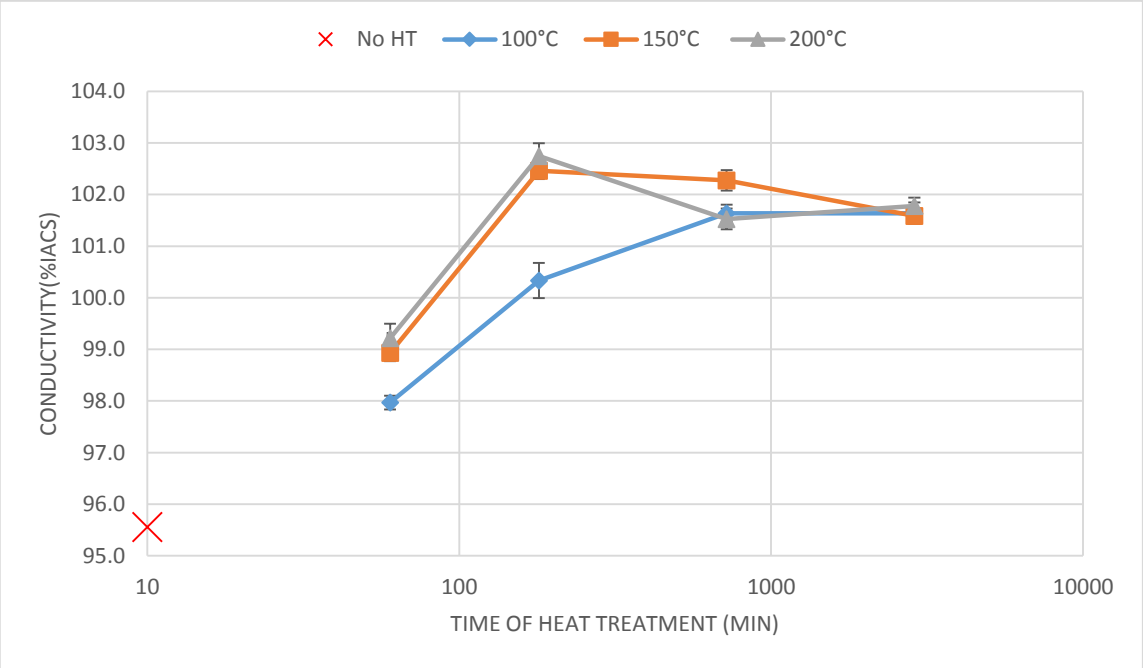


Figure 33. The conductivity of copper C101 after long-term heat treatment (route 4Bc).

### 4.2.2. Commercially Pure Copper (C110)

#### 4.2.2.1. After Equal Channel Angular Extrusion (ECAE)

The conductivity results of copper C110 before and after ECAE without subsequent heat treatment are shown in Fig.34. The conductivity of C110 increased significantly after annealing, due to dislocation elimination. After ECAE, the imposed strain decreased the conductivity, but different passes and routes have little effect. On the other hand, the ECAE process considerably impaired the conductivity of C110 after one pass; more passes of ECAE had little influence. Therefore, the sample that had the highest conductivity was the one annealed without ECAE.

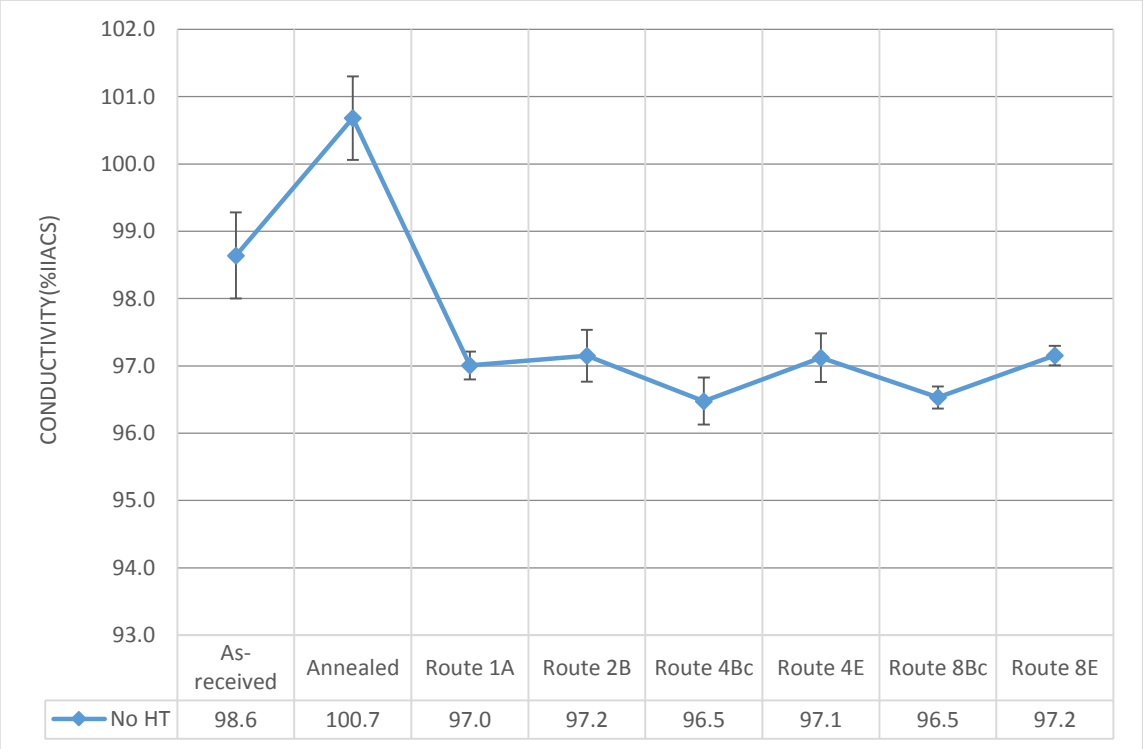


Figure 34. The conductivity of copper C110 before and after ECAE without subsequent heat treatment.

#### 4.2.2.2. Different Temperatures of Heat Treatment

The conductivity of copper C110 after ECAE with a one-hour heat treatment at different temperatures is shown in Fig.35. After the heat treatment for one hour at 100 ºC, the conductivity increased obviously. However, the conductivity of the samples decreased after heat treatment at 125 ºC, and it showed an apparent difference. When the temperature of heat treatment was above 125 ºC, the conductivity regularly increased with increasing temperature. The conductivity of the sample heat-treated for one hour at 400 ºC was the highest and similar to the annealed material.

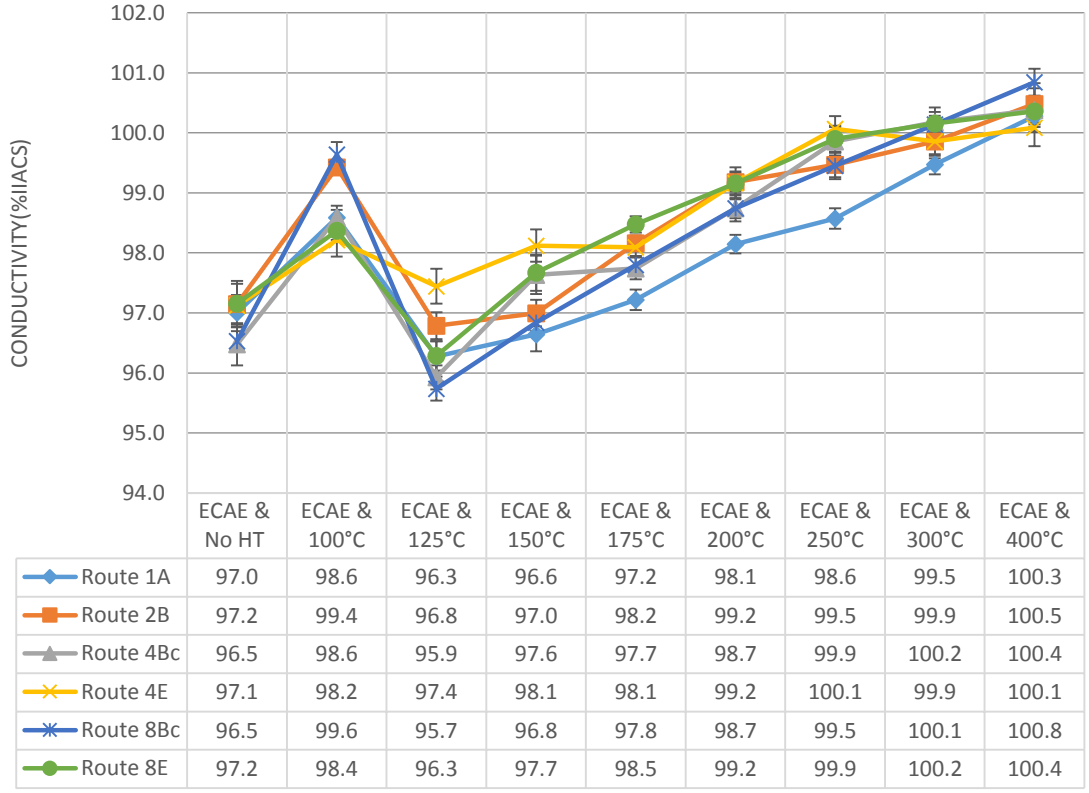


| | ECAE & No HT | ECAE & 100°C | ECAE & 125°C | ECAE & 150°C | ECAE & 175°C | ECAE & 200°C | ECAE & 250°C | ECAE & 300°C | ECAE & 400°C |
|---|---|---|---|---|---|---|---|---|---|
| Route 1A | 97.0 | 98.6 | 96.3 | 96.6 | 97.2 | 98.1 | 98.6 | 99.5 | 100.3 |
| Route 2B | 97.2 | 99.4 | 96.8 | 97.0 | 98.2 | 99.2 | 99.5 | 99.9 | 100.5 |
| Route 4Bc | 96.5 | 98.6 | 95.9 | 97.6 | 97.7 | 98.7 | 99.9 | 100.2 | 100.4 |
| Route 4E | 97.1 | 98.2 | 97.4 | 98.1 | 98.1 | 99.2 | 100.1 | 99.9 | 100.1 |
| Route 8Bc | 96.5 | 99.6 | 95.7 | 96.8 | 97.8 | 98.7 | 99.5 | 100.1 | 100.8 |
| Route 8E | 97.2 | 98.4 | 96.3 | 97.7 | 98.5 | 99.2 | 99.9 | 100.2 | 100.4 |

Figure 35. The conductivity of copper C110 after ECAE and one-hour heat treatment at different temperatures.

#### 4.2.2.3. Different Times of Heat Treatment

The samples processed by route 1A and route 4Bc were selected for the long-term heat treatment; the results of conductivity are shown in Fig.36 and Fig.37. For the samples produced by route 1A, the conductivity increased with time. When the time of the heat treatment was longer, the conductivity became higher. However, after the heat treatment for three hours, the conductivity tends to saturate.

For the samples processed by route 4Bc, the conductivity increased after the heat treatment for three hours at 150 ºC and 200 ºC. When the time was longer than three hours, the conductivity decreased slightly and remained constant. On the other hand, when the heat treatment was at 100 ºC, the conductivity decreased slightly after three hours. Once the time became longer, the conductivity started to increase.

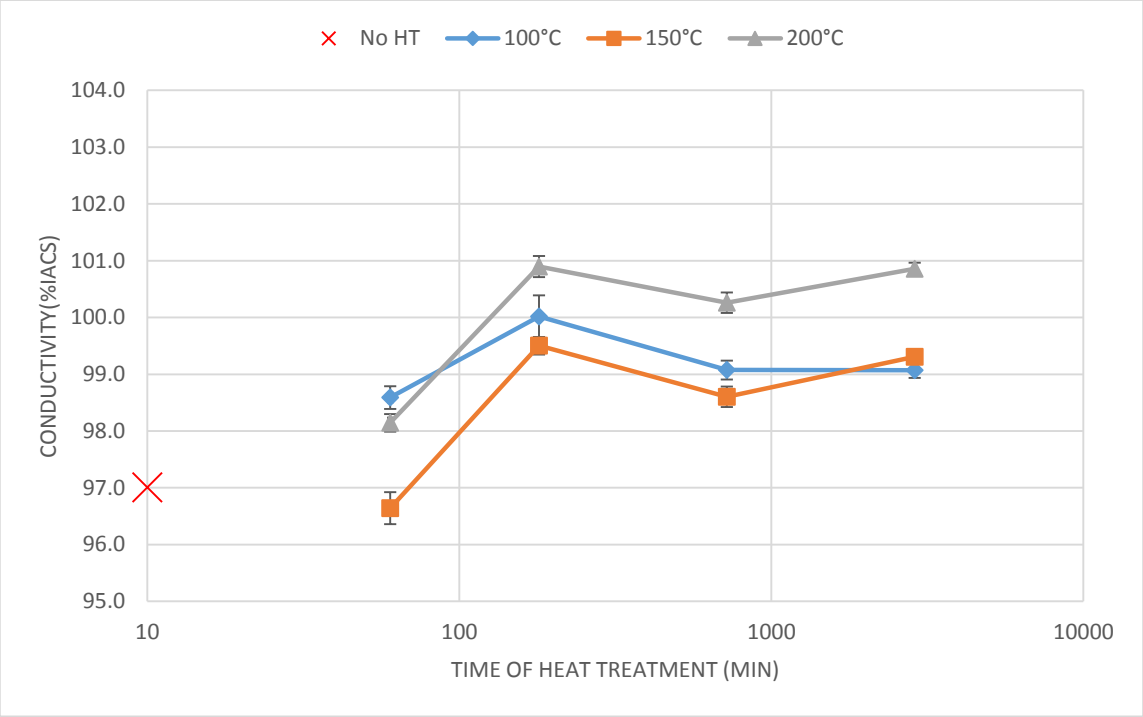


Figure 36. The conductivity of copper C110 after long-term heat treatment (route 1A).

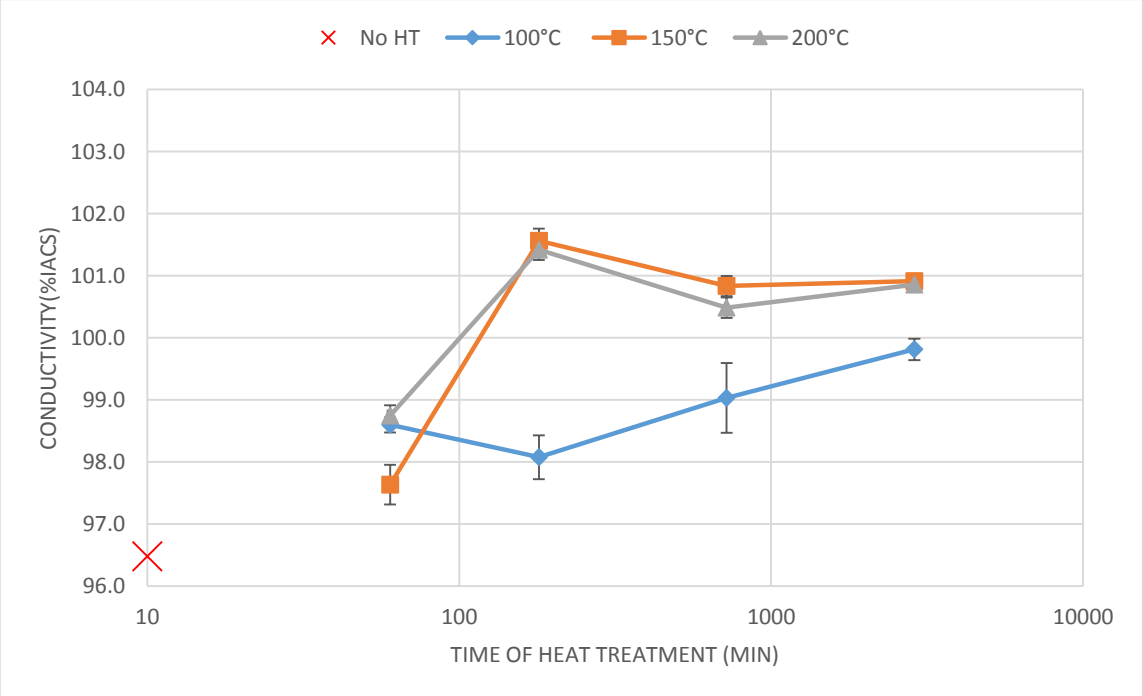


Figure 37. The conductivity of copper C110 after long-term heat treatment (route 4Bc).

### 4.2.3. Chromium Copper Alloy (C182)

#### 4.2.3.1. After Equal Channel Angular Extrusion (ECAE)

The conductivity of copper C182 before and after ECAE without subsequent heat treatment is shown in Fig.38. Before ECAE, solution heat treatment and quenching caused the conductivity to drop dramatically. This result is explained by the creation of solid solution. After ECAE, a higher density of dislocations resides in the microstructure. Therefore, the conductivity dropped again. The lowest conductivity was the sample processed by route 8Bc. Moreover, different passes and routes of ECAE have no marked effect on the conductivity. In other words, the conductivity of C182 tends to saturate after one pass of ECAE; more imparted strain induced no difference on the conductivity.

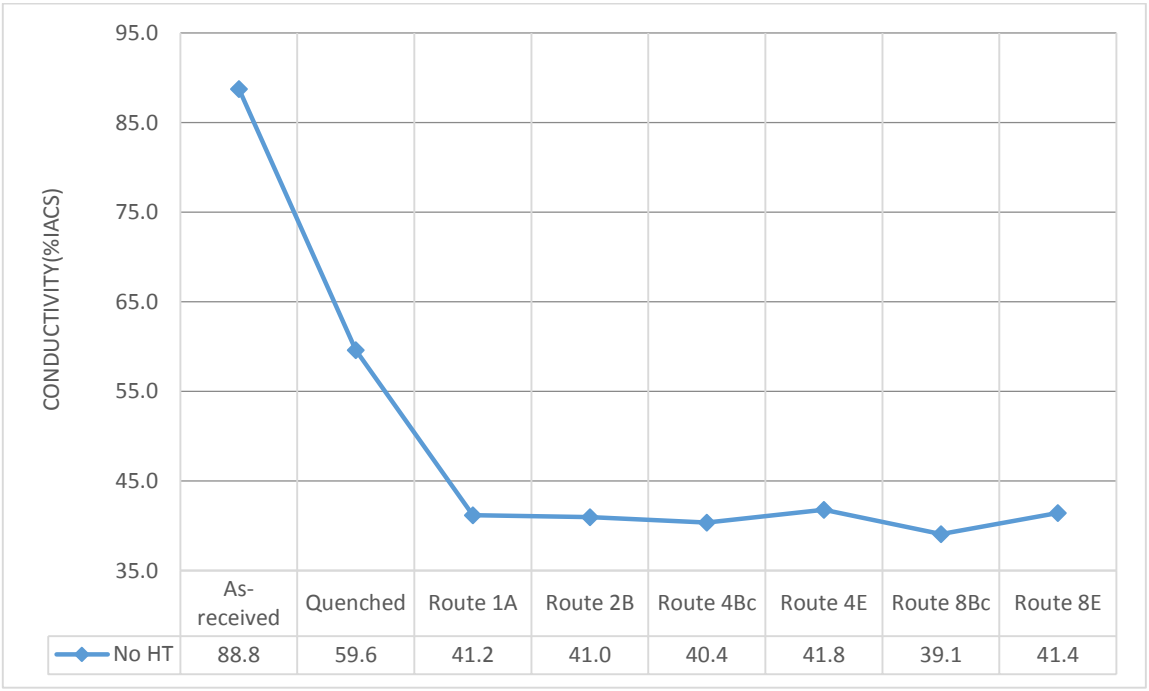


Figure 38. The conductivity of copper C182 before and after ECAE without subsequent heat treatment.

#### 4.2.3.2. Different Temperatures of Heat Treatment

The conductivities of copper C182 samples after different routes of ECAE and heat treatment at different temperatures are shown in Fig.39, Fig 40, and Fig.41. These plots represent the same samples heat-treated for different times, which are 10 min., 10+20 min., and 10+20+60 min., respectively.

These three plots all show similar results: the higher temperatures of heat treatment enhanced the conductivity more. For example, in the sample processed by route 8Bc and heat treated at 500 ºC for 10 min., the conductivity enhanced ~119.8% compared to the sample without heat treatment. However, for the same sample, when the 10-minute heat treatment was 350 ºC, the conductivity only enhanced ~14.2%. This could be explained by the precipitation process.

Furthermore, the number of passes and the different routes of ECAE are not the critical factors that influence the conductivity. However, the samples processed by eight passes of ECAE carried the highest conductivity, and the samples through one pass of ECAE carried the lowest conductivity.

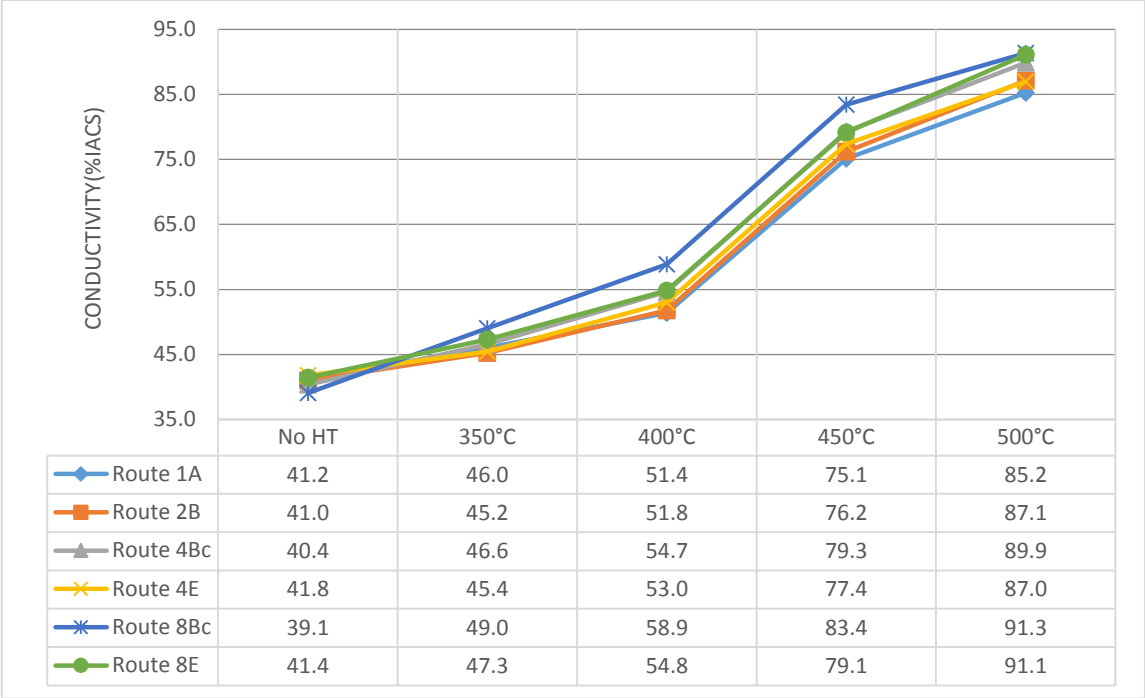


| | No HT | 350°C | 400°C | 450°C | 500°C |
|---|---|---|---|---|---|
| Route 1A | 41.2 | 46.0 | 51.4 | 75.1 | 85.2 |
| Route 2B | 41.0 | 45.2 | 51.8 | 76.2 | 87.1 |
| Route 4Bc | 40.4 | 46.6 | 54.7 | 79.3 | 89.9 |
| Route 4E | 41.8 | 45.4 | 53.0 | 77.4 | 87.0 |
| Route 8Bc | 39.1 | 49.0 | 58.9 | 83.4 | 91.3 |
| Route 8E | 41.4 | 47.3 | 54.8 | 79.1 | 91.1 |

Figure 39. The conductivity of copper C182 processed through different routes of ECAE and heat treatment for 10 minute at different temperatures.

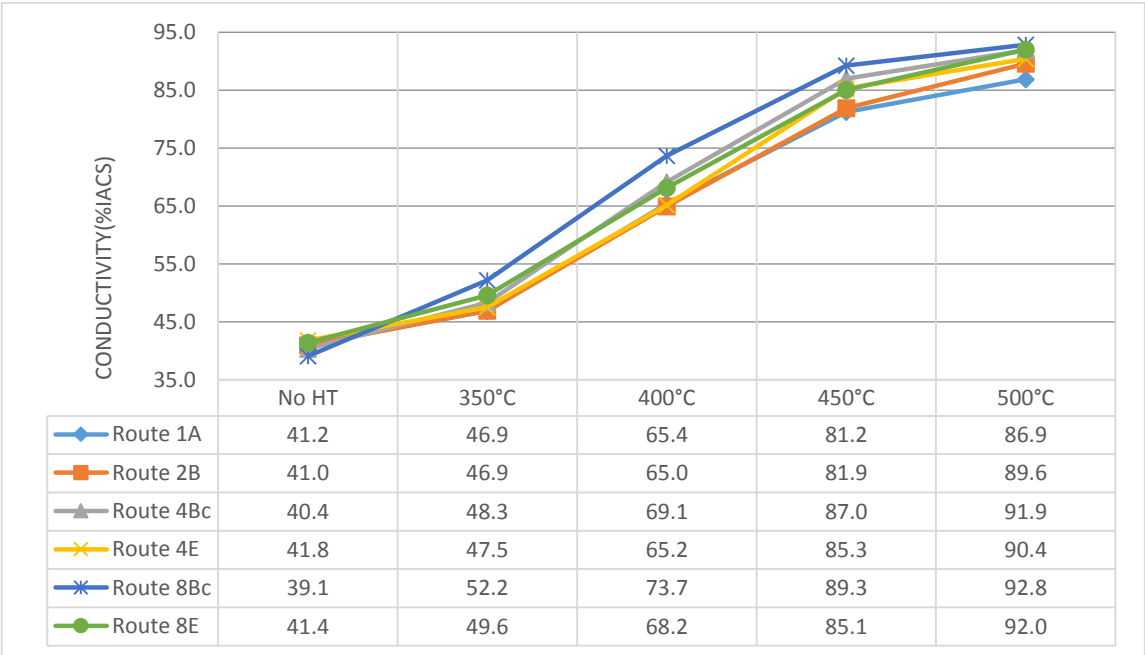


| | No HT | 350°C | 400°C | 450°C | 500°C |
|---|---|---|---|---|---|
| Route 1A | 41.2 | 46.9 | 65.4 | 81.2 | 86.9 |
| Route 2B | 41.0 | 46.9 | 65.0 | 81.9 | 89.6 |
| Route 4Bc | 40.4 | 48.3 | 69.1 | 87.0 | 91.9 |
| Route 4E | 41.8 | 47.5 | 65.2 | 85.3 | 90.4 |
| Route 8Bc | 39.1 | 52.2 | 73.7 | 89.3 | 92.8 |
| Route 8E | 41.4 | 49.6 | 68.2 | 85.1 | 92.0 |

Figure 40. The conductivity of copper C182 processed through different routes of ECAE and heat treatment for 10+20 minute at different temperatures.

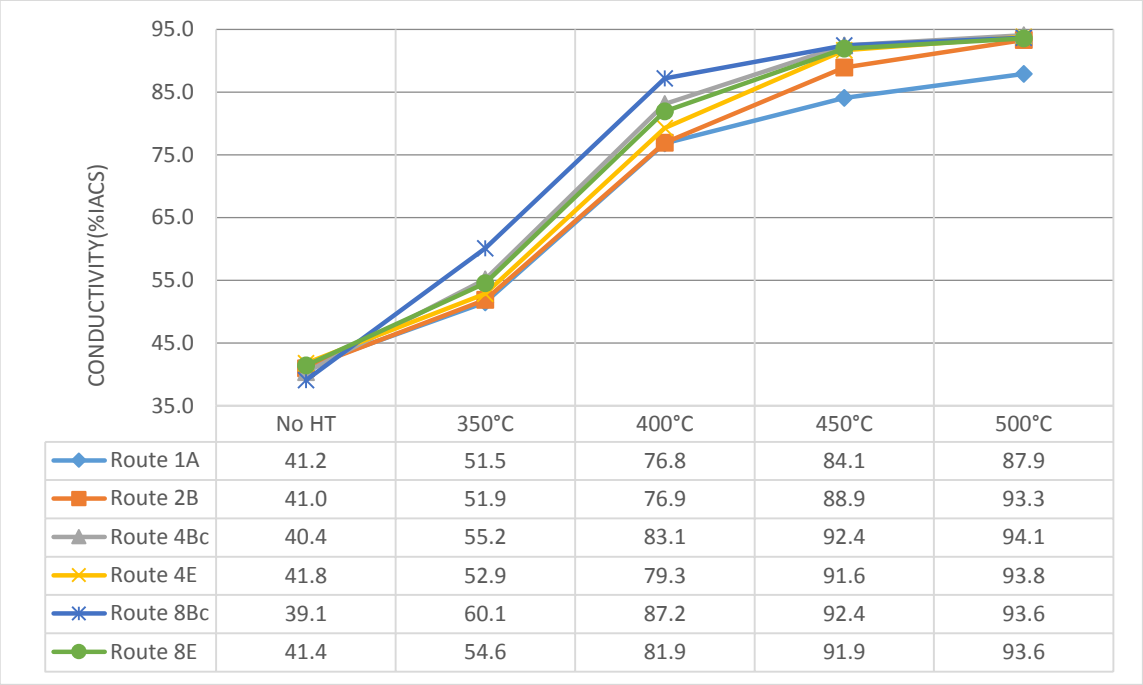


| | No HT | 350°C | 400°C | 450°C | 500°C |
|---|---|---|---|---|---|
| Route 1A | 41.2 | 51.5 | 76.8 | 84.1 | 87.9 |
| Route 2B | 41.0 | 51.9 | 76.9 | 88.9 | 93.3 |
| Route 4Bc | 40.4 | 55.2 | 83.1 | 92.4 | 94.1 |
| Route 4E | 41.8 | 52.9 | 79.3 | 91.6 | 93.8 |
| Route 8Bc | 39.1 | 60.1 | 87.2 | 92.4 | 93.6 |
| Route 8E | 41.4 | 54.6 | 81.9 | 91.9 | 93.6 |

Figure 41. The conductivity of copper C182 processed through different routes of ECAE and heat treatment for 10+20+60 minute at different temperatures.

#### 4.2.3.3. Different Times of Heat Treatment

The conductivities of copper C182 after ECAE and heat treatment for different times and different temperatures are shown in Fig. 42, Fig.43, Fig.44, and Fig.45, which are for heat treatments at 350 °C, 400 °C, 450 °C, and 500 °C, respectively.

As expected, the conductivity of C182 increased as the time of heat treatment increased. When the temperature of heat treatment was 350°C and 400°C, the longest time had the highest conductivity. However, when the heat-treatment temperature was 450 °C, the highest conductivity appeared after 90 min., but it had no obvious difference to the sample heat-treated for 60 min. When the temperature was 500°C, after 10-min. heat treatment, the conductivity became static.

The routes and the passes of ECAE have little effect on the conductivity. However, for the samples that carried more imposed strain, the conductivity is higher after heat treatment. Nevertheless, the difference is small.

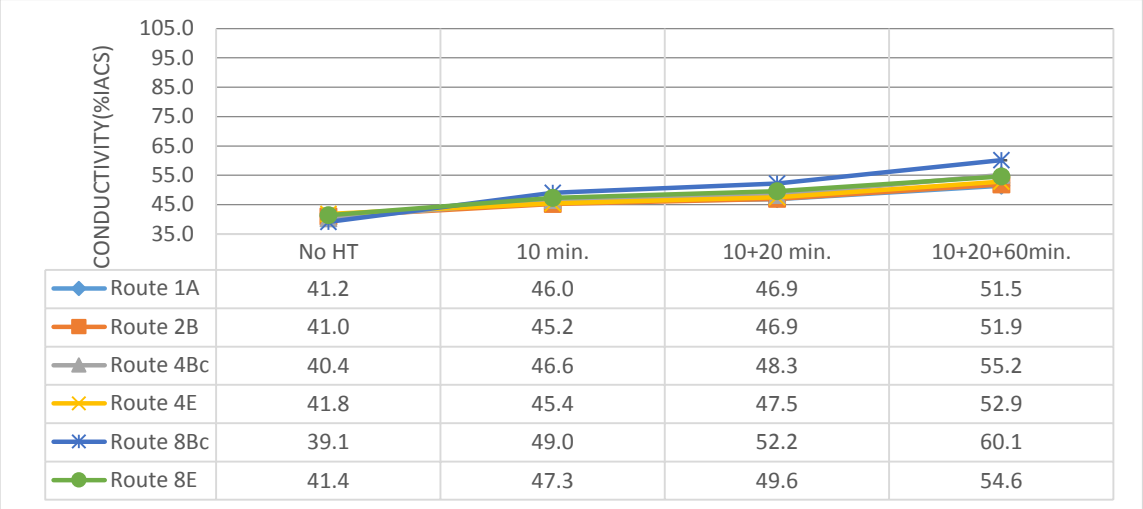


| | No HT | 10 min. | 10+20 min. | 10+20+60min. |
|---|---|---|---|---|
| Route 1A | 41.2 | 46.0 | 46.9 | 51.5 |
| Route 2B | 41.0 | 45.2 | 46.9 | 51.9 |
| Route 4Bc | 40.4 | 46.6 | 48.3 | 55.2 |
| Route 4E | 41.8 | 45.4 | 47.5 | 52.9 |
| Route 8Bc | 39.1 | 49.0 | 52.2 | 60.1 |
| Route 8E | 41.4 | 47.3 | 49.6 | 54.6 |

Figure 42. The conductivity of copper C182 after ECAE and heat treatment at 350 ºC for different times.

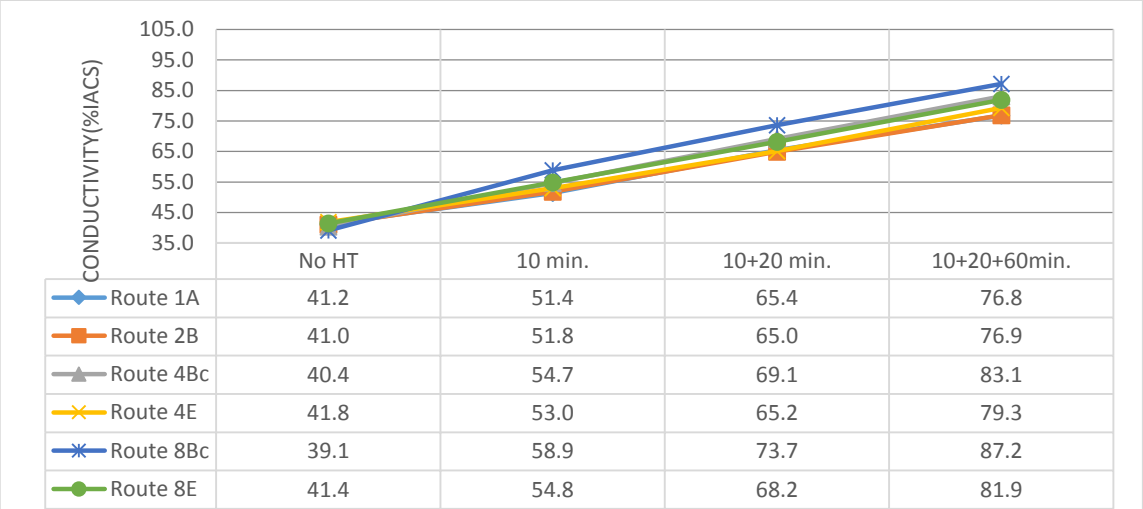


| | No HT | 10 min. | 10+20 min. | 10+20+60min. |
|---|---|---|---|---|
| Route 1A | 41.2 | 51.4 | 65.4 | 76.8 |
| Route 2B | 41.0 | 51.8 | 65.0 | 76.9 |
| Route 4Bc | 40.4 | 54.7 | 69.1 | 83.1 |
| Route 4E | 41.8 | 53.0 | 65.2 | 79.3 |
| Route 8Bc | 39.1 | 58.9 | 73.7 | 87.2 |
| Route 8E | 41.4 | 54.8 | 68.2 | 81.9 |

Figure 43. The conductivity of copper C182 after ECAE and heat treatment at 400 ºC for different times.

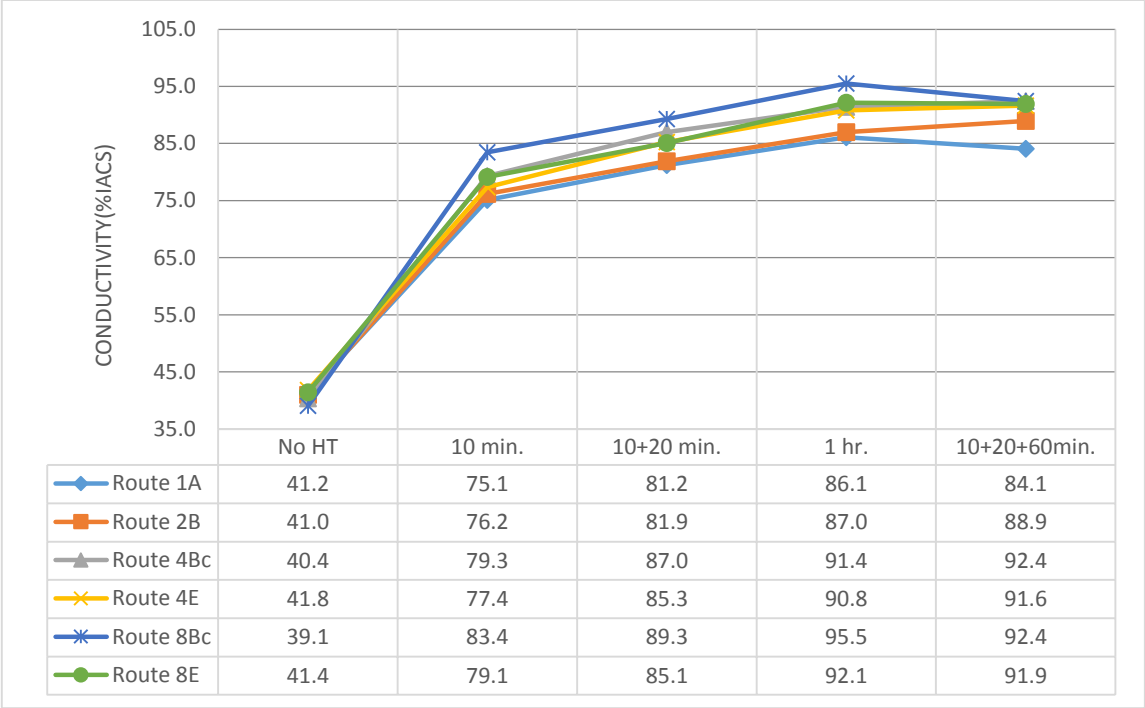


| | No HT | 10 min. | 10+20 min. | 1 hr. | 10+20+60min. |
|---|---|---|---|---|---|
| Route 1A | 41.2 | 75.1 | 81.2 | 86.1 | 84.1 |
| Route 2B | 41.0 | 76.2 | 81.9 | 87.0 | 88.9 |
| Route 4Bc | 40.4 | 79.3 | 87.0 | 91.4 | 92.4 |
| Route 4E | 41.8 | 77.4 | 85.3 | 90.8 | 91.6 |
| Route 8Bc | 39.1 | 83.4 | 89.3 | 95.5 | 92.4 |
| Route 8E | 41.4 | 79.1 | 85.1 | 92.1 | 91.9 |

Figure 44. The conductivity of copper C182 after ECAE and heat treatment at 450 ºC for different times.

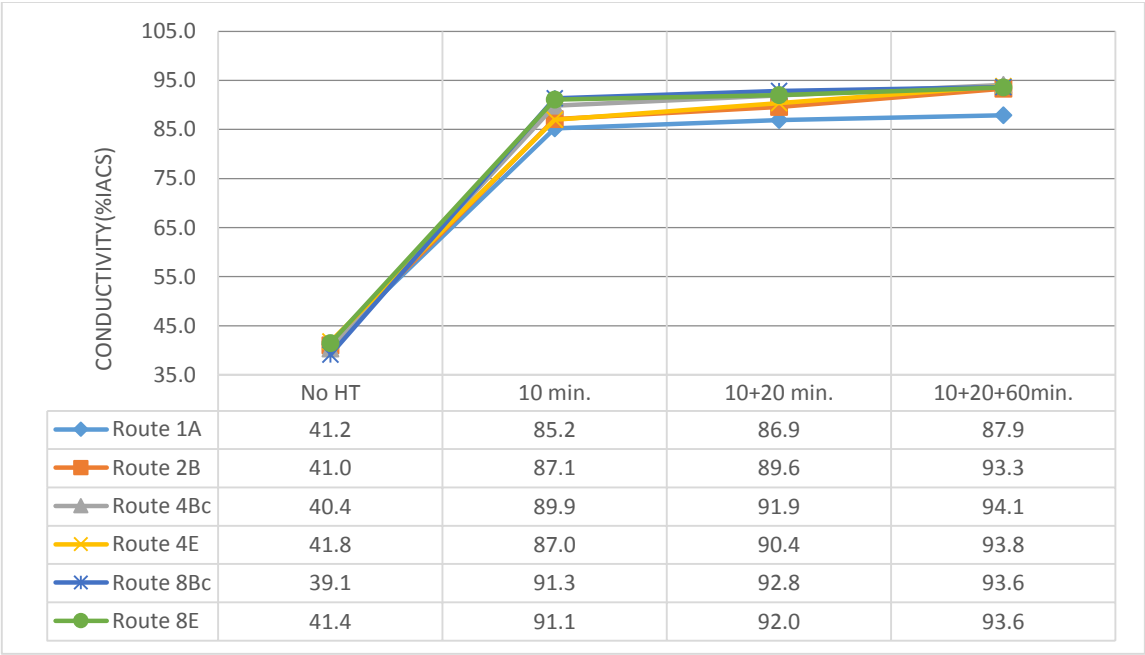


| | No HT | 10 min. | 10+20 min. | 10+20+60min. |
|---|---|---|---|---|
| Route 1A | 41.2 | 85.2 | 86.9 | 87.9 |
| Route 2B | 41.0 | 87.1 | 89.6 | 93.3 |
| Route 4Bc | 40.4 | 89.9 | 91.9 | 94.1 |
| Route 4E | 41.8 | 87.0 | 90.4 | 93.8 |
| Route 8Bc | 39.1 | 91.3 | 92.8 | 93.6 |
| Route 8E | 41.4 | 91.1 | 92.0 | 93.6 |

Figure 45. The conductivity of copper C182 after ECAE and heat treatment at 500 ºC for different times.

Fig.46 shows the conductivity of C182 after long-term heat treatment. For the samples heat treated at 350 ºC, the conductivity increased as the time increased. The speed of increase was slower for the sample processed by route 1A. For this sample, the highest conductivity presented after forty-eight-hours heat treatment. When the temperature was 450 ºC, the conductivity increased as the time increased. However, for the sample processed by route 1A, the conductivity tends to saturate after twelve hours. The conductivity of sample produced by route 4Bc tends to saturate after three hours.

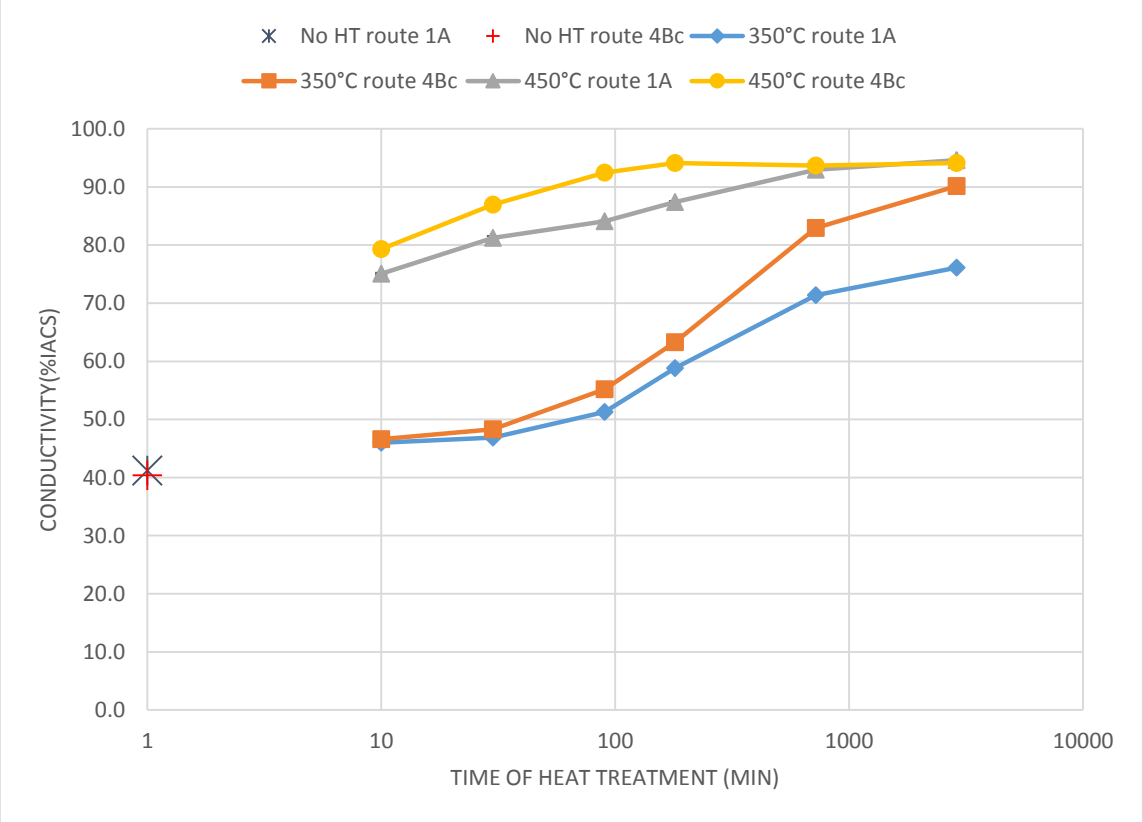


Figure 46. The conductivity of copper C182 after long-term heat treatment.

# V. DISCUSSION

## 5.1. Effect of Routes and Passes

In this study, different routes and passes of ECAE were applied to the samples to determine the effect. The number of passes affects the degree of the imposed plastic strain, which can be calculated by Eq.(2) [36]. For the die of ECAE used in this study, each pass can supply a true strain of ~1.15. Furthermore, different routes of ECAE affect the shearing characteristics, as explained in Chapter 2.

### 5.1.1. Routes and Passes Versus Hardness

Fig.47 presents a summary of hardness measurements from samples subjected to different routes and passes of ECAE. Before ECAE, the hardness significantly dropped after annealing or quenching. There are three reasons for this drop in hardness: (1) increase of grain size, (2) the elimination of dislocations, and (3) movement of impurities from precipitates to substitution defects. For C101 and C110, the impurities are limited, so the main reasons for the hardness decrease are the elimination of dislocations and an increase in grain size. On the other hand, the hardness of C182 dramatically dropped after solution heat treatment and quench; the reasons for the dropping became of reasons (1) and (3).

After ECAE, the hardness significantly increased. This increase is explained by the higher density of dislocations [64]. Moreover, the hardness of these three materials tends to saturate after the second pass of ECAE. This saturation indicates that the more imposed

strain has no effect on the hardness. The results are consistent with N. Lugo et al. [65] and K.X. Wei [6].

Copper C182 possesses much higher hardness than copper C101 and copper C110, due to the chrome in the copper matrix. C101 and C110 present a similar result because the impurities in the copper matrix have no significant influence on the hardness.

The routes of ECAE produced no obvious difference on the hardness. However, the samples processed by route Bc show a slightly higher hardness compared to the samples processed by route E, and these three different materials presented similar strain-hardness results.

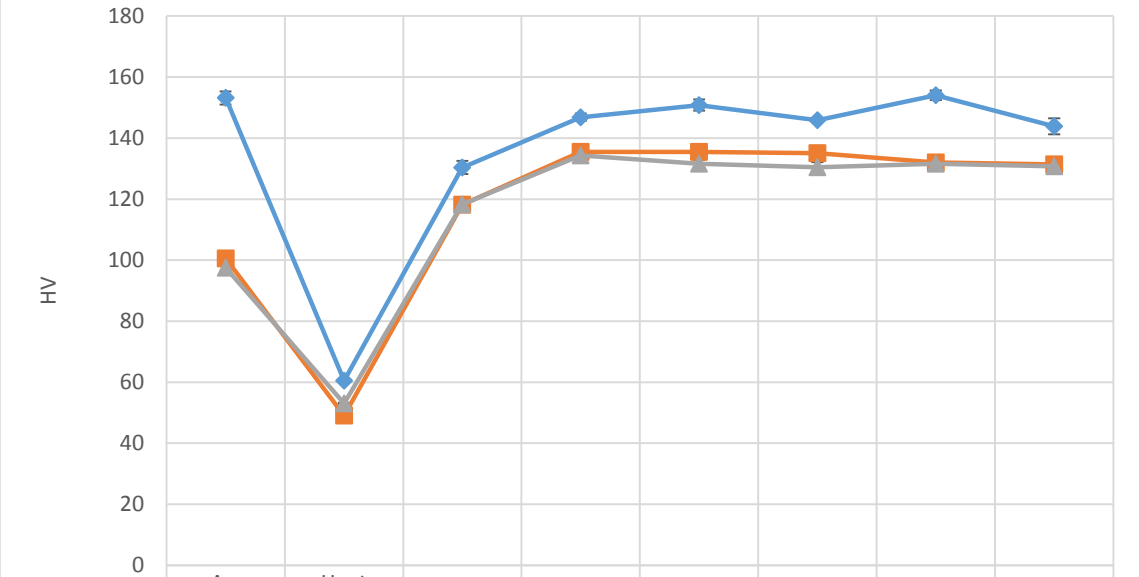


| | As-received | Heat treatment | Route 1A | Route 2B | Route 4Bc | Route 4E | Route 8Bc | Route 8E |
|---|---|---|---|---|---|---|---|---|
| C101 | 101 | 49 | 118 | 136 | 135 | 135 | 132 | 131 |
| C110 | 97 | 53 | 118 | 134 | 132 | 130 | 132 | 131 |
| C182 | 153 | 60 | 130 | 147 | 151 | 146 | 154 | 144 |

Figure 47. The summary of hardness measurements.

### 5.1.2. Routes and Passes Versus Conductivity

The conductivity of the copper and copper alloy before and after ECAE are shown in Fig.48. For C101 and C110, the conductivity slightly increased after annealing. The elimination of dislocations is probably the reason for the increase. After dislocations are eliminated by the annealing, conductive electrons move more easily through the lattice and the conductivity increase. However, the conductivity decreased dramatically for C182 after solution heat treat and quench. This decrease is explained by the solid solution that is produced after the heat treatment. The results as C182 indicate that the formation of a solid solution has more influence on the conductivity than elimination of dislocations.

After the ECAE process, the conductivity decreased for all three materials. This is explained by the higher density of dislocations caused by the strain. Moreover, for C182, the combination of higher density of dislocations and solid solution are the reasons for the significant drop in conductivity.

Additionally, the conductivity results of C101 and C110 are similar to each other. Before ECAE, C101 possesses a slightly higher of conductivity than C110. This result indicates that the impurities have an influence on the conductivity before ECAE. However, after the ECAE process, the density of dislocations becomes a more important factor that affects the conductivity. Therefore, the conductivity becomes similar for these two materials. Furthermore, according to the research by K. Edalati [58], the conductivity of pure copper after eight passes is similar to the results of twenty passes. This result indicated that more imposed strain on the materials might not cause any difference to the conductivity. On the other hand, the conductivity of C182 is much lower than the C101

and C110, due to the chromium in the copper matrix. The conductivity results for C182 are slightly higher than the results of Cu–0.5%Cr alloy [6]; it could be explained by the content of Cr is different in these two studies.

For the conductivity measurements, the routes of ECAE are still not an important factor that affects the results. Although the materials processed by route Bc had a lower conductivity than the materials processed by route E, the difference between them is small.

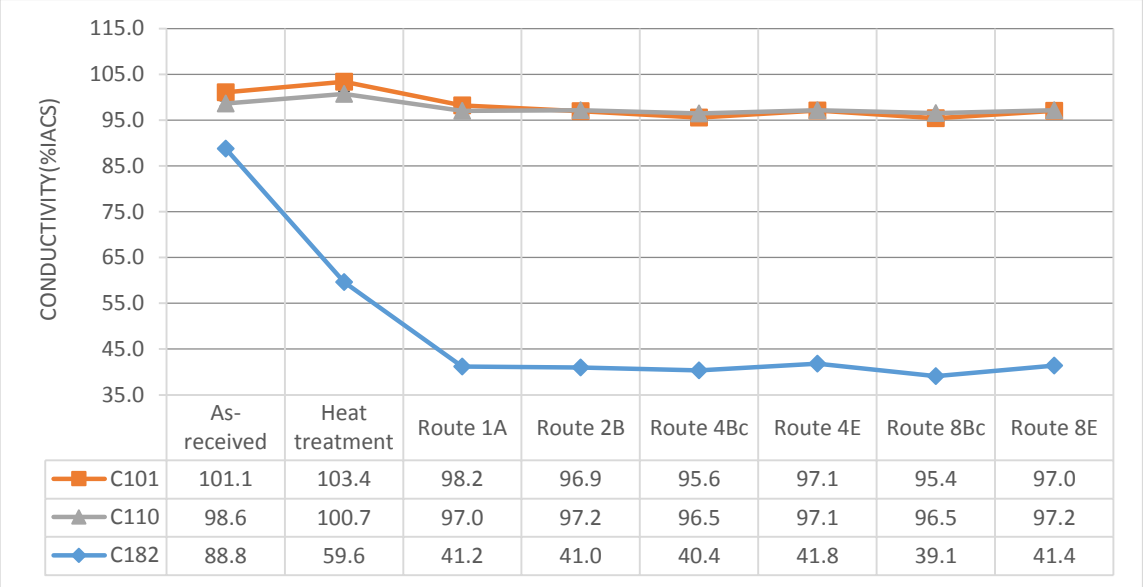


| | As-received | Heat treatment | Route 1A | Route 2B | Route 4Bc | Route 4E | Route 8Bc | Route 8E |
|---|---|---|---|---|---|---|---|---|
| C101 | 101.1 | 103.4 | 98.2 | 96.9 | 95.6 | 97.1 | 95.4 | 97.0 |
| C110 | 98.6 | 100.7 | 97.0 | 97.2 | 96.5 | 97.1 | 96.5 | 97.2 |
| C182 | 88.8 | 59.6 | 41.2 | 41.0 | 40.4 | 41.8 | 39.1 | 41.4 |

Figure 48. The summary of conductivity measurements.

## 5.2. Effect of Heat-Treatment Temperature

The samples of C101 and C110 processed by route 1A, 2B and 8Bc are chosen for a discussion of the influence of heat-treatment temperature. Because the results of route

4Bc, 4E, and 8E are similar to the result of route 8Bc, these comparisons are neglected in this discussion.

### 5.2.1. Heat-Treatment Temperature Versus Hardness

A summary of hardness measurements after ECAE and heat treatment for C101 and C110 is shown in Fig.49. The hardness significantly decreased when the temperature of heat treatment was higher, and the pass of ECAE was the most important factor that influenced the considerable decrease at different temperatures.

The different level of hardness for the samples given different passes of ECAE is explained by the different degrees of imposed strain. A higher degree of imposed strain causes a higher density of dislocations in the material, so the heat treatment has more influence to eliminate the dislocations. Therefore, for the samples possessed through a higher degree of imposed strain, the elimination of dislocations occurred at lower temperatures. On the other hand, for the samples possessed at a lower imposed strain, the elimination of dislocations needs a higher temperature to activate dislocation movement.

Furthermore, the hardness of C101 and C110 is slightly different after heat treatment. The hardness of C101 is slightly lower than C110. This is because the higher levels of impurities in C110 can more effecting impede the movement of dislocations. Therefore, dislocation elimination is slower in the C110 material compared to that in C101.

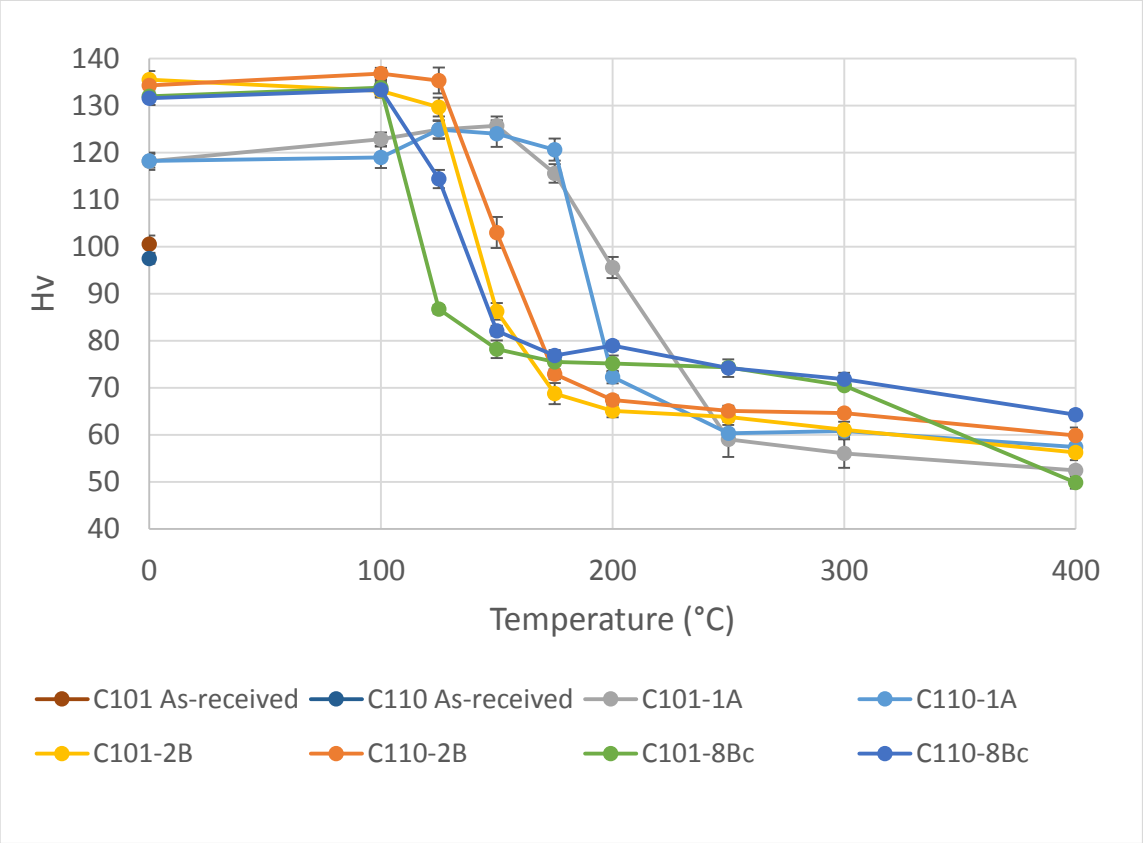


Figure 49. Summary of hardness measurements after ECAE for C101 and C110.

Fig.50 presents the hardness of C182 after ECAE and heat treatment for 10 minutes at different temperatures. Precipitation at 450 ºC appears to be the most effective at this temperature. This result is consistence with that of K.X. Wei et al. [6], but slightly higher than A. Vinogradov et al. [66]. However, the amount of difference is small.

For the samples processed by routes 4Bc and 8Bc, the hardness decreases after heat treatment at all temperatures, which might mean the elimination of dislocations has more influence than precipitation for these two samples. Furthermore, the hardness of all samples heat-treated at 500 ºC is much lower than the samples heat-treated at 450 ºC, except the sample processed by route 1A. This lower hardness at 500 ºC can be explained

by the distribution of precipitations. At 450 ºC, the precipitations might distribute around the dislocations and impede the dislocations moving. However, at 500 ºC, the precipitations might be larger and spread further apart, so the dislocations move easier and the hardness become lower. The samples processed by route 1A have the same hardness at these two temperatures because the density of dislocations is low, and the distribution of precipitates is not much different.

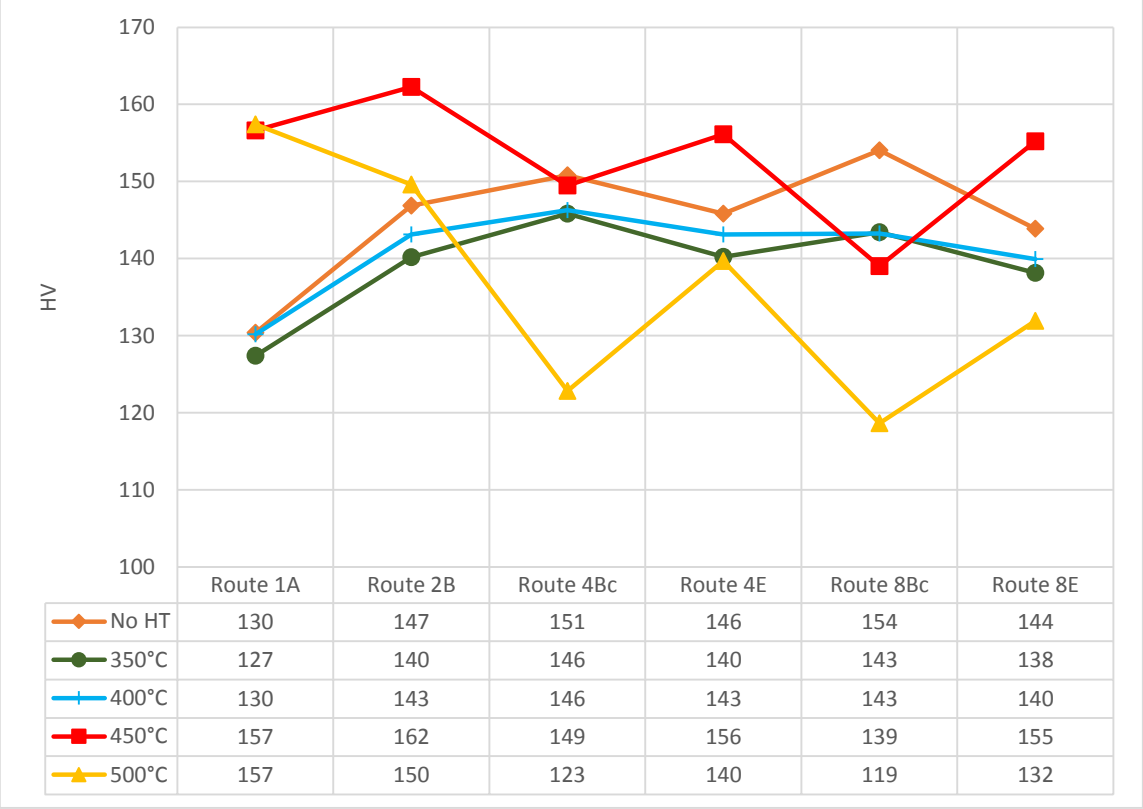


| | Route 1A | Route 2B | Route 4Bc | Route 4E | Route 8Bc | Route 8E |
|---|---|---|---|---|---|---|
| No HT | 130 | 147 | 151 | 146 | 154 | 144 |
| 350°C | 127 | 140 | 146 | 140 | 143 | 138 |
| 400°C | 130 | 143 | 146 | 143 | 143 | 140 |
| 450°C | 157 | 162 | 149 | 156 | 139 | 155 |
| 500°C | 157 | 150 | 123 | 140 | 119 | 132 |

Figure 50. The hardness of C182 after ECAE and heat treatment at 350,400,450 and 500 ºC for 10 minutes.

### 5.2.2. Heat-Treatment Temperature Versus Conductivity

A summary of the conductivity measurements after ECAE and heat treatment at different temperatures for C101 and C110 is shown in Fig. 51. For copper C101, after the heat treatment, the conductivity continuously increased as temperature increased, which is explained by the elimination of dislocations. This conductivity measurement compared to the hardness measurement has a slight difference. The hardness dropped significantly at 125 ºC and 150 ºC, but the conductivity has no obvious change at different temperatures. This might indicates that the recrystallization has a greater effect on the hardness.

Copper C101 and C110 show a similar tendency after the heat treatment, but the amount of conductivity for C101 is higher than C110. Before the heat treatment, the conductivity of these two materials is almost the same, but after the heat treatment, the annealing enhanced the conductivity of C101 more significantly than C110. The impurities in C110 retard the speed of dislocations elimination, and this can be the reason for the lower conductivity. Furthermore, although the higher temperatures can increase the speed of aging, the samples heat-treated at 100 ºC showed a contradiction. When the temperature of the heat treatment was 100 ºC, the conductivity of C110 showed a peak, which was much higher than the samples heat-treated at 125 ºC. This peak can be explained by the impurities being around the dislocations at this temperature. The concentration of impurities is high around dislocations, but the concentration of impurities is low everywhere else. Therefore, the electrons have fewer obstacles for moving. However, when the temperature is higher, the impurities regularly distribute around the materials and the dislocation density is small, so the conductivity becomes lower.

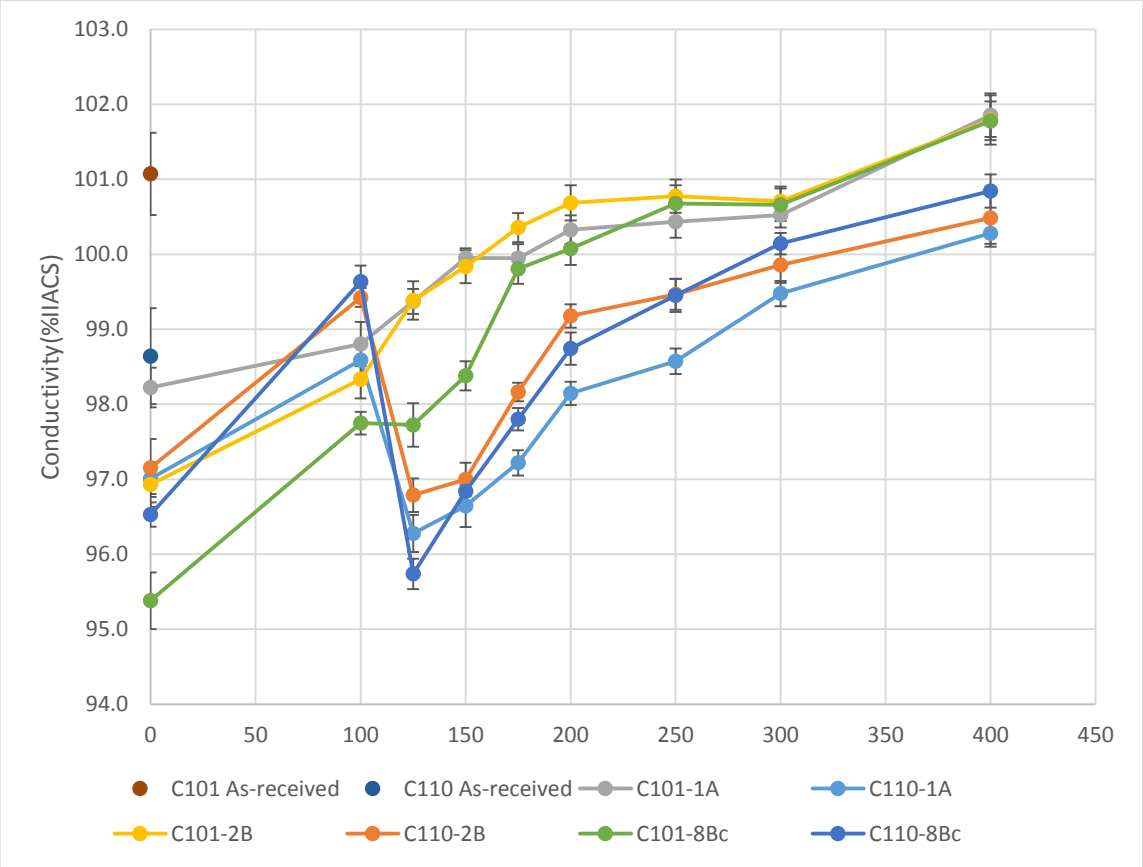


Figure 51. Summary of conductivity measurements after ECAE for copper C101 and C110.

Fig.52 presents the conductivity of C182 after ECAE and heat treatment at different temperatures. As expected, the conductivity increased after the heat treatment, and higher temperatures of the heat treatment increased the conductivity. When the temperature is above 450 ºC, the conductivity increased dramatically. This indicates the precipitation occurred at 450 ºC, and shows agreement with the hardness results.

ECAE produces a supersaturating crystal defects. Therefore, after ECAE, the precipitation and elimination of dislocations occur during the heat treatment; these can significantly increase the conductivity of the samples. Therefore, the increase of

conductivity for copper C182 is higher than copper C101 and C110. Moreover, this tendency of the heat treatment temperature show the agreement to K.X. Wei et al.[6], Moreover, the Cu-Cr-Zr alloy [67] and Cu-Cr-Zr-Mg alloy [68] also present a consistent tendency after heat treatment.

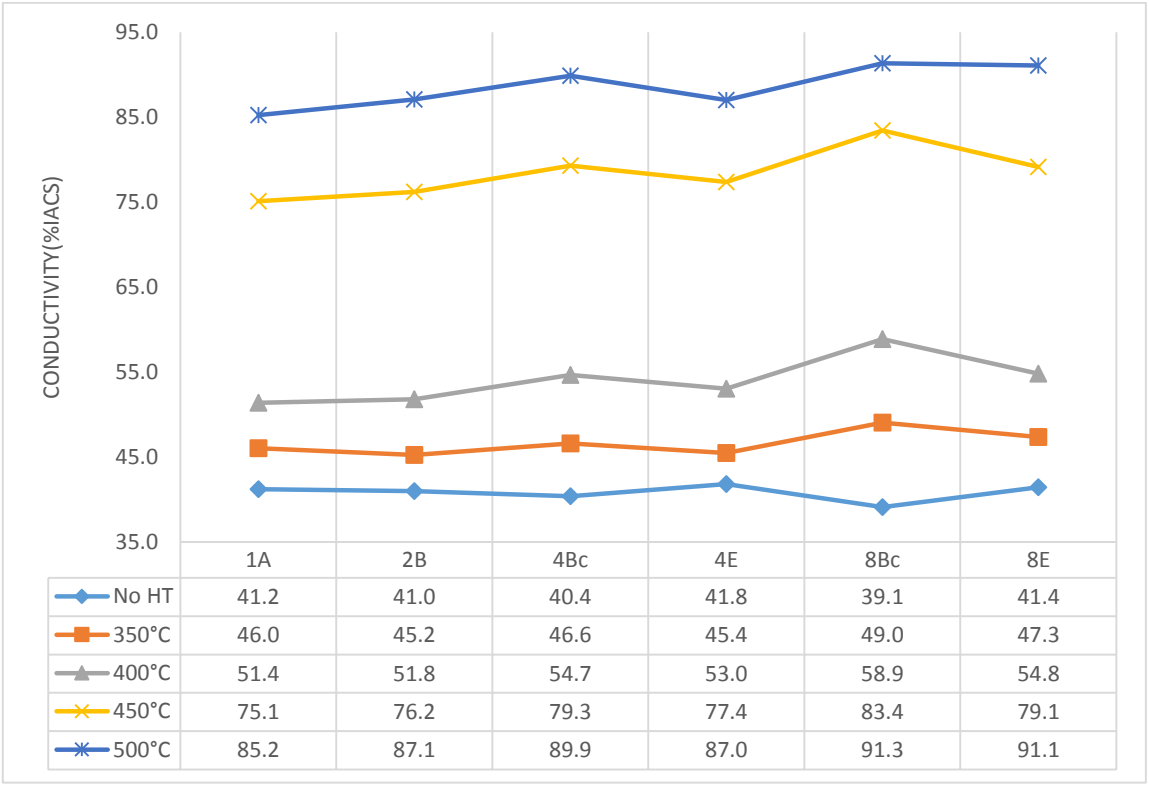


| | 1A | 2B | 4Bc | 4E | 8Bc | 8E |
|---|---|---|---|---|---|---|
| No HT | 41.2 | 41.0 | 40.4 | 41.8 | 39.1 | 41.4 |
| 350°C | 46.0 | 45.2 | 46.6 | 45.4 | 49.0 | 47.3 |
| 400°C | 51.4 | 51.8 | 54.7 | 53.0 | 58.9 | 54.8 |
| 450°C | 75.1 | 76.2 | 79.3 | 77.4 | 83.4 | 79.1 |
| 500°C | 85.2 | 87.1 | 89.9 | 87.0 | 91.3 | 91.1 |

Figure 52. The conductivity of copper C182 after ECAE and heat treatment at 350, 400, 450 and 500 ºC for 10 minutes.

## 5.3. Effect of Heat-Treatment Time

The aging treatment can be accelerated by the cold-working deformation [69] and aging temperature, which is confirmed by previous results and other research [70].

Although the aging treatment is slow at low temperature, the conductivity usually can achieve to a higher level after long-term heat treatment.

### 5.3.1. Heat-Treatment Time Versus Hardness

Fig. 53 and Fig 54 present the hardness measurements of C101 and C110 after ECAE and long-term heat treatment. The hardness continuously decreased as time increased because longer time increased the elimination of dislocations.

When the temperature is 100 ºC, the hardness of route-1A sample kept constant after heat treatment. This result indicates that elimination of dislocations does not occur at this temperature. However, for the samples processed by route 4Bc, the hardness decreased continuously as time increased at 100 ºC. This difference is caused by higher cold-working deformation and consequent higher level of strained energy in the dislocation strain fields. This reason can also explain the differences between these two materials at 150 ºC and 200 ºC.

The results of the hardness for copper C101 and C110 might indicate that, the low-temperature aging cannot eliminate the dislocations in a short time, but longer time causes elimination of the dislocations. On the other hand, high-temperature heat treatment decreased the hardness significantly in a short time.

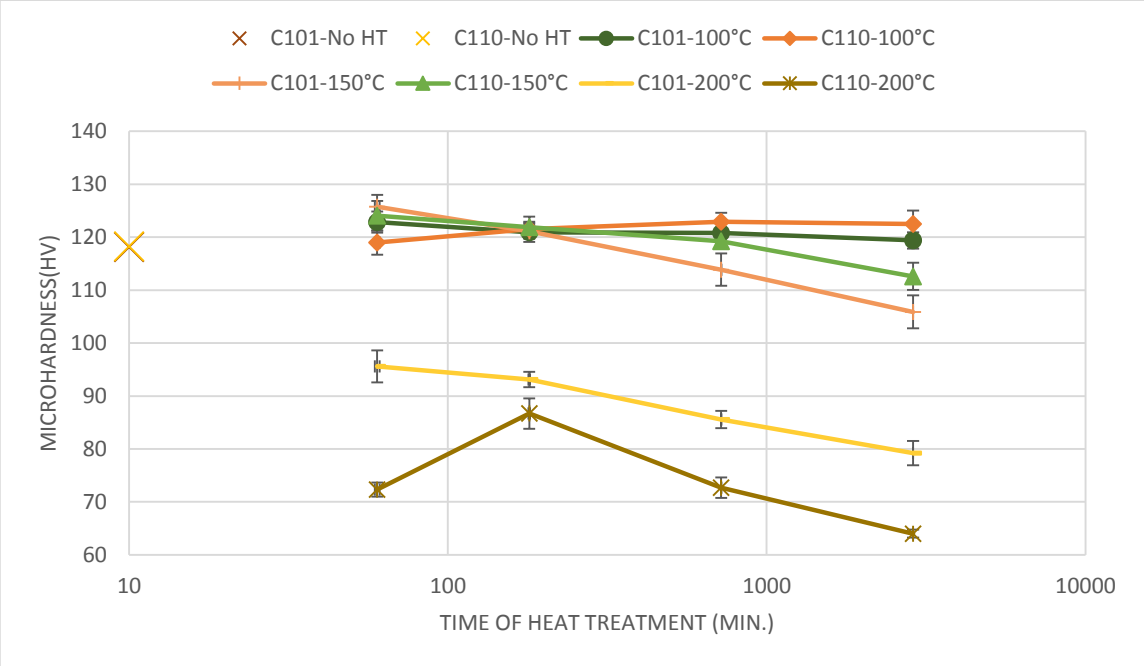


Figure 53. Summary of hardness measurements on copper C101 and C110 for long-term heat treatment (route 1A).

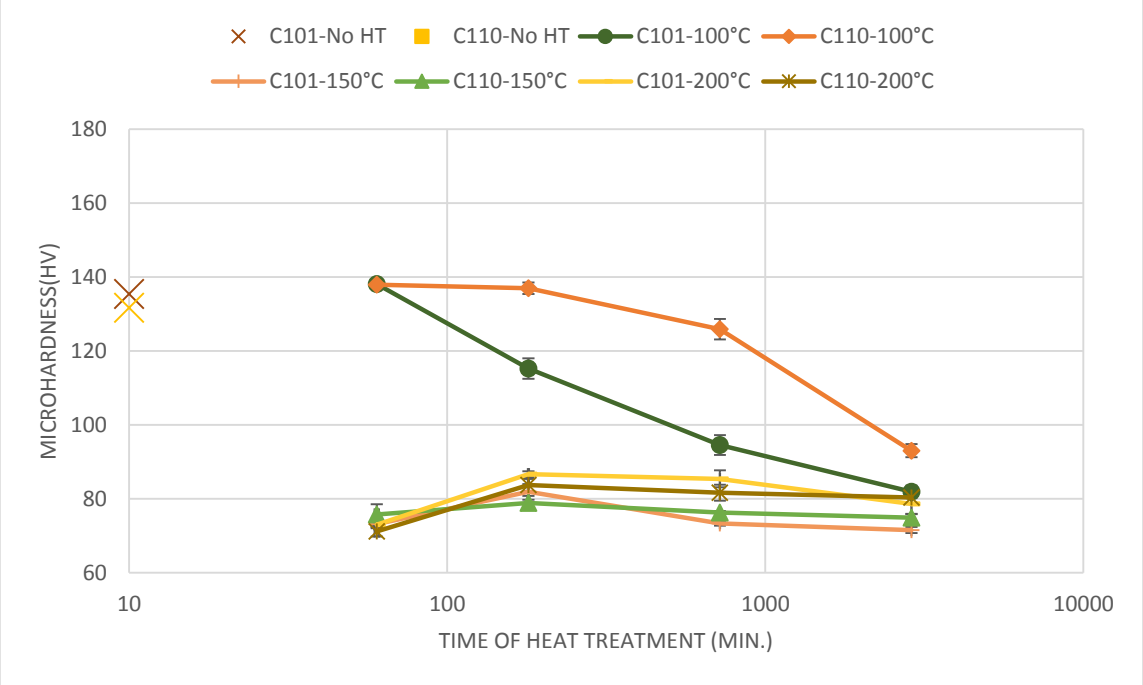


Figure 54. Summary of hardness measurements on copper C101 and C110 for long-term heat treatment (route 4Bc).

The results of hardness measurements for copper C182 after ECAE and long-term heat treatment are presented in Fig.55. This result proves that the time of heat treatment has a significant influence on the hardness of C182. The higher temperatures and high-imposed strain accelerate the aging treatment. Therefore, when the heat treatment is at high temperatures or the sample imparted high strain, the highest hardness occurred in a short time. However, longer time of heat treatment at high temperatures impair the hardness. Furthermore, when both the temperature and imposed strain are low, the hardness kept increasing as time increased.

Different routes of ECAE and different temperatures of heat treatment can affect the highest hardness occurred at different times of heat treatment. The highest hardness is similar for all the samples, which have different processes. These similar results can be explained by the saturation of dislocation density and precipitations, which are similar for the different samples.

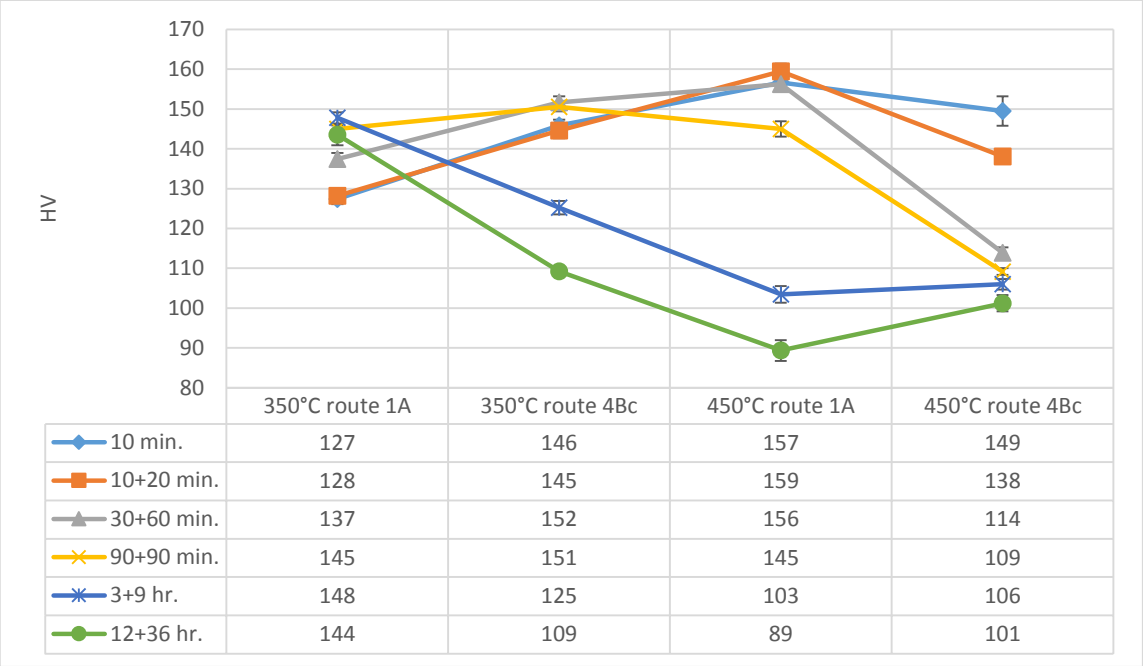


| | 350°C route 1A | 350°C route 4Bc | 450°C route 1A | 450°C route 4Bc |
|---|---|---|---|---|
| 10 min. | 127 | 146 | 157 | 149 |
| 10+20 min. | 128 | 145 | 159 | 138 |
| 30+60 min. | 137 | 152 | 156 | 114 |
| 90+90 min. | 145 | 151 | 145 | 109 |
| 3+9 hr. | 148 | 125 | 103 | 106 |
| 12+36 hr. | 144 | 109 | 89 | 101 |

Figure 55. The hardness of copper C182 after ECAE and long-term heat treatment**.**

### 5.3.2. Heat-Treatment Time Versus Conductivity

Fig.56 and Fig.57 present the conductivity measurements of copper C101 and C110 after long-term heat treatment. The elimination of dislocations caused by the heat treatment after ECAE can considerably increase the conductivity. For C110, the results show a peak after three hours heat treatment, and the conductivity fluctuated after three hours. This result might be explained by the distribution of the impurities. The impurities move during the heat treatment, so the conductivity keep decreasing. This fluctuation indicates C110 is not stable after a 48-hour heat treatment. The distribution of impurities also can explain the result that, the conductivities are higher at 100 ºC than 150 ºC even if the time is longer. In other words, longer time do not have influence on the distribution of the impurities.

Additionally, although the hardness of C101 and C110 after long-term heat treatment has no big difference, the conductivities of C101 are higher than the C110. This trend can be explained by that the impurities in C110 have more influence on hardness than conductivity.

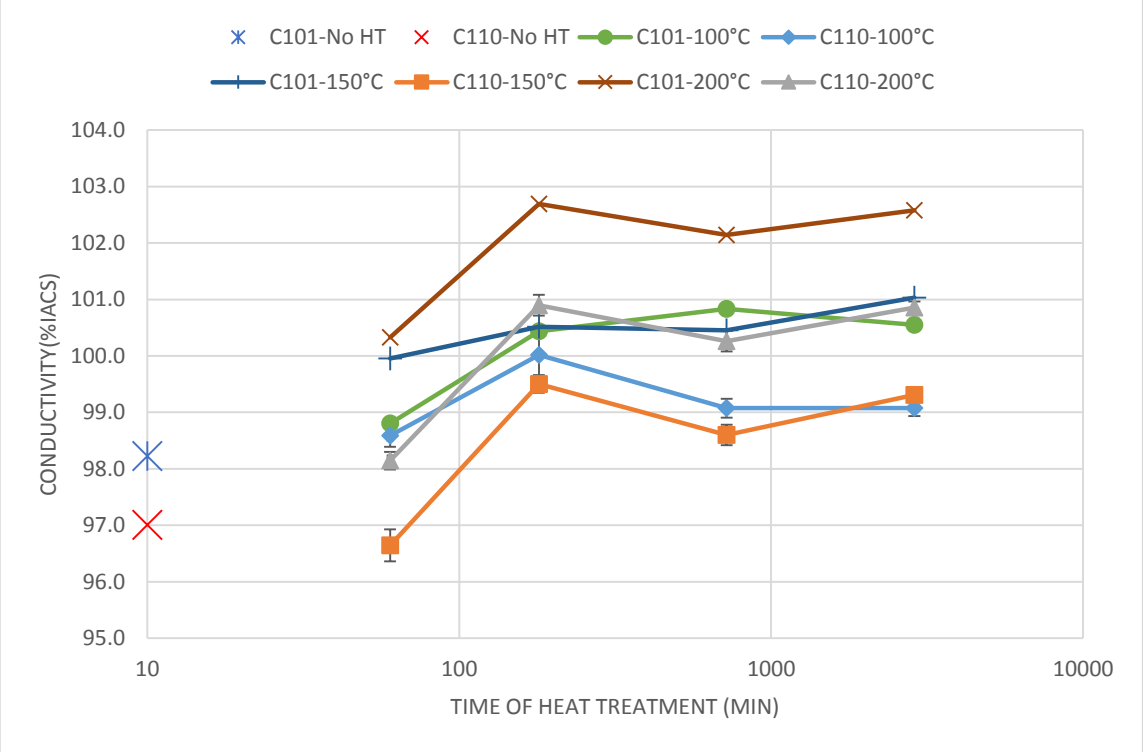


Figure 56. The conductivity of copper C101 and C110 after ECAE (1A) and long-term heat treatment.

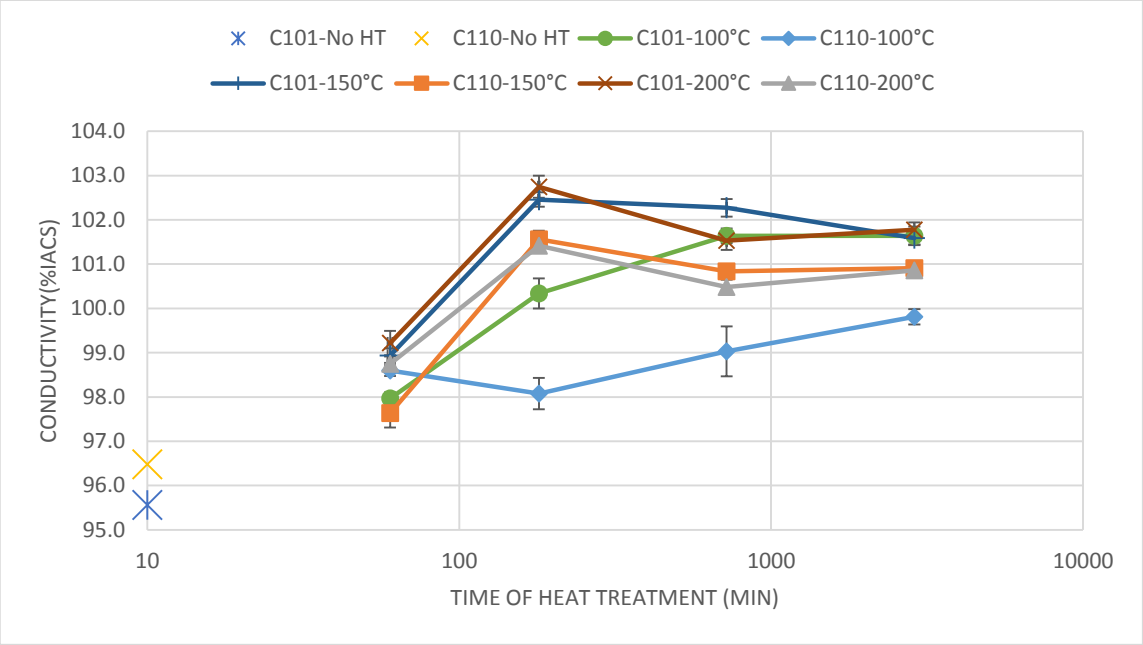


Figure 57. The conductivity of copper C101 and C110 after ECAE (4Bc) and long-term heat treatment.

The conductivity of C182 after ECAE and long-term heat treatment is shown in Fig.58. The reasons that the conductivity of C182 kept increasing after long-term heat treatment are elimination of dislocations and precipitation of chrome. However, when the heat treatment is long enough, the elimination of dislocations and precipitations might not occur anymore. Therefore, the conductivity tends to saturate, and the time of saturation is the same for different samples processed by different routes and different temperatures.

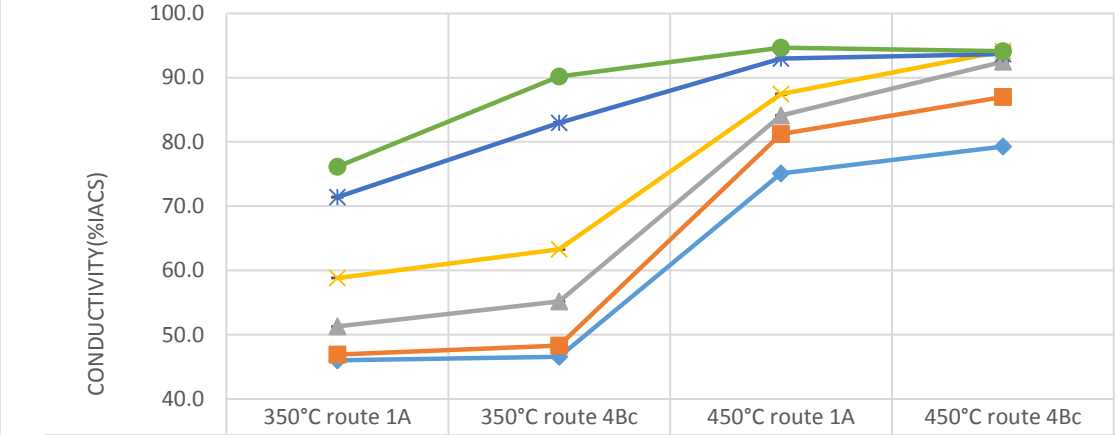


| | 350°C route 1A | 350°C route 4Bc | 450°C route 1A | 450°C route 4Bc |
|---|---|---|---|---|
| 10 min. | 46.0 | 46.6 | 75.1 | 79.3 |
| 10+20 min. | 46.9 | 48.3 | 81.2 | 87.0 |
| 30+60 min. | 51.3 | 55.2 | 84.1 | 92.4 |
| 90+90 min. | 58.8 | 63.3 | 87.4 | 94.1 |
| 3+9 hr. | 71.4 | 83.0 | 92.9 | 93.7 |
| 12+36 hr. | 76.1 | 90.2 | 94.6 | 94.1 |

Figure 58. The conductivity of copper C182 after ECAE and long-term heat treatment

## 5.4. Balancing Hardness and Conductivity

Fig.59 shows the hardness versus the conductivity for all samples and all heat treatments of the materials, C101, C110, C182, and some other commercial Cu-based alloys. The results of C101, C110, and C182 include the as-received, annealed, quenched, ECAEed materials and the materials after ECAE and heat treatment at different temperatures for different times. The results of other Cu-based alloys are from the literature [2, 7]. In this study, the annealed C101 possesses the highest conductivity, which is 103.37 %IACS, but the hardness is only 49 Hv. The highest hardness appeared on C182 processed by route 2B of ECAE and heat treated at 450 ºC for 10 minutes. The hardness of this sample is 162 Hv, but the conductivity is 76.18 %IACS. For the results from other

reports, the hardness of 211.5 Hv and conductivity of 74.9 %IACS were reported in Cu-0.5%Cr [7]. Although the specifications of Cu-0.5%Cr alloy are similar to C182, the hardness of this Cu-0.5%Cr alloy showed a higher hardness than the C182 in this study. This might be explained by the priority of the heat treatment. In Xu's research, the heat treatment came after the quench, and the extrusion came after the heat treatment. However, in this study, the copper C182 was extruded after quenching and then heat-treated after ECAE. Therefore, the differences between these two results should be the order of the heat treatment. On the other hand, a combination of 148.4 Hv and 87 %IACS were presented in Cu-0.2%Mg, and a combination of 157.5 Hv and 80 %IACS were reported in Cu-0.4%Mg [2]. These results are similar to C182. Therefore, Mg and Cr seem to behave similarly in Cu-based alloys.

Table 5 shows different figures of merit (FOM) terms for the combination of hardness and conductivity. In percentage terms, the highest hardness and conductivity value in this analysis are 100%; the lowest hardness and conductivity value are 0%. Other value of hardness and conductivity are calculated by percentage. In this table, the percentages are the average of these two values. The sample of C110 processed by route B and heat-treated at 100 ºC for one hour shows the highest average percentage in this study, which is 85.8. This sample had 137 Hv and 99.42 %IACS. For the other FOM terms, (A) the hardness is multiplied by conductivity, and (B) the hardness is multiplied by conductivity and divided by density, also showed this sample possessed the best combination of hardness and conductivity. For C101, the sample processed by route 4Bc and heat-treated at 100 ºC for 1 hour showed the best combination compared to other C101 sample. On the other hand,

for C182, although ECAE and heat treatment can enhance hardness and conductivity, they cannot enhance these properties simultaneously. The copper C182 processed by route 1A and heat-treated at 500 ºC for 10 minutes possesses the highest average of hardness and conductivity in this study. However, the as-received C182 had the better amount in other FOM terms. In conclusion, there is no improvement to the properties of copper C182. Other combinations of plastic strain and heat treatment might give a better combination. Severe plastic deformation definitely improved the properties combination of copper C101 and C110.

According to these results, the samples processed by fewer passes of ECAE possess a better combination of hardness and conductivity than the samples processed by more passes of ECAE. Because more passes of ECAE can only increase the hardness slightly but decreased the conductivity considerably. For copper C101 and C110, the best combination was obtained when the temperature of heat treatment was 100ºC. The longer time heat treatment does not improve the combination. For C182, when the temperature of heat treatment was higher than the optimum precipitation temperature, the combination becomes better. The shorter time of heat treatment for C182 may produce the better combination. In conclusion, there is no best sample, which possesses both the highest conductivity and the highest hardness values together. The increased conductivity usually occurs with decreasing hardness. However, this study shows that ECAE can enhance the hardness of conductor materials and without much degradation in electrical conductivity.

Table 5. Figures of merit for the combination of hardness and conductivity.

| Material | Process | $\frac{(H)+(C)}{2}$ | (H) × (C) | $\frac{\frac{(H)-H_{min}}{H_{max}-H_{min}}+\frac{(C)-C_{min}}{C_{max}-C_{min}}}{2}\times 100$ |
|---|---|---|---|---|
| C101 | As-received | 100.8 | 10166 | 71.0 |
| | Annealed | 76.2 | 5075 | 50.0 |
| | Route 4Bc 100°C 1 hr. | 118.0 | 13530 | 85.2 |
| C110 | As-received | 98.1 | 9616 | 67.8 |
| | Annealed | 76.9 | 5345 | 49.7 |
| | Route 2B 100°C 1 hr. | 118.1 | 13603 | 85.8 |
| | Route 4Bc 100°C 1 hr. | 118.3 | 13601 | 85.6 |
| C182 | As-received | 121.0 | 13595 | 84.7 |
| | Quenched | 60.0 | 3603 | 21.0 |
| | Route 1A 500°C 10 min. | 121.3 | 13417 | 83.8 |
| Cu-0.2% Mg | ECAE + cold rolling + drawing | 117.7 | 12911 | 81.2 |
| Cu-0.4% Mg | ECAE + cold rolling + drawing | 118.8 | 12600 | 79.8 |
| Cu-0.5%Cr | Quench + aging + ECAE | 143.2 | 15841 | 99.7 |

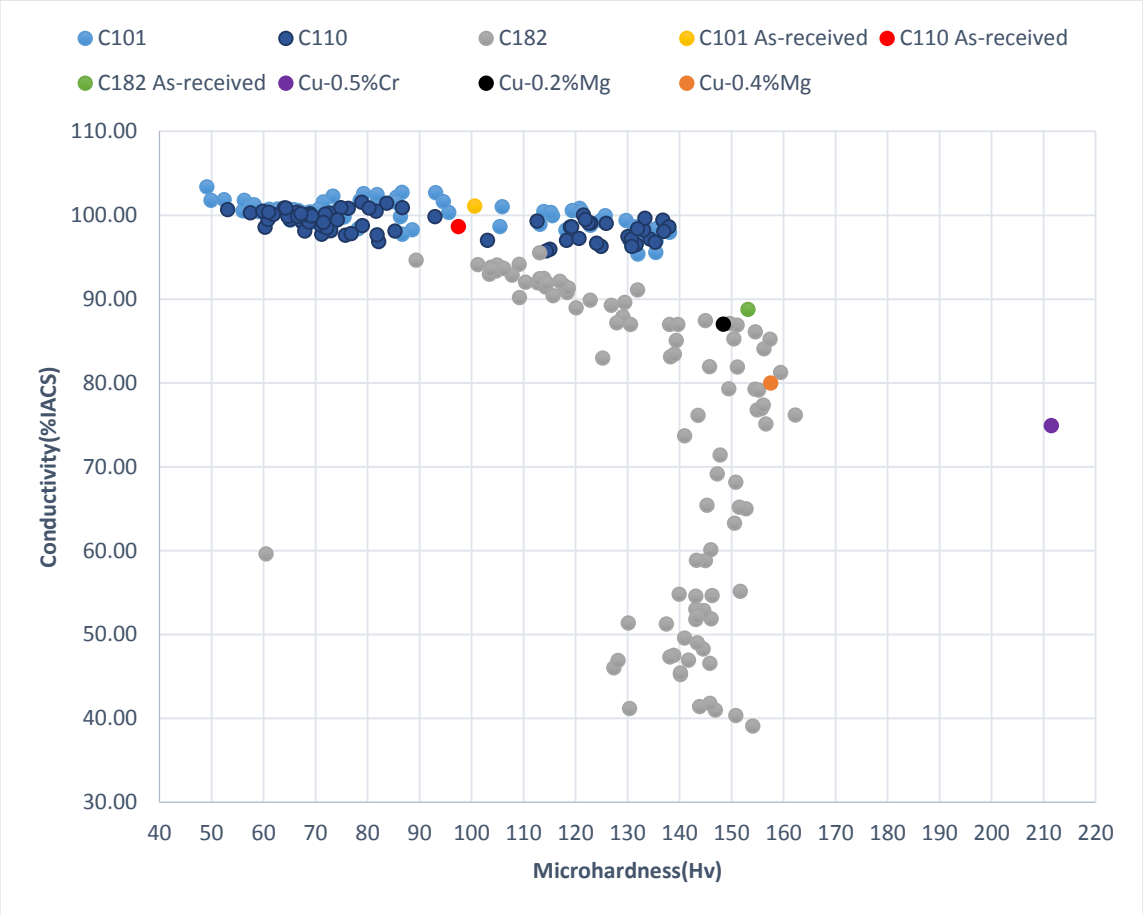


Figure 59. Hardness versus conductivity of all materials and processing conditions in this research and literatures.

# VI. SUMMARY AND CONCLUSION

In this study, different numbers passes and routes of equal-channel angular extrusion (ECAE) were successfully applied to oxygen-free high conductivity (OFHC) copper (C101), commercially pure copper (C110), and copper chromium alloy (C182). Different temperatures and times of heat treatment were applied these materials after ECAE. The hardness and electrical conductivity of the materials were measured. The main findings are summarized here:

1. ECAE successfully enhanced the hardness of all materials but decreased the electrical conductivity at the same time.
2. Both hardness and electrical conductivity tend to saturate after the second pass of ECAE; further extrusion process have no significant influence. In addition, route Bc (4 and 8 passes) has more influence on material properties than route E (4 and 8 passes), but the differences between them are small.
3. After ECAE, heat treatment (annealing) increases the electrical conductivity but decreases the hardness, and the higher temperatures of heat treatment increase the speed of properties change.
4. Longer periods of heat treatment continually affect the properties of C182, but the properties of C101 and C110 stabilize after long-term heat treatment.
5. Lower temperatures of heat treatment continually affect the properties of copper alloys, but the properties saturate faster at higher temperatures of heat treatment.

Furthermore, higher levels of plastic strain also cause the properties of copper alloys to saturate faster than samples with lower levels of plastic strain.

6. For C101, the best combination of hardness and conductivity occurred on the sample processed by route 1A of ECAE and heat-treated at 100 ºC for 12 hours. The conductivity reached 100.83 %IACS and the hardness reached 121 Hv.
7. The results of C110 show that the small amounts of impurities in the copper slightly lower the conductivity and hardness but the influence is small. The best combination of hardness and conductivity occurred for the sample processed by route 2B of ECAE and heat treated at 100 ºC for 1 hour. The conductivity reached 99.42 %IACS and the hardness reached 137 Hv.
8. The hardness and the electrical conductivity of C101 and C110 are similar after all processing conditions.
9. For C182, the Cr inside the copper matrix greatly increases the hardness, but also decreases the conductivity significantly. The precipitation of Cr occurred most effectively after ECAE and heat treatment at 450 ºC. This precipitation enhanced both hardness and conductivity. The best combination of hardness and conductivity occurred after route 1A of ECAE and heat treatment at 500 ºC for 10 minutes. For this processing, the conductivity is 86.11 %IACS and the hardness is 155 Hv.

From these results, the following conclusions are drawn:

1. SPD resulting from ECAE and post ECAE heat treatment can improve the combination of hardness and electrical conductivity of Cu-based alloys for electrical conductor applications.
2. For a room temperature copper alloy conductor, the best strength-conductivity combination where both these factors are considered to have equal importance can be realized in copper C110.
3. SPD resulting from ECAE has more effect on the strength and electrical conductivity of pure copper than on a precipitation hardenable copper alloy.
4. The above three conclusions can also applied to other metals such as Al and silver contemplated for electrical conductor applications.

# VII. SUGGESTIONS FOR FUTURE STUDY

There remain some unresolved problems for Cu alloys processed by severe plastic deformation. First, the microstructure changes induced by SPD and heat treatment need to be determined. The reasons for the change of the properties are not confined by microstructural evidence. Therefore, using different methods to determine the distribution of dislocations, average grain size, and impurities precipitations are important. Second, the experiments conducted in this study did not measure the tensile properties of SPD processed materials, such as strength, elongation, and stress-strain curve. Although, the other mechanical properties should be related to the hardness, these properties still need to be measured.

Additionally, conducting ECAE under cryogenic temperature for copper alloys is another interesting topic. In this study, it was shown that the hardness and conductivity of C182 could be changed by ECAE. Moreover, a literature study mentions how the fraction of twins inside the copper alloys can affect the resistivity. The resistivity of nano-twin Cu possess similar resistivity to coarse-grain Cu but much higher strength, and this resistivity is much lower than the nanocrystalline copper [71]. On the other hand, Y.S. Li et al. [72] represented a result that pure copper processed by dynamic plastic deformation (DPD) can increase the fraction of twins in the microstructure. According to these three different studies, copper chromium alloy is an interesting material to process through ECAE at a cryogenic temperature.

REFERENCES


1. Çetinarslan, C.S., *Effect of cold plastic deformation on electrical conductivity of various materials.* Materials & Design, 2009. **30**(3): p. 671-673.
2. Zhu C.C., et al., *Effect of ECAP combined cold working on mechanical properties and electrical conductivity of Conform-produced Cu–Mg alloys.* Journal of Alloys and Compounds, 2014. **582**: p. 135-140.
3. Han, K., et al., *High strength and high electrical conductivity bulk Cu.* Philosophical Magazine, 2004. **84**(34): p. 3705-3716.
4. Rangaraju, N., et al., *Effect of cryo-rolling and annealing on microstructure and properties of commercially pure aluminium.* Materials Science and Engineering: A, 2005. **398**(1-2): p. 246-251.
5. Lee, S., et al., *Thermophysical properties of aluminum 1060 fabricated by equal channel angular pressing.* International Journal of Thermophysics, 2012. **33**(3): p. 540-551.
6. Wei, K.X., et al., *Microstructure, mechanical properties and electrical conductivity of industrial Cu–0.5%Cr alloy processed by severe plastic deformation.* Materials Science and Engineering: A, 2011. **528**(3): p. 1478-1484.
7. Xu, C.Z., et al., *Microstructure and properties of ultra-fine grain Cu–Cr alloy prepared by equal-channel angular pressing.* Materials Science and Engineering: A, 2007. **459**(1-2): p. 303-308.
8. Davis, J.R., *Copper and copper alloys.* 2001, Materials Park, OH : ASM International.
9. International, A., *ASM handbooks online*. 2002, Materials Park, OH : ASM International.
10. T. W. Ebbesen, et al., *Electrical conductivity of individual carbon nanotubes.* Nature, 1996. **382**: p. 54-56.
11. Furukawa, M., et al., *The use of severe plastic deformation for microstructural control.* Materials Science and Engineering: A, 2002. **324**(1-2): p. 82-89.
12. Kim, A.P.Z.-K., et al., *Orientation imaging microscopy of ultrafine-grained nickel.* Scripta Materialia, 2002. **46**: p. 575-580.
13. Islamgaliev, R.K., et al., *The nanocrystalline structure formation in germanium subjected to severe plastic deformation.* Nanostructured Materials, 1994. **4**: p. 387-395.
14. Lowe, T.C. and R.Z. Valiev, *Producing nanoscale microstructures through sever plastic deformation.* JOM, 2000. **52**(4): p. 27-28.

15. Zhilyaev, A.P., et al., *Experimental parameters influencing grain refinement and microstructural evolution during high-pressure torsion.* Acta Materialia, 2003. **51**(3): p. 753-765.

16. Huang, J.Y., et al., *Microstructures and dislocation configurations in nanostructured cu processed by repetitive corrugation and straightening.* Acta Materialia, 2001. **49**(9): p. 1497-1505.

17. Valiev, R.Z., et al., *Producing bulk ultrafine-grained materials by severe plastic deformation* JOM, 2006. **58**(4): p. 33-39.

18. Saito, Y., et al., *Novel ultra-high straining process for bulk materials-development of the accumulative roll-bonding (ARB) process.* Acta Materialia, 1999. **47**(2): p. 579-583.

19. Lu, C., K. Tieu, and D. Wexler, *Significant enhancement of bond strength in the accumulative roll bonding process using nano-sized SiO2 particles.* Journal of Materials Processing Technology, 2009. **209**(10): p. 4830-4834.

20. Beygelzimer, Y., et al., *Useful properties of twist extrusion.* Materials Science and Engineering: A, 2009. **503**(1-2): p. 14-17.

21. Segal, V.M., V.I. Reznikov, and A.E. Drobyshevskiy, *Plastic working of metals by simple shear.* Metall, 1981. **1**: p. 99.

22. Segal, V.M., *Materials processing by simple shear.* Materials Science and Engineering: A, 1995. **197**: p. 157-161.

23. Valiev, R.Z. and T.G. Langdon, *Principles of equal-channel angular pressing as a processing tool for grain refinement.* Progress in Materials Science, 2006. **51**(7): p. 881-981.

24. Petch, N.J., *The cleavage strength of polycrystals.* J. Iron Steel Inst., 1953. **174**: p. 25.

25. Hall, E.O., *The deformation and ageing of mild steel:III discussion of results.* Proceedings of the Physical Society. Section B, 1951. **64**: p. 747-753.

26. Chokshi, A.H., et al., *On the validity of the hall-petch relationship in nanocrystalline materials.* Scripta Metallurgica, 1989. **23**(10): p. 1679-1683.

27. Kumar, N., et al., *The effect of friction stir processing on the microstructure and mechanical properties of equal channel angular pressed 5052Al alloy sheet.* Journal of Materials Science, 2011. **46**(16): p. 5527-5533.

28. Hebesberger, T., et al., *Structure of Cu deformed by high pressure torsion.* Acta Materialia, 2005. **53**(2): p. 393-402.

29. Zhilyaev, A. and T. Langdon, *Using high-pressure torsion for metal processing: Fundamentals and applications.* Progress in Materials Science, 2008. **53**(6): p. 893-979.

30. Orlov, D., et al., *Evolution of microstructure and hardness in pure al by twist extrusion.* Materials Transactions, 2008. **49**(1): p. 2-6.

31. Rajinikanth, V., et al., *Effect of repetitive corrugation and straightening on Al and Al–0.25Sc alloy.* Materials Letters, 2008. **62**(2): p. 301-304.

32. Morisada, Y., et al., *MWCNTs/AZ31 surface composites fabricated by friction stir processing.* Materials Science and Engineering: A, 2006. **419**(1-2): p. 344-348.

33. Su, J.-Q., T.W. Nelson, and C.J. Sterling, *Friction stir processing of large-area bulk UFG aluminum alloys.* Scripta Materialia, 2005. **52**(2): p. 135-140.

34. Zhao, X., J.-f. Wang, and T.-f. Jing, *Gray cast iron with directional graphite flakes produced by cylinder covered compression process.* Journal of Iron and Steel Research, International, 2007. **14**(5): p. 52-55.

35. Yeh, J.W., S.Y. Yuan, and C.H. Peng, *A reciprocating extrusion process for producing hypereutectic Al–20wt.% Si wrought alloys.* Materials Science and Engineering: A, 1998. **252**(2): p. 212-221.

36. Iwahashi, Y., et al., *Principle of equal-channel angular pressing for the processing of ultra-fine grained materials.* Scripta Materialia, 1996. **35**(2): p. 143-146.

37. Nakashima, K., et al., *Influence of Channel Angle on the Development of Ultrafine Grains in Equal-Channel Angular Pressing.* Acta Materialia, 1998. **46**(5): p. 1589-1599.

38. Zhu, Y.T. and T.C. Lowe, *Observations and issues on mechanisms of grain refinement during ECAP process.* Materials Science and Engineering: A, 2000. **291**: p. 46-53.

39. Furuno, K., et al., *Microstructural development in equal-channel angular pressing using a 60° die.* Acta Materialia, 2004. **52**(9): p. 2497-2507.

40. Suh, J.Y., et al., *Finite element analysis of material flow in equal channel angular pressing.* Scripta Materialia, 2001. **44**: p. 677-681.

41. Park, J.W. and J.Y. Suh, *Effect of die shape on the deformation behavior in equal-channel angular pressing.* Metallurgical and Materials Transactions A, 2001. **32**(12): p. 3007-3014.

42. Kim, H.S., M.H. Seo, and S.I. Hong, *Finite element analysis of equal channel angular pressing of strain rate sensitive metals.* Journal of Materials Processing Technology, 2002. **130-131**: p. 497-503.

43. Berbon, P.B., et al., *Influence of pressing speed on microstructural development in equal-channel angular pressing.* Metallurgical and Materials Transactions A, 1999. **30**(8): p. 1989-1997.

44. Yamaguchi, D., et al., *Significance of adiabatic heating in equal-channel angular pressing.* Scripta Materialia, 1999. **41**(8): p. 791-796.

45. Yamashita, A., et al., *Influence of pressing temperature on microstructural development in equal-channel angular pressing.* Materials Science and Engineering: A, 2000. **287**(1): p. 100-106.

46. Shin, D.H., et al., *Effect of pressing temperature on microstructure and tensile behavior of low carbon steels processed by equal channel angular pressing.* Materials Science and Engineering: A, 2002. **323**(1-2): p. 409-415.

47. Huang, W.H., et al., *The effect of strain path and temperature on the microstructure developed in copper processed by ECAE.* Materials Science and Engineering: A, 2004. **366**(2): p. 221-228.

48. Stolyarov, V.V. and R. Lapovok, *Effect of backpressure on structure and properties of AA5083 alloy processed by ECAP*. Journal of Alloys and Compounds, 2004. **378**(1-2): p. 233-236.

49. Stolyarov, V.V., et al., *Ultrafine-grained Al–5 wt.% Fe alloy processed by ECAP with backpressure.* Materials Science and Engineering: A, 2003. **357**(1-2): p. 159-167.

50. Lapovok, R.Y., *The role of back-pressure in equal channel angular extrusion.* Journal of Materials Science, 2005. **40**(2): p. 341-346.

51. Furukawa, M., et al., *The shearing characteristics associated with equal-channel angular pressing.* Materials Science and Engineering: A, 1998. **257**(2): p. 328-332.

52. Ferrasse, S., et al., *Texture evolution during equal channel angular extrusion.* Materials Science and Engineering: A, 2004. **368**(1-2): p. 28-40.

53. Dalla Torre, F., et al., *Microstructures and properties of copper processed by equal channel angular extrusion for 1–16 passes.* Acta Materialia, 2004. **52**(16): p. 4819-4832.

54. Lugo, N., et al., *Microstructures and mechanical properties of pure copper deformed severely by equal-channel angular pressing and high pressure torsion.* Materials Science and Engineering: A, 2008. **477**(1-2): p. 366-371.

55. Nagarjuna, S. and K. Balasubramanian, *Effect of prior cold work on mechanical properties, electrical conductivity and microstructure of aged Cu-Ti alloys.* Journal of Materials Science, 1999. **34**: p. 2929-2942.

56. Ferrasse, S., et al., *Microstructure and properties of copper and aluminum alloy 3003 heavily worked by equal channel angular extrusion*. Metallurgical and Materials Transactions A, 1997. **28**(4): p. 1047-1057.

57. Higuera-Cobos, O.F. and J.M. Cabrera, *Mechanical, microstructural and electrical evolution of commercially pure copper processed by equal channel angular extrusion.* Materials Science and Engineering: A, 2013. **571**: p. 103-114.

58. Edalati, K., et al., *Equal-Channel angular pressing and high-pressure torsion of pure copper: evolution of electrical conductivity and hardness with strain.* Materials Transactions, 2012. **53**(1): p. 123-127.

59. Hosseini, S.A. and H.D. Manesh, *High-strength, high-conductivity ultra-fine grains commercial pure copper produced by ARB process.* Materials & Design, 2009. **30**(8): p. 2911-2918.

60. Ko, Y.G., et al., *Mechanical and electrical responses of nanostructured Cu–3wt%Ag alloy fabricated by ECAP and cold rolling.* Journal of Alloys and Compounds, 2010. **504**: p. S448-S451.

61. Shan'gina, D.V., N.R. Bochvar, and S.V. Dobatkin, *Structure and properties of Cu-Cr alloys subjected to shear under pressure and subsequent heating.* Russian Metallurgy (Metally), 2011. **2010**(11): p. 1046-1052.

62. Wenner, F., *A method of measuring earth resistivity.* National Bureau of Standards, 1916. **12**(4): p. 469-478.

63. Valdes, L.B., *Resistivity measurements on germanium for transistors.* Proceedings of the IRE, 1954. **42**(2): p. 420-427.

64. Lu, L., *Superplastic extensibility of nanocrystalline copper at room temperature.* Science, 2000. **287**(5457): p. 1463-1466.

65. Lugo, N., et al., *Thermal stability of ultrafine grains size of pure copper obtained by equal-channel angular pressing.* Journal of Materials Science, 2010. **45**(9): p. 2264-2273.

66. Vinogradov, A., et al., *Structure and properties of ultra-fine grain Cu–Cr–Zr alloy produced by equal-channel angular pressing.* Acta Materialia, 2002. **50**(7): p. 1639-1651.

67. Batra, I.S., et al., *Microstructure and properties of a Cu-Cr-Zr alloy.* Journal of Nuclear Materials, 2001. **299**(2): p. 91-100.

68. Liu, P., et al., *Aging precipitation and recrystallization of rapidly solidified Cu-Cr-Zr-Mg alloy.* Materials Science and Engineering: A, 1999. **265**(1-2): p. 262-267.

69. Christman, T. and S. Suresh, *Microstructural development in an aluminum alloy-sic whisker composite.* Acta Metallurgica, 1988. **36**(7): p. 1691-1704.

70. Jin, Y., et al., *Correlation between the cold-working and aging treatments in a cu-15 wt pct cr in situ composite.* Metallurgical and Materials Transactions A, 1998. **29**(8): p. 2195-2203.

71. Lu, L., et al., *Ultrahigh strength and high electrical conductivity in copper.* Science, 2004. **304**(5669): p. 422-6.

72. Li, Y.S., N.R. Tao, and K. Lu, *Microstructural evolution and nanostructure formation in copper during dynamic plastic deformation at cryogenic temperatures.* Acta Materialia, 2008. **56**(2): p. 230-241.